Vrije Universiteit Brussel

Aspects of Resurgence

Proefschrift ingediend met het oog op het behalen van de graad van
Master in de Fysica en Sterrenkunde

Jeriek Paul Van den Abeele

Promotors:
Prof. dr. Alexander Sevrin
Prof. dr. Daniel Thompson

Faculteit Wetenschappen en Bio-Ingenieurswetenschappen
Vakgroep Fysica en Sterrenkunde

Juni 2016

Aspects of Resurgence

Samenvatting

Niet-perturbatieve fenomenen zijn alomtegenwoordig in de natuur, zowel in kwantummechanica als in kwantumveldentheorieën. Algemene argumenten tonen dat de problemen met storingsrekening zelfs niet beperkt zijn tot fysische contexten met sterke koppeling, maar dat perturbatietheorie in het algemeen divergeert, ook in de kwantumelektrodynamica en kwantummechanische problemen. Borelsommatie leidt soms tot een oplossing, maar voor vele niet-sommeerbare reeksen geeft de procedure aanleiding tot imaginaire bijdragen met een ambigu teken. Voor de energie van een instabiele toestand kan daaraan een betekenis gegeven worden, maar anders zijn zulke bijdragen vaak problematisch en een signaal dat perturbatietheorie onvolledig is. Immers, belangrijke gevolgen van tunneling zoals de splitsing van energieniveaus en het ontstaan van energiebanden kunnen niet met storingsreeksen beschreven worden. In het padintegraalformalisme van de kwantummechanica ontstaan dergelijke kenmerken ten gevolge van instantonen, oplossingen voor de klassieke bewegingsvergelijkingen in een Euclidische ruimtetijd die een eindige actie hebben.

In deze thesis werd specifiek de periodische sine-Gordonpotentiaal bestudeerd, met als motivatie de relevantie ervan in modellen voor de sterke kernkracht. Voor de benadering van de grondtoestand werden met behulp van recurrentierelaties tot 1000 orden in perturbatietheorie berekend, zodat het asymptotische gedrag van de storingsreeks zeer precies bepaald kon worden. Een analyse daarvan toonde dat de groei van de coefficiënten gerelateerd is aan een niet-perturbatieve instanton–anti-instanton-bijdrage. Dit bevestigt het resurgence-paradigma, dat stelt dat perturbatietheorie en niet-perturbatieve effecten heel nauw verband houden met elkaar. Verder bewijs voor dit idee volgde uit het bepalen van de groei van de correctietermen op het asymptotisch gedrag van de perturbatiecoefficiënten. Dit toonde een niet-triviale connectie aan met een 4-instantoneffect, zoals verwacht in het kader van resurgence.

In het laatste deel van dit werk werd het voorkomen van resurgente transreeksen bestudeerd in het kwantumprobleem van de sine-Gordonpotentiaal. De transreeksen bieden de mogelijkheid om systematisch rekening te houden met niet-perturbatieve bijdragen, zodanig dat ambigue imaginaire contributies uit verschillende sectoren elkaar kunnen opheffen. Op die manier kan wiskundig een rigoureuze betekenis gegeven worden aan divergerende asymptotische expansies van waarneembare grootheden.

Contents

Acknowledgments

I would like to dedicate my thesis to my grandfather, Henri Van den Abeele. Opa, ik had u beloofd dat ik mijn best ging doen voor u.

I am forever indebted to my friends and family for their unfailing support and generous help when I needed it the most.

My gratitude goes as well to Prof. Alexander Sevrin and Prof. Daniel Thompson, for introducing me to the field of mathematical physics and for their suggestions. I also want to thank Prof. Ben Craps for his helpful advice.

1 Introduction

1.1 Context

Physical problems rarely have exact solutions, in the sense that interesting observables, like interaction cross-sections or ground-state energies, cannot generally be computed in an analytical way. Faced with the absence of closed-form solutions, the standard mathematical tool one resorts to is perturbation theory. After identifying a small perturbation parameter in the problem at hand, one can expand the quantity of interest as a power series in the parameter and iteratively compute the influence of higher-order processes. Perhaps the ultimate triumph of this approach is the 5-loop calculation of the anomalous magnetic moment of the electron in quantum electrodynamics (QED), yielding a value agreeing with experimental measurements – up to 10 significant figures [6]. The strategy seems to work well ... or does it?

1.1.1 QCD, or the importance of strong-coupling effects

Firstly, the outlined method is only natural for weakly-coupled theories. However, it is well-known that couplings in quantum field theory (QFT) are scale-dependent, af-

ter regularisation and renormalisation. These procedures are necessary to resolve the generic divergences due to the very nature of perturbation theory in Lorentz-invariant quantum theories: at each order, a summation over the infinity of virtual intermediate states is involved, typically leading to UV-divergent loop integrals unless regulated [7]. Reparametrising the perturbative expansions in terms of renormalised, physical coupling constants allows hiding the divergences in the non-physical, bare couplings. The other side of the coin, however, is that the new couplings depend on the renormalisation energy scale μ. Although the final, physical predictions should not depend on this scale, it affects the results of individual diagrams and hence indicates the way the theory itself behaves effectively when probed [7, 8].

Quantum chromodynamics (QCD), the non-Abelian $SU(3)$ gauge theory describing the strong nuclear force, is renormalisable, like QED. The running of its renormalised, dimensionless coupling α_s is encoded by the β function [9, 10]:

$$\beta(\alpha_s) = \mu \frac{\mathrm{d}\alpha_s}{\mathrm{d}\mu} = -\left(\frac{11}{3}N_c - \frac{2}{3}N_f\right)\frac{\alpha_s^2}{4\pi} + \mathcal{O}\left(\alpha_s^3\right) = -\frac{7\alpha_s^2}{4\pi} + \mathcal{O}\left(\alpha_s^3\right) < 0. \tag{1.1}$$

Its negative value in the Standard Model case with $N_c = 3$ colours and $N_f = 6$ flavours indicates that QCD is weakly coupled at high energies, but has strong coupling in the low-energy regime. This *asymptotic freedom* towards high energies manifests itself in deep inelastic proton scattering, where experiments show that the quarks inside the proton can be described as quasi-free rather than strongly bound. On the other hand, the strong coupling at low energies is consistent with the observed *confinement* of quarks and gluons, which carry colour charge, inside colour-neutral hadrons. In this regime, at scales $\mu \lesssim 1$ GeV, perturbation theory is no longer viable, since α_s grows to order unity and larger [11].

A non-perturbative understanding of field theory is indispensable for a full description of the QCD vacuum and the hadronic spectrum. Chiral perturbation theory leads to some quantitative predictions, like the pseudoscalar-meson masses, by exploiting how non-vanishing quark masses explicitly break chiral flavour symmetry in QCD [12]. This is an example of an effective field theory, formulated in terms of the observed hadronic degrees of freedom, rather than the quarks and gluons that do not appear as asymptotic states. Other approaches to calculate QCD predictions at low energies include lattice gauge theory, the attempts to calculate the QCD path integrals on a discre-

tised spacetime grid, and studying large-N expansions of the properties of Yang-Mills theories with gauge group $SU(N)$ [13].

For a successful account of the short range of the strong interaction, QCD has to have a dynamically generated mass gap, at the quantum level [14], between the vacuum and the first excited state of the theory. In more physical terms, the question is: can glueballs, colourless states composed of self-interacting gluons, be rigorously proven to be the lightest bound states in the QCD spectrum and have non-zero mass? QED has no such gapped energy spectrum, since photons can have arbitrarily long wavelengths. Perturbative QCD cannot explain the mass gap, nor confinement, both occurring in the strong-coupling regime, yet insights from both lattice simulations and experiments suggest such properties, and the lowest glueball mass is expected in a range of 1 to 1.7 GeV [15–17].

1.1.2 Beyond perturbation theory

There is another problem with perturbation theory, besides the issues for strongly-coupled theories. While sketching the natural procedure in the weak-coupling case, an important final step was neglected: summing all higher-order corrections. In principle, an infinite number of these terms is necessary to get the exact result. However, a priori there is often no guarantee of convergence. Seemingly making matters even worse, a heuristic argument by Dyson [18], based on how physical instabilities imply non-analyticity, asserts the generic divergence of perturbative expansions in QED and quantum mechanics. These typically diverge factorially, which is mathematically related to the growth of the number of higher-order Feynman diagrams [13, 19].

Nevertheless, exact physical quantities should be finite and when their perturbative approximations diverge, it is a meaningful sign indicating an incomplete description. Such series should typically only be interpreted as asymptotic expansions of an exact solution in a certain limit of the expansion parameter, yielding accurate results when appropriately truncated. After all, important physical phenomena like quantum tunnelling cannot even be captured in a perturbative description [20]. The magnitude of the related effects depends on non-perturbative, exponentially small factors like $e^{-C/g}$, for a constant C, leading to a vanishing Taylor series around its essential singularity $g = 0$.

One can still hope, however, that the information encoded in a perturbation series can be reinterpreted in a sensible way to reconstruct the observable quantity. The *Borel resummation* procedure offers a way out, for factorially divergent series, essentially by replacing the factorials in the series coefficients by their integral representation as a gamma function. As a matter of fact, the factorial divergence and exact behaviour of late terms in the series turn out to be precisely linked to singularities of the Borel-transformed series [13]. An integration is required in the attempt to reconstruct the exact result, which is problematic for non-Borel summable series, where the singularities occur along the integration path. The price one pays to avoid these via contour deformation is an imaginary contribution to the reconstructed quantity, with an ambiguous sign depending on the chosen contour. From the physical point of view, the imaginary part can be desirable, as for the energy of an unstable state, but for the energy of a stable state it definitely is not. An explicit account of non-perturbative effects is crucial to eliminate such unphysical, ambiguous imaginary energy contributions, which render perturbation theory ill-defined and incomplete [13, 21–24].

1.2 Motivation: resurgence and trans-series

Trans-series expansions provide a framework for the construction of non-perturbative solutions, where asymptotic perturbation series on their own are insufficient. By explicitly incorporating summations over both perturbative and non-perturbative contributions, the trans-series provide possibilities to cancel out the imaginary ambiguities incurred by non-Borel summable series. The fact that such cancellations indeed do occur, in various physical contexts [2, 4, 5, 21, 22, 25–30], is a highly non-trivial manifestation of *resurgence*, a mathematical theory rigorously developed by Écalle in the 1980s [31].

The resurgence framework is deeply rooted in the study of analytic functions with isolated singularities, and reveals surprising similarities between their behaviour at these singular points and at the origin. When expanding solutions of differential equations like the Schrödinger equation as trans-series, such relations between singularities translate to an intricate connections between the series coefficients in the perturbative and non-perturbative sectors. Opportunities for the exact cancellation of ambiguous contributions ensue [4, 21, 22].

In quantum theories, tunnelling is linked to instantons, classical solutions of the equations of motion in Euclidean spacetime with a finite action. They are directly associated to the non-perturbative effects which prevent the convergence of perturbative expansions, e. g. for the ground-state energy in the double-well potential. For some quantum-mechanical settings with degenerate minima, Bogomolny [32] and Zinn-Justin [33, 34] (BZJ) discovered how the ambiguity in non-Borel summable perturbation series cancels out, to leading order, against another ambiguous contribution found by accounting for instanton contributions. Full, resurgent trans-series expansions are believed to go even further, with cancellations claimed to continue throughout all higher orders, ultimately leading to real and ambiguity-free observables [21, 22].

Resurgent structures are prevalent as well in QFTs with degenerate classical vacua [4, 21]. Perturbative expansions in QCD and asymptotically free, QCD-like theories (like 4d Yang-Mills theories and the 2d $\mathbb{CP}^{N-1}$ non-linear sigma model) also suffer from non-Borel summability due to singularities of their Borel transform [4, 21, 25]; however, more dominant, problematic singularities arise, called *infrared renormalons*, which are related to the scale-dependence of the renormalised coupling. 't Hooft speculated about their connection to the confinement problem, given that they can originate from infrared divergences in the contributions from fermion loops in a gluon line [35–37]. The renormalons lead to ambiguous non-perturbative contributions that are parametrically different (viz. depending on the gauge or global symmetry group rank N) from the contributions from instanton events [4, 21, 25, 35, 36], so the BZJ cancellation mechanism from quantum mechanics is insufficient.

An ambitious aim of the resurgence program in QFT is to enable a non-perturbative, semi-classical continuum definition, as opposed to lattice formulations. To get to that point, a cancellation of the renormalon ambiguities is in order. Recent proposals [4, 25] suggest the solution might be achieved by addressing another issue, the invalidity of the dilute instanton gas approximation, which is used to obtain semi-classical expansions in quantum mechanics. Spatial compactifications were found to lead to new configurations, called fractionalised instantons, which (in appropriate combinations named bions) indeed appear to give rise to ambiguities able to cancel those from IR renormalons exactly for $\mathbb{CP}^{N-1}$ models [4].

While studying the applications of resurgence theory in quantum field theory is, on the face of it, highly technical, it turns out a lot can already be learnt about non-

perturbative effects from the study of periodic potentials in quantum mechanics, which were studied early-on in the context of the Bogomolny–Zinn-Justin mechanism. The underlying reason is that several 2d field theories (especially the $SU(N)$ principal chiral model and the $\mathbb{CP}^{N-1}$ model), acting as QCD toy models with asymptotic freedom, confinement and a dynamically generated mass gap, can be continued to a calculable, weak-coupling regime. This is achieved by compactification on a circle ($\mathbb{R}^2 \to \mathbb{R} \times S^1_L$) with sufficiently small radius L and specific boundary conditions. Effectively, in the small-L limit, the 2d QFTs boil down to quantum mechanics after Kaluza-Klein reduction[1], with low-energy dynamics and in particular the properties of the ground state governed by a Hamiltonian with a periodic sine-Gordon (or equivalently, cosine-well) potential [3, 4, 27]. Calculated quantities like the free energy remain meaningful in the large-circle limit, owing to the property of adiabatic continuity permitting a continuous connection to the strong-coupling regime, without rapid cross-overs between deconfined and confined regimes or phase transitions. Therefore, it is definitely worthwhile to explore the techniques used to determine the divergence of perturbative energy expansions with such potentials and look at singularities of the Borel transforms. Especially in the light of resurgence theory, the asymptotic series get new meaning and deep relations between perturbative and non-perturbative physics can be uncovered.

1.3 Thesis structure

- Chapter 2 provides an introduction to Euclidean path integrals and instantons. As an illustration of the importance of non-perturbative, single-instanton effects, the explicit calculations are shown in this framework, leading to the well-known level splitting in the double-well and band structure in the energy spectrum of the periodic cosine-well.
- In Chapter 3, a brief description is given of the mathematical tools necessary to analyse the behaviour of divergent asymptotic series occurring in interesting physical problems. An account is given of the notion of asymptoticity, the Stokes phenomenon, some practical possibilities and limitations of Borel resummation and the use of Padé approximants in the analysis of the singularities of the Borel

[1] The key idea is that extra compact dimensions, when small enough, would only affect high-energy features of the theory.

transform. At the end of the chapter, the idea behind dispersion relations for non-analytic functions is reviewed.

- Chapter 4 subsequently details the application of these techniques in the specific problem of the periodic sine-Gordon potential, mathematically known as the Mathieu equation [38–40]. This chapter extends the numerical Stone–Reeve analysis [41] of the Mathieu problem and precise links between perturbation theory and instanton effects are highlighted.

  In particular, after calculating the first 1000 orders in perturbation theory exactly, the large-order behaviour of the perturbative expansion was determined to an unprecedented accuracy: the first 32 sub-leading corrections were found in exact rational form, and up to 65 in reliable numerical approximations. These correspond to fluctuation coefficients around the non-perturbative instanton–anti-instanton sector. In turn, those fluctuation coefficients are shown to determine a divergent asymptotic series themselves, of which the leading asymptotics were also found and associated to a higher-order non-perturbative effect involving a part of the 4-instanton sector.

- In Chapter 5, it is explained how resurgent trans-series arise in quantum mechanical problems, in a very natural way, when the potentials display degenerate harmonic minima as for the sine-Gordon well. The discussion, based on recent insights obtained using the uniform WKB approximation [21,22], sheds light on the surprisingly close relations between perturbation theory and non-perturbative contributions to observables. These intricate connections are summarised in the resurgence triangle. Consequently, the results from the large-order behaviour in the Mathieu problem are demonstrated to be concrete, non-trivial manifestations of such an underlying resurgent structure.

- The final chapter is followed by the Conclusions and Outlook, several appendices with more details and a bibliography.

2

Instantons and quantum tunnelling

2.1 Introduction

In quantum mechanics, particles retain a non-vanishing probability to traverse a potential barrier even when their energy is classically insufficient to surmount it. Such tunnelling events are intimately related to *instantons*, a class of objects uncovered by working in the path integral formulation of quantum mechanics [20, 42]. They are classical solutions to the equations of motion in Euclidean spacetime, characterised by a finite action and non-trivial trajectories. Aptly called instantons by 't Hooft, they represent instantaneous jumps between potential minima, leading to a localised structure in spacetime.

Classically, of course, there can be no potential barrier penetration. However, the transition from Minkowski spacetime to Euclidean spacetime requires rotating the real time axis to the imaginary axis of the complex plane. Tunnelling paths in real time then turn out to be described by classical trajectories in imaginary time [20, 42]. The relevance of looking at tunnelling in this way is illustrated by considering the example of the double-well potential, a simple setting where tunnelling arises between the symmetric potential minima. In the classical analysis, the lowest energy states have a twofold

degeneracy, as the particle could be located in the left or the right minimum. Quantum tunnelling then alters this picture, lifting the degeneracy by giving rise to even and odd states with a different energy.

Effects like this energy splitting can be evaluated in the semi-classical limit, where quantum effects and hence Planck's constant are considered small with respect to the classical action involved. In that case, it suffices to compute the contributions of instantons to leading order, by applying the steepest-descent method to the path integral, i. e. expanding the integrand around saddle points. In the end, the more common WKB approximation for solving the Schrödinger equation would yield the same results as the instanton approach, but the latter has a more immediate generalisation to quantum field theory.

This chapter mainly discusses how instantons arise in the quantum-mechanical context of the potentials with degenerate minima, along the lines of [20, 42–44]. The analysis provides key insights into the physical meaning of instanton solutions and their importance in the connection with leading-order quantum corrections. The first step in illuminating their main features and technicalities consists of taking a closer look at path integrals and the Euclidean framework, in order to ensure a well-defined integral.

2.2 Path integrals in quantum mechanics

The dynamics of physical systems is often described by the principle of stationary action, with the classical path taken by the system characterised as a trajectory of which the first-order variation leaves the action invariant. The path integral formalism still involves the action of a path to quantify the probability amplitude of a process, but in an integral reflecting the fact that all possible trajectories should be considered in quantum mechanics [45]. One has to account for any path in configuration space connecting the initial and final state of the process, essentially a statement of the superposition principle in quantum mechanics.

As a starting point, it is instructive to focus on the motion of a single spinless particle of unit mass, travelling in a one-dimensional potential $V(x)$. Now, one can envisage a process where the particle moves from its initial position x_i at time $-t_0/2$ to a point x_f, where it arrives at time $+t_0/2$. Feynman's method to find the transition amplitude for this propagation process prescribes integrating over all paths connecting the space-

time points $(-t_0/2, x_i)$ and $(+t_0/2, x_f)$, even those not satisfying the classical equations of motion [45]. Each of these superposed paths $x(t)$ gets assigned a weighting factor $e^{iS[x(t)]/\hbar}$ in the path integral, where

$$S[x(t)] = \int_{-t_0/2}^{+t_0/2} \mathrm{d}t\, L(x, \dot{x}) = \int_{-t_0/2}^{+t_0/2} \mathrm{d}t \left[\frac{1}{2} \left(\frac{\mathrm{d}x}{\mathrm{d}t} \right)^2 - V(x) \right] \tag{2.1}$$

is the classical action, given by the integral over time of the Lagrangian $L(x, \dot{x})$ along the particle's path. The action is a functional: it maps an element of a vector space to its underlying scalar field, in this case a path $x(t)$ in an infinite-dimensional function space to a real number.

In the Schrödinger picture of quantum mechanics (Appendix A), Feynman's sum over all possible histories for this process is then related to its quantum mechanical probability amplitude by [45]

$$\langle x_f | e^{-iHt_0/\hbar} | x_i \rangle = N \int \mathcal{D}[x(t)]\, e^{iS[x(t)]/\hbar}. \tag{2.2}$$

In the expression on the left-hand side, x_i and x_f label position eigenstates and H denotes the Hamiltonian operator (assumed to be time-independent), entering in the time-evolution operator $e^{-iHt_0/\hbar}$ for the system. On the right-hand side, N is a formal normalisation factor, introduced to keep that side finite and determined later on. The integration $\int \mathcal{D}[x(t)]$ refers to summing over all paths $x(t)$ in configuration space satisfying the boundary conditions $x(-t_0/2) = x_i$ and $x(+t_0/2) = x_f$. The concrete procedure for performing this integral in practice is the subject of the next sections.

2.2.1 The classical limit

One observes that the weight for each path is just a pure phase, its unit modulus ensuring each path is equally important. However, the summation over paths occurs in the amplitude of the process. Hence, interference between different paths may alter its probability significantly, a typical feature of quantum mechanics. In the classical limit, where one considers $S \gg \hbar$, or equivalently "$\hbar \to 0$", the integrand $e^{iS[x(t)]/\hbar}$ becomes very oscillatory [45]. Intuitively, it is clear how sinusoidal waves with quickly varying phase cancel out when added, due to destructive interference – only sinusoids with ap-

proximately the same phase add coherently. Applying this idea to oscillatory integrals is called the *stationary-phase approximation*: dominant contributions to an oscillatory integral come from regions where the phase is nearly constant. In this case, requiring the phase to be invariant (to first order) under variations[1] of its argument, the path $x(t)$,

$$\delta S \equiv S[x(t) + \delta x(t)] - S[x(t)] = 0 \tag{2.3}$$

leads to the classical path $x_{cl}(t)$ [45]. After all, by definition this path is the one in accordance with the principle of stationary action. It is no surprise only the classical path will describe the motion and contribute to the transition amplitude in the classical limit, so that

$$N \int \mathcal{D}[x(t)]\, \mathrm{e}^{iS[x(t)]/\hbar} \sim \mathrm{e}^{iS_{\mathrm{cl}}/\hbar}, \tag{2.4}$$

where $S_{\mathrm{cl}} = S[x_{cl}(t)]$ is the action of the classical path. Implicitly, it was assumed that the action has only one critical point, where the first-order variation vanishes. If multiple such points exist, their contributions have to be summed. However, all (2.4) gives is just an asymptotic description of the integral's behaviour as $\hbar$ tends to zero. In order to include contributions due to quantum effects, it is necessary to expand the path integral more systematically.

2.2.2 The stationary-phase approximation

The *stationary-phase approximation* is the standard approach to handle oscillatory integrals of the type

$$I[f] = \int_{-\infty}^{+\infty} \mathrm{d}x\, \mathrm{e}^{(i/g)f(x)}, \tag{2.5}$$

where f is a real function and g a real, positive constant [46]. As mentioned earlier, rapid oscillations of the integrand as $g \to 0$ cancel each other out when integrated, leaving only dominating contributions from the neighbourhood of stationary points x_k, where no oscillations occur to first order: $f'(x_k) = 0$. Hence, in the small-g limit the integral can be approximated by a Taylor expansion of f around the stationary points

[1] The functional $S[x(t)]$ can be differentiated with respect to its argument, the function $x(t)$, yielding the functional derivative $\frac{\delta S[x(t)]}{\delta x(t)}$. Requiring $\delta S = 0$ to first order is equivalent to stating that the first functional derivative vanishes.

x_k:

$$f(x) = f(x_k) + \frac{1}{2} f''(x_k)(x - x_k)^2 + R(x - x_k), \tag{2.6}$$

where the remainder $R(x - x_k)$ contains cubic and higher-order terms in the deviation $x - x_k$. Summing over the contributions in small neighbourhoods $(x_k - \epsilon, x_k + \epsilon)$ around the stationary points x_k, one finds that approximately,

$$I[f] \simeq \sum_k \mathrm{e}^{(i/g) f(x_k)} \int_{x_k - \epsilon}^{x_k + \epsilon} \mathrm{d}x \, \mathrm{e}^{(i/g)[f''(x_k)(x - x_k)^2/2 + R(x - x_k)]}. \tag{2.7}$$

The integrations around the stationary points can be extended to infinity, as the resulting error is exponentially suppressed and vanishes in the limit of $g \to 0$. Then, writing $y = (x - x_k)/\sqrt{g}$, the integral becomes[2]

$$I[f] \simeq \sum_k \mathrm{e}^{(i/g) f(x_k)} \int_{-\infty}^{+\infty} \mathrm{d}y \, \mathrm{e}^{i[f''(x_k) y^2/2 + (1/g) R(\sqrt{g} y)]} \tag{2.8}$$

$$= \sum_k \sqrt{\frac{2\pi i g}{f''(x_k)}} \mathrm{e}^{(i/g) f(x_k)} [1 + g(\ldots) + g^2(\ldots) + \ldots] \tag{2.9}$$

In the last line, neglecting the remainder term and claiming it leads to subleading contributions of order $\mathcal{O}(g)$ should still be justified. This immediately follows from the realisation that $R(\sqrt{g} y)$ contains cubic and higher orders of $\sqrt{g} y$ [46], so that

$$\frac{1}{g} R(\sqrt{g} y) = \frac{1}{3!} \sqrt{g} f^{(3)}(x_k) y^3 + \frac{1}{4!} g f^{(4)}(x_k) y^4 + \mathcal{O}\left(g^{3/2}\right) \tag{2.10}$$

has (half-)integer powers of g in the coefficients for even (odd) powers of y. Now, the exponential factor $\mathrm{e}^{(i/g) R(\sqrt{g} y)}$ can be expanded in even powers of y only, since odd powers vanish in the integral. Hence, only integer powers of g enter in the expansion of (2.8), for example the first-order term

$$\mathrm{e}^{\frac{i}{g} R(\sqrt{g} y)} \Big|_{\mathcal{O}(g)} = g \left[\frac{1}{4!} f^{(4)}(x_k) y^4 + \frac{1}{12} f^{(3)}(x_k)^2 y^6 \right]. \tag{2.11}$$

In this way, the stationary-phase approximation in (2.9) is established.

[2] To be exact, this step requires a generalisation of the Gaussian integral called the Fresnel integral: $\int_{-\infty}^{+\infty} \mathrm{d}x \exp\left(i a x^2/2\right) = \sqrt{2\pi i/a}$ for real $a \neq 0$.

Applying the stationary-phase method to path integrals essentially amounts to expanding the action $S[x(t)]$ around its critical points. If there is only one, the classical solution $x_{cl}(t)$ of the Euler-Lagrange equations, one can expand any path as $x(t) = x_{cl}(t) + \delta x(t)$ so that

$$S[x(t)] = S_{cl} + \frac{1}{2}\int_{-t_0/2}^{+t_0/2} \mathrm{d}t \int_{-t_0/2}^{+t_0/2} \mathrm{d}t' \left.\frac{\delta S[x(t)]}{\delta x(t)\delta x(t')}\right|_{x=x_{cl}} \delta x(t)\delta x(t') + \dots \tag{2.12}$$

In this expansion, the term with the first functional derivative of the action was omitted since it vanishes for $x(t) = x_{cl}(t)$. The first term will give rise to the exponential factor noted in (2.4). As in (2.9), the higher-order fluctuations result in a pre-exponential factor and an expansion in orders of $\hbar$, a so-called *semiclassical expansion* [46]. It is possible to continue and determine the pre-exponential factor at this point already, yet given the main objective of studying instanton solutions, it is more practical to calculate it further on, in the convenient framework of Euclidean spacetime.

2.3 Euclidean path integrals

Interesting new solutions for the quantum mechanical equations of motion will be obtained by turning from Minkowski spacetime to working in Euclidean spacetime [20, 42–44]. Formally, this Wick rotation amounts to analytic continuation in the time coordinate t, letting it assume values on the imaginary axis of the complex plane:

$$t = -i\tau, \tag{2.13}$$

where $t = x^0$ and $\tau = x^4$ are respectively the Minkowski time and the Euclidean time[3].

The Euclidean action S_E and the Minkowski action S are related as

$$S = \int_{-t_0/2}^{t_0/2} \mathrm{d}t \left[\frac{1}{2}\left(\frac{\mathrm{d}x}{\mathrm{d}t}\right)^2 - V(x)\right] = i\int_{-T/2}^{T/2} \mathrm{d}\tau \left[\frac{1}{2}\left(\frac{\mathrm{d}x}{\mathrm{d}\tau}\right)^2 + V(x)\right] = iS_E. \tag{2.14}$$

Here, $[-t_0/2, t_0/2]$ denotes the interval for the calculation in Minkowski time and the

[3]Euclidean time τ is often referred to as 'imaginary time', despite being a real quantity. Minkowski time t is called 'real time', even though it is analytically continued to imaginary values.

analogue with $T = it_0$ gives the Euclidean interval. At this point, one observes that the transition to imaginary time flips the potential present in the action: the Euclidean Lagrangian is given by

$$L_E = \frac{1}{2}\left(\frac{\mathrm{d}x}{\mathrm{d}\tau}\right)^2 - (-V(x)). \tag{2.15}$$

Furthermore, since Wick rotation turns the exponential weighting factor for the path $x(t)$ into $\mathrm{e}^{-S_E[x(\tau)]/\hbar}$ and the time evolution operator into $\mathrm{e}^{-HT/\hbar}$, the Euclidean path integral becomes [20, 42–44]

$$\langle x_f|\mathrm{e}^{-HT}|x_i\rangle = N\int \mathcal{D}[x(\tau)]\,\mathrm{e}^{-S_E[x(\tau)]/\hbar}. \tag{2.16}$$

The integration runs over all imaginary-time paths $x(\tau)$ with fixed endpoints $x(-T/2) = x_i$ and $x(+T/2) = x_f$.

In this way, the oscillating integrand of the real-time path integral, complicating convergence, has conveniently changed to a decreasing exponential. The resulting integral is well-defined and known as a Wiener integral[4]. For if one assumes the potential is bound from below, with minimum fixed at zero (if necessary by means of an additive constant), it is clear from (2.15) that the Euclidean action is positive, so paths with large action are exponentially suppressed and concerns about convergence disappear.

2.3.1 The partition function

The transition to imaginary time has practical implications, apart from leading to a rigorous mathematical definition of the path integral with a simple, positive action. One consequence is that the ground state energy can be obtained in a straightforward limit from the path integral [20, 42–44]. To see this, one uses the completeness of energy eigenstates $|n\rangle$ with $H|n\rangle = E_n|n\rangle$ and inserts into (2.16) a resolution of unity to write position eigenstates $|x\rangle$ in terms of energy eigenstates:

$$\sum_n |n\rangle\langle n| = \mathbb{1} \qquad \Longrightarrow \qquad |x\rangle = \sum_n \langle n|x\rangle\,|n\rangle\,. \tag{2.17}$$

[4] The problem with the regular Feynman path integral is in defining the integration measure on the infinite-dimensional space of Minkowski-spacetime paths. However, one can define it as the analytic continuation of a Wiener integral to purely imaginary τ [47].

Then (2.16) yields

$$N \int \mathcal{D}x \, \mathrm{e}^{-S_E[x(\tau)]/\hbar} = \sum_n \mathrm{e}^{-E_n T/\hbar} \, \langle x_f|n\rangle \, \langle n|x_i\rangle \, . \tag{2.18}$$

One observes that the imaginary-time evolution operator is Hermitian and no longer unitary. The limit of large $T \to \infty$ projects out the lowest-level term of the sum,

$$\mathrm{e}^{-E_0 T} \psi_0(x_f) \psi_0^*(x_i), \tag{2.19}$$

as dominant contribution, where the wavefunction of the n-th energy eigenstate at position x is identified as $\psi_n(x) = \langle x|n\rangle$.

Furthermore, the partition function $Z(\beta)$ in the Euclidean formulation enables an interesting connection between quantum mechanics and statistical physics [45]. Defined as function of $\beta = 1/(k_B T_0)$, where T_0 denotes temperature, the partition function

$$Z(\beta) = \mathrm{Tr}\left(\mathrm{e}^{-\beta H}\right) \tag{2.20}$$

resembles the trace of the Euclidean time evolution operator when the energies $k_B T_0$ and $\hbar/\tau$ are identified. Indeed, the amplitude for a process where the system goes from any state back to the same state after some time τ is in fact given by the partition function for the system:

$$Z(\tau) = \mathrm{Tr}\left(\mathrm{e}^{-H\tau/\hbar}\right). \tag{2.21}$$

Evaluating the trace in (2.20) in a basis of energy eigenstates and the trace in (2.21) in a basis of position eigenstates should then be equivalent:

$$Z\left(\beta = \frac{\tau}{\hbar}\right) = \sum_n \langle n|\mathrm{e}^{-\beta H}|n\rangle = \sum_n \mathrm{e}^{-E_n \tau/\hbar} \tag{2.22}$$

$$= \int \mathrm{d}x \, \langle x|\mathrm{e}^{-H\tau/\hbar}|x\rangle = N \int_{x_i = x_f} \mathcal{D}[x(\tau)] \, \mathrm{e}^{-S_E[x(\tau)]/\hbar}. \tag{2.23}$$

The path integral runs over all closed loops and since the trace is invariant under a change of basis, calculating the integral should enable one to read off the energy spectrum, i. e. the E_n values. The ground-state energy can be found by taking the limit $\beta \to \infty$, as in

$$E_0 = -\lim_{\beta \to \infty} \frac{1}{\beta} \ln Z(\beta). \tag{2.24}$$

2.3.2 The semiclassical approximation

At this point, it is natural to wonder how the path integral can be calculated in practice. Section 2.2.2 on the stationary-phase method already showed the way to go in the case of Minkowski time: in the limit where $\hbar \to 0$, expanding the action around the classical path leads to a semi-classical expansion of the path integral in orders of $\hbar$. Shifting to the Euclidean path integral, (2.16), the exponential suppression factor immediately shows the integral is dominated by the stationary points of the positive action[5] S_E. No stationary-phase argument is required now, as the exponent is real. In this case, the integral is approximated using Laplace's method: a straightforward Taylor expansion of the action about the classical solution $x_{cl}(\tau)$ in the $\hbar \to 0$ limit suffices to turn the integral into a product of simple Gaussian integrals [20, 42–44].

The first step to a more explicit integration measure is to zoom in on the variable being integrated, in this case the path connecting two fixed boundary points at specific times. If there is a countable basis of real orthonormal functions $x_n(\tau)$, vanishing at those boundaries, such that

$$\int_{-T/2}^{+T/2} \mathrm{d}\tau \; x_n(\tau) x_m(\tau) = \delta_{nm} \qquad \text{and} \qquad x_n\left(\pm\frac{T}{2}\right) = 0 \tag{2.25}$$

for all positive integers n, m, then any path satisfying the two boundary conditions $x_i = x(-\tau/2)$ and $x_f = x(+\tau/2)$ can be expanded as a fluctuation about the classical path using the $x_i(\tau)$ basis [20, 42]:

$$x(\tau) = x_{cl}(\tau) + \sum_{n=0}^{\infty} c_n x_n(\tau). \tag{2.26}$$

Then the path integration is a series of integrations over the real coefficients c_n of the linear combination:

$$\mathcal{D}[x(\tau)] = \prod_{n=0}^{\infty} \frac{\mathrm{d}c_n}{\sqrt{2\pi\hbar}}. \tag{2.27}$$

The multiplicative factor is chosen for convenience, but remains meaningless until the normalisation factor N is fixed.

The requirement for the classical path to be a stationary point of the action (for sim-

[5] Since all calculations will be made in the Euclidean formalism, the subscript E will be dropped: no confusion can arise.

plicity assumed to be the only one now) translates to the first-order invariance of its action under a small perturbation $\delta x(\tau)$ [20, 42–44]:

$$0 = \delta S = \int_{-T/2}^{+T/2} \mathrm{d}\tau \left[-\ddot{x}_{cl}(\tau) + V'(x_{cl}) \right] \delta x(\tau). \tag{2.28}$$

Primes denote differentiation with respect to the position x and dots refer to Euclidean time derivatives. Since the perturbation is arbitrary, the integrand must vanish. In this way, one recovers the classical equation of motion

$$\ddot{x}_{cl}(\tau) = V'(x_{cl}). \tag{2.29}$$

The left-hand side is the particle's acceleration, the right-hand side gives the force the particle is subjected to in the potential $-V(x)$. This result immediately implies that the (imaginary-)time derivative of the energy

$$E = \frac{1}{2}\dot{x}_{cl}(\tau)^2 - V(x_{cl}) \tag{2.30}$$

vanishes, so the classical path conserves energy.

As it is now known that the first-order deviation of the action for the perturbed classical path $x_{cl}(\tau) + \delta x(\tau)$ is zero, with inclusion of the second-order deviation the action becomes

$$S[x_{cl} + \delta x] \simeq S_{cl} + \frac{1}{2} \int_{-T/2}^{+T/2} \mathrm{d}\tau \int_{-T/2}^{+T/2} \mathrm{d}\tau' \, \frac{\delta^2 S[x_{cl}(\tau)]}{\delta x(\tau) \delta x(\tau')} \, \delta x(\tau) \delta x(\tau'). \tag{2.31}$$

Here, the second functional derivative is given by

$$\frac{\delta^2 S[x_{cl}(\tau)]}{\delta x(\tau) \delta x(\tau')} = \left[-\frac{\mathrm{d}^2}{\mathrm{d}\tau^2} + V''(x_{cl}) \right] \delta(\tau - \tau'). \tag{2.32}$$

The operator between brackets is a linear Hermitian operator. One can choose the orthonormal basis of paths $x_n(\tau)$ in (2.26) to be its eigenfunctions, with discrete eigenvalues λ_n:

$$\left[-\partial_\tau^2 + V''(x_{cl}) \right] x_n(\tau) = \lambda_n x_n(\tau). \tag{2.33}$$

Subsequently replacing the perturbation δx by the linear combination of terms $c_n x_n$

and using the orthonormality condition (2.25), the leading-order approximation of the action is significantly simplified to

$$S[x] = S[x_{cl} + \delta x] \simeq S_{cl} + \frac{1}{2}\sum_n \lambda_n c_n^2. \tag{2.34}$$

Bringing all elements together, the path integral (2.16) becomes a product of Gaussian integrals over c_n [20, 42–44] and hence,

$$\langle x_f|\mathrm{e}^{-HT/\hbar}|x_i\rangle = N\mathrm{e}^{-S_{cl}/\hbar}\prod_n \int_{-\infty}^{+\infty} \frac{\mathrm{d}c_n}{\sqrt{2\pi\hbar}}\,\mathrm{e}^{\frac{\lambda_n c_n^2}{2\hbar}}\,[1+\mathcal{O}(\hbar)] \tag{2.35}$$

$$= N\mathrm{e}^{-S_{cl}/\hbar}\prod_n \lambda_n^{-1/2}\,[1+\mathcal{O}(\hbar)]. \tag{2.36}$$

The subleading terms of order $\hbar$ arise from the truncation of the Taylor expansion of the action, as in (2.9). The product of the eigenvalues of the second variational derivative can also be defined as the determinant of this operator, so

$$\prod_n \lambda_n^{-1/2} = \det\left(-\partial_\tau^2 + V''(x_{cl})\right)^{-1/2}. \tag{2.37}$$

It is important to note that (2.36-2.37) are only valid when all eigenvalues are positive and non-zero, which is not generally true. This subtlety will be addressed in Section 2.5.1.

2.4 The simple harmonic oscillator

To fix the factor N, one can examine the example of a one-dimensional harmonic oscillator-like potential. Actually, the exact form is not important, but the potential should have a single *harmonic minimum*. This means that the potential (Fig. 2.1a) encountered by a particle can be described by

$$V(x) = \frac{1}{2}\omega^2 x^2 + \mathcal{O}\left(x^4\right) \tag{2.38}$$

near this minimum.

In the imaginary-time description, the particle moves in the inverted potential $-V(x)$

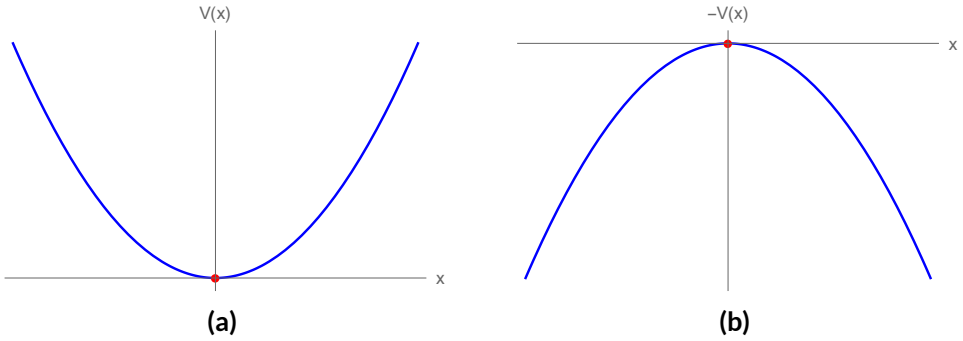

Figure 2.1: Harmonic oscillator potential *(a)* and inverted potential *(b)*.

(Fig. 2.1b). If one fixes the boundaries of its trajectory by $x_i = 0 = x_f$, the figure shows that the only conceivable path obeying the classical equation of motion (2.29) is a constant one: $x_{cl}(\tau) = 0$. The action for this trivial path is zero, since the potential was chosen to vanish at the minimum:

$$S_{cl} = \int_{-T/2}^{T/2} \mathrm{d}\tau \left[\frac{1}{2} \left(\frac{\mathrm{d}x_{cl}}{\mathrm{d}\tau} \right)^2 + V(x_{cl}(\tau)) \right] = 0. \tag{2.39}$$

To calculate the amplitude of this process, one has to solve the eigenvalue problem for the operator $-\partial_\tau^2 + \omega^2$:

$$\left[-\partial_\tau^2 + \omega^2 \right] x_n(\tau) = \lambda_n x_n(\tau). \tag{2.40}$$

The eigenfunctions are sinusoids [20]. With the boundary requirements that $x_n(\pm T/2) = 0$, the solution can be specified for integer n alternately with cosines and sines, as

$$x_0(\tau) = \cos\left(\frac{\pi\tau}{T}\right),\ x_1(\tau) = \sin\left(\frac{2\pi\tau}{T}\right),\ \ldots \text{ and } \lambda_n = \omega^2 + \frac{\pi^2 n^2}{T^2}. \tag{2.41}$$

In the limit of small $\hbar$, one can then use (2.36) to write the amplitude:

$$\langle 0|\mathrm{e}^{-HT/\hbar}|0\rangle \simeq N\prod_{n=1}^{\infty}\left(\omega^2+\frac{\pi^2n^2}{T^2}\right)^{-\frac{1}{2}} \tag{2.42}$$

$$= \left[N\prod_{n=1}^{\infty}\left(\frac{\pi^2n^2}{T^2}\right)^{-\frac{1}{2}}\right]\left[\prod_{n=1}^{\infty}\left(1+\frac{\omega^2T^2}{\pi^2n^2}\right)\right]^{-\frac{1}{2}}. \tag{2.43}$$

The second factor in brackets yields $\sinh(\omega T)/\omega T$, using the infinite product representation [20]

$$\sinh(z) = z\prod_{n=1}^{\infty}\left(1+\frac{z^2}{\pi^2n^2}\right). \tag{2.44}$$

If there would be no potential, then $\omega = 0$ and the first brackets contain the corresponding free-particle amplitude. Hence, an equivalent result can be obtained from the left-hand expression by writing $H_0 = \hat{p}^2/2$ for the free Hamiltonian and inserting the resolution of unity with momentum eigenstates.

$$N\prod_{n=1}^{\infty}\left(\frac{\pi^2n^2}{T^2}\right)^{-\frac{1}{2}} \simeq \langle 0|\mathrm{e}^{-\frac{1}{2\hbar}\hat{p}^2T}|0\rangle \tag{2.45}$$

$$= \int_{-\infty}^{+\infty}\mathrm{d}p\,\mathrm{e}^{-\frac{1}{2\hbar}p^2T}|\,\langle x=0|p\rangle\,|^2 = \frac{1}{\sqrt{2\pi\hbar T}} \tag{2.46}$$

In the last line, substituting the bracket $\langle x|p\rangle = \mathrm{e}^{ipx/\hbar}/\sqrt{2\pi\hbar}$ led to a Gaussian integral. In a sense, (2.46) fixes the formal normalisation constant N, which should be infinite to compensate for the infinite product yielding $1/\infty$.

With these results, the amplitude is readily rewritten as [20]

$$\langle 0|\mathrm{e}^{-HT/\hbar}|0\rangle \simeq \left(\frac{\omega}{\pi\hbar}\right)^{\frac{1}{2}}(2\sinh(\omega T))^{-\frac{1}{2}} = \left(\frac{\omega}{\pi\hbar}\right)^{\frac{1}{2}}\mathrm{e}^{-\frac{\omega T}{2}}\left(1-\mathrm{e}^{-2\omega T}\right)^{-\frac{1}{2}}. \tag{2.47}$$

The limit of large imaginary time T projects out the lower energy states, which can be read off by comparison to (2.18). Indeed, in this limit the Taylor expansion of the right-hand factor yields

$$\langle 0|\mathrm{e}^{-HT/\hbar}|0\rangle \overset{T\to\infty}{\longrightarrow} \left(\frac{\omega}{\pi\hbar}\right)^{\frac{1}{2}}\left(\mathrm{e}^{-\frac{1}{2}\omega T}+\frac{1}{2}\mathrm{e}^{-\frac{5}{2}\omega T}+\ldots\right), \tag{2.48}$$

so that the first energy eigenvalues are $E_0 = \hbar\omega/2$ and $E_2 = 5E_0$, exactly as expected for the harmonic oscillator: in general, $E_n = (n + 1/2)\hbar\omega$. The probability to find the particle in the associated energy eigenstates at $x = 0$ is given by $|\psi_0(0)|^2 = \sqrt{\omega/\pi\hbar}$ and $|\psi_2(0)|^2 = \sqrt{\omega/4\pi\hbar}$. There is no contribution to the amplitude from eigenstates with odd n, since these have vanishing $\psi_n(0)$ – the Hermite polynomials are alternately even and odd.

2.5 Instantons in the double-well potential

A double-well potential for a spinless, unit-mass particle can generally be described by

$$V(x) = \lambda(x^2 - \eta^2)^2, \tag{2.49}$$

where $\lambda > 0$ and the axes have been chosen so that the potential is an even function with minimum value zero (Fig. 2.2a). In close analogy to the previous subsection, one can define the curvature at the minima by $\omega^2 = V''(\pm\eta) = 8\lambda\eta^2$. The potential reduces to a single well when η is set to zero.

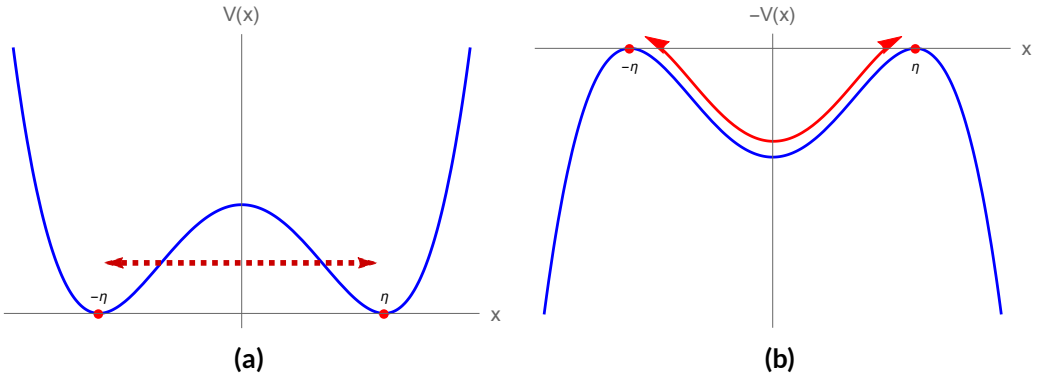

Figure 2.2: Double-well potential *(a)* and inverted potential *(b)*.

Superficially, the double well looks like two harmonic oscillators glued together. In a picture where the wall between the wells would be infinite, the energy eigenstates would indeed be doubly degenerate: particles could stay in either potential well, but never cross the barrier. The expected particle position in the two distinct ground states would be either η or $-\eta$, and these states would spontaneously break the reflection

symmetry of the system under the transformation $x \to -x$. However, quantum mechanics renders this picture incorrect when the wall height, $V(0) = \omega^4/64\lambda$, is finite. In that case, particles are able to tunnel through the wall, even in the lowest-energy state. The corresponding ground state wave function is not localised in any minimum; instead, it is a symmetric superposition of the two localised states describing the true vacuum [20]. Tunnelling lifts the degeneracy of the energy states. The first two, symmetric and anti-symmetric combinations of wavefunctions localised at the two vacua, are split by an exponentially small energy proportional to $\exp\left(-\omega^3/12\lambda\hbar\right)$. This fact cannot be described by perturbation theory, which yields the wrong double-oscillator picture, essentially because the series expansion of the exponential factor around $\lambda = 0$ gives zero.

The energy splitting can be obtained by the WKB method or through calculations with instantons [20]. The latter is less familiar from textbooks and clarifies how this non-perturbative effect arises from tunnelling paths. Here lies the connection with the idea of new trajectories emerging as classical solutions by switching to the Euclidean formalism. The pivotal point is the associated inversion of the potential, from (2.15). For the double-well potential, this means there are possibilities other than a trivial constant path at a potential minimum, which was the only stable possibility for the single well. The fact that there are two degenerate minima now enables a tunnelling trajectory connecting them. In real time, there is no classically allowed path connecting $x = -\eta$ and $x = \eta$, but in imaginary time, there is: due to the inversion of the potential, a classical trajectory connects the top of one hump to the other top (Fig. 2.2b). Another way to look at it: in tunnelling regions, the kinetic energy $E - V$ is formally negative, which corresponds to imaginary-time evolution in Euclidean spacetime [43].

As in the previous section, a solution is sought for the classical equation of motion (2.29). However, not a constant path on top of one of the hills, which has zero action, but a topologically non-trivial one. More specifically, one requires a solution satisfying boundary conditions like $x(\pm T/2) = \pm\eta$ (or $\mp\eta$, the other way round) and having a finite action in the limit where T becomes infinite. This limit yields the lowest-energy path, which is of special interest in the semi-classical path integral approximation, as opposed to paths with finite T or with infinite action and often $x(\tau \to \infty) \to \pm\infty$ [20].

Knowing that the particle starts at rest at $\tau = -\infty$ and with zero potential, conservation of energy (2.30) implies that the whole trajectory has vanishing energy. Thus,

this classical solution of the equation of motion must satisfy $\dot{x} = \pm\sqrt{2V(x)}$. Hence, together with the boundary conditions, the potential implicitly defines the path through

$$\tau = \tau_c \pm \int_0^{x_{cl}} \mathrm{d}x \, (2V(x))^{-1/2}, \tag{2.50}$$

where τ_c is the integration constant corresponding to the time when the particle reaches the half-way mark $x = 0$ between the potential hills. A more explicit result is obtained by substituting $V(x)$ and integrating:

$$\dot{x}_{cl}(\tau) = \pm\sqrt{2\lambda}(\eta^2 - x_{cl}^2) \implies x_{cl}(\tau) = \pm\eta \tanh\left(\frac{\omega(\tau - \tau_c)}{2}\right). \tag{2.51}$$

Taking the positive and negative square root leads to two solutions. The hyperbolic tangent path interpolates between the vacua and the trajectory $x_{cl}(\tau)$ with the $+$ sign is called an *instanton*, centred at time τ_c, the other one is the related *anti-instanton* [20, 42–44]. The former is the kink solution (Fig. 2.3a) where the particle tunnels from $x = -\eta$ to $x = \eta$, whereas the latter goes in the opposite direction (Fig. 2.3b). The top of the potential is only reached in the limit where $T \to \infty$.

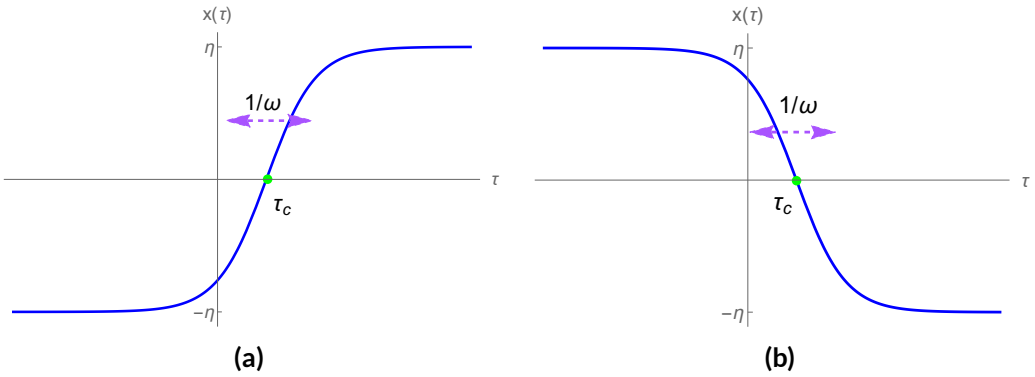

Figure 2.3: Instanton *(a)* and anti-instanton *(b)* solutions for the double-well potential, centred at time τ_c.

The action for the instanton solution ($\mathcal{I}$) is calculated using (2.14) and the fact that

$E = 0$ implies $\dot{x}^2 = 2V(x)$:

$$S_I = \int_{-\infty}^{+\infty} \mathrm{d}\tau\, \dot{x}_{cl}^2 = \int_{-\eta}^{+\eta} \mathrm{d}x\, \dot{x}_{cl} = \int_{-\eta}^{+\eta} \mathrm{d}x\, \sqrt{2V(x)} \tag{2.52}$$

$$= \sqrt{2\lambda} \int_{-\eta}^{+\eta} \mathrm{d}x\, (\eta^2 - x^2) = \frac{\omega^3}{12\lambda}. \tag{2.53}$$

The anti-instanton solution ($\overline{\mathcal{I}}$) has the same action, $S_{\bar{I}} = S_I$, thanks to the symmetry of the potential.

2.5.1 One-instanton effects in the double well

At late imaginary times $\tau \to \infty$, a particle moving according to the instanton solution will reach the top of the potential hill at $x = \eta$. Expanding the double-well potential in that area, the leading-order approximation is a harmonic oscillator and the equation of motion (2.51) becomes

$$\dot{x}_{cl}(\tau) \simeq -2\eta\sqrt{2\lambda}(x_{cl} - \eta) = -\omega(x_{cl} - \eta). \tag{2.54}$$

Hence, $|x - \eta| \propto \mathrm{e}^{-\omega\tau}$ in the limit of large τ: the particle comes exponentially closer to the top, only really reaching it as time tends to infinity. This implies instantons are confined in time, meaning that most of the jump between the vacua essentially takes place in a short time of the order of $1/\omega$. This limited characteristic width explains why such topological configurations are called instantons.

As mentioned in the introduction, $\exp(-S_I/\hbar)$ will be the leading, exponentially small factor in the splitting between the lowest energy levels, but the pre-exponential factor still requires some work. After all, the determinant in the one-instanton amplitude for the tunnelling process (2.36) now depends on a non-constant $V''(x_{cl})$, unlike the simple potential well:

$$\langle \eta | \mathrm{e}^{-HT/\hbar} | -\eta \rangle_{1\text{ inst}} = N \mathrm{e}^{-S_I/\hbar} \det\left(-\partial_\tau^2 + V''(x_{cl})\right)^{-1/2} [1 + \mathcal{O}(\hbar)]. \tag{2.55}$$

Nevertheless, most of the time the particle can be found near one of the potential wells, locally described as harmonic oscillator potentials. Therefore, the resulting determinant should be very similar, so the corrections can be encapsulated in a multiplicative

factor K [20]:

$$N \det\left(-\partial_\tau^2 + V''(x)\right)^{-\frac{1}{2}} = KN \det\left(-\partial_\tau^2 + \omega^2\right)^{-\frac{1}{2}} \overset{T\to\infty}{\longrightarrow} K \left(\frac{\omega}{\pi\hbar}\right)^{\frac{1}{2}} \mathrm{e}^{-\frac{\omega T}{2}}, \tag{2.56}$$

where (2.47) was used.

Describing the factor K requires a closer look at the operator $-\partial_\tau^2 + V''(x)$ entering the eigenvalue equation (2.33). By taking the time derivative of the equation of motion (2.29), one finds an eigenfunction of this operator with eigenvalue zero[6]:

$$x_0(\tau) = \frac{1}{\sqrt{S_I}} \dot{x}_{cl}(\tau). \tag{2.57}$$

At first sight, this zero mode is problematic: the integral over the expansion coefficient c_0 in (2.35) is no longer Gaussian and would make the amplitude diverge! Fortunately, the solution is near.

Unlike the constant solutions for the equation of motion, instanton solutions depend on the instanton centre τ_c and hence lack invariance under time translations. Integrating over this time parameter is required to account for all instanton contributions to the path integral. Since varying τ_c shifts the whole instanton trajectory in time, it is called a *collective coordinate* [44]. Fluctuations changing the τ_c value are not Gaussian, even large shifts are important and should not be damped. As this coincidence with the non-Gaussianity from the zero mode suggests, a translation of the instanton location $\mathrm{d}\tau_c$ can directly be related to a deviation of the expansion coefficient $\mathrm{d}c_0$. This is done by equating the effect of these changes on the instanton path $x_{cl}(\tau)$:

$$\mathrm{d}x_{cl} = \dot{x}_{cl}\mathrm{d}\tau_c \text{ and } \mathrm{d}x_{cl} = x_0 \mathrm{d}c_0 = \frac{1}{\sqrt{S_I}} \dot{x}_{cl} \mathrm{d}c_0 \quad \Longrightarrow \quad \frac{\mathrm{d}c_0}{\sqrt{2\pi\hbar}} = \sqrt{\frac{S_I}{2\pi\hbar}} \mathrm{d}\tau_c. \tag{2.58}$$

Therefore, looking at 2.56, K can be written as the ratio of two determinants, with a small twist. The zero eigenvalue should be omitted (indicated by a prime) and replaced by the pre-factor in 2.58, as the integral over τ_c replaces the one over c_0, yielding

$$K = \sqrt{\frac{S_I}{2\pi\hbar}} \left[\frac{\det\left(-\partial_\tau^2 + V''(x)\right)}{\det(-\partial_\tau^2 + \omega^2)}\right]^{-1/2} \tag{2.59}$$

[6]The normalisation factor $S_I^{-1/2}$ is necessary to comply with (2.25).

Calculating the ratio of determinants explicitly is non-trivial and in practice proceeds using the Van Vleck-Pauli-Morette formula or the Gelfand-Yaglom formula [46]. Both tricks simplify the problem of multiplying all operator eigenvalues in a remarkable way: the former method only requires the action, the latter amounts to solving a differential equation.

2.5.2 The dilute-gas approximation

Due to the transient nature of the instanton transition, it is easy to imagine attaching an anti-instanton after it, so that the particle returns to the vacuum where it started. This would also solve the equations of motion, approximately[7], just like any chain of well-separated alternating instantons and anti-instantons (Fig. 2.4) would, leading to trajectories oscillating between the minima.

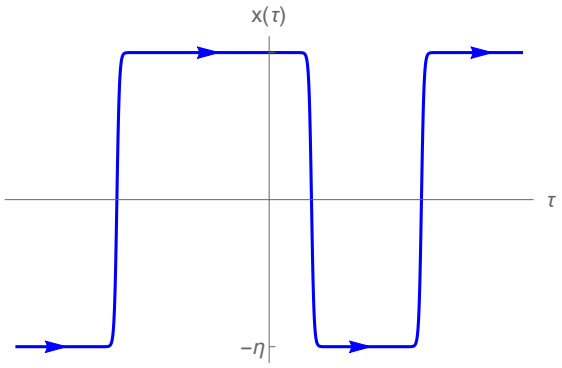

Figure 2.4: String of alternating instanton and anti-instanton trajectories between the double-well minima, with large separation in time.

Considering these path integral contributions with multiple separated instantons, say n, is called the *dilute-gas approximation* [20, 42–44]. Of course, one has to integrate over all n (anti-)instanton centre locations τ_i, while keeping the right ordering, here

[7] This subtle point is emphasised by Coleman [20]: paths containing a string of instantons and anti-instantons are just approximate stationary points of the action. They only become true stationary points in the limit of infinite distance between neighbouring (anti-)instantons, when the exponentially small overlap between the patched trajectories (and hence any instanton interaction) vanishes and the total action is really the sum of each individual (anti-)instanton action.

taken to be $\tau_{i+1} > \tau_i$. This amounts to an integral familiar from computations in quantum field theory [20, 42–44]:

$$\int_{-T/2}^{+T/2} \mathrm{d}\tau_1 \int_{-T/2}^{\tau_1} \mathrm{d}\tau_2 \ldots \int_{-T/2}^{\tau_{n-1}} \mathrm{d}\tau_n = \frac{1}{n!} \int_{-T/2}^{+T/2} \mathrm{d}\tau_1 \ldots \int_{-T/2}^{+T/2} \mathrm{d}\tau_n = \frac{T^n}{n!}. \tag{2.60}$$

If the time evolution throughout the tunnelling process in Fig. 2.4 is seen as a sequence of regular evolution periods[8] in a single-well potential with constant $V''(x) = \omega^2$, interspersed by short instanton flashes, the amplitude can be written as

$$\begin{aligned}\langle \eta | \mathrm{e}^{-H(\eta)\Delta\tau_{n+1}/\hbar} | \eta \rangle \, \langle \eta | \mathcal{I}(\tau_n) | -\eta \rangle \, \langle -\eta | \mathrm{e}^{-H(-\eta)\Delta\tau_n/\hbar} | -\eta \rangle \, \langle -\eta | \overline{\mathcal{I}}(\tau_{n-1}) | \eta \rangle \\ \ldots \langle \eta | \mathrm{e}^{-H(\eta)\Delta\tau_2/\hbar} | \eta \rangle \, \langle \eta | \mathcal{I}(\tau_1) | -\eta \rangle \, \langle -\eta | \mathrm{e}^{-H(-\eta)\Delta\tau_1/\hbar} | -\eta \rangle \,.\end{aligned} \tag{2.61}$$

The instanton corrections to single-well behaviour, indicated by $\mathcal{I}(\tau_i)$, are precisely the effects captured in the factor K introduced in (2.56). It follows, then, that the tunnelling amplitude with n individual instanton objects (and hence action nS_I) contains a factor K^n [20]. Summing over all odd numbers n, necessary for tunnelling from one minimum to the other, yields

$$\langle \eta | \mathrm{e}^{-HT/\hbar} | -\eta \rangle \overset{T\to\infty}{\longrightarrow} \left(\frac{\omega}{\pi\hbar}\right)^{\frac{1}{2}} \mathrm{e}^{-\frac{\omega T}{2}} \sum_{n \text{ odd}} \frac{(\mathrm{e}^{-S_I/\hbar} K T)^n}{n!} \left[1 + \mathcal{O}(\hbar)\right]. \tag{2.62}$$

Clearly, the same expression holds for the inverted process, from η to $-\eta$, and the sum over even n yields the amplitude for a particle staying at its original position. To summarise,

$$\langle \pm\eta | \mathrm{e}^{-HT/\hbar} | -\eta \rangle \overset{T\to\infty}{\longrightarrow} \frac{1}{2} \left(\frac{\omega}{\pi\hbar}\right)^{\frac{1}{2}} \mathrm{e}^{-\frac{\omega T}{2}} \left[\mathrm{e}^{\mathrm{e}^{-S_I/\hbar} KT} \mp \mathrm{e}^{-\mathrm{e}^{-S_I/\hbar} KT}\right] \left[1 + \mathcal{O}(\hbar)\right]. \tag{2.63}$$

Looking back to (2.18), this large-T limit immediately allows identifying the lowest energy eigenstates as a spatially symmetric and anti-symmetric linear combinations [20, 44], respectively

$$|+\rangle \propto |\eta\rangle + |-\eta\rangle \quad \text{and} \quad |-\rangle \propto |\eta\rangle - |-\eta\rangle \,, \tag{2.64}$$

[8] These intervals are denoted by $\Delta\tau_i = \tau_i - \tau_{i-1}$, with $\tau_{n+1} = T/2$ and $\tau_0 = -T/2$.

with corresponding energies[9]

$$E_{\pm} \simeq \frac{1}{2}\hbar\omega \mp \hbar K \mathrm{e}^{-S_I/\hbar}. \tag{2.65}$$

The conclusion is simple: tunnelling breaks the degeneracy of the perturbative ground state, splitting it into an even ground state and an odd first excited state with an exponentially small, non-perturbative energy difference.

On a final note, the dilute instanton gas approximation should still be verified. This is achieved by showing that the dominant contribution to the energy splitting comes from temporal sections with low instanton density. After all, as n is increased, the 'instanton gas' in the interval T becomes less and less dilute. However, using Stirling's formula ($n! \propto n^n$ for large n) ensures that the exponential terms $x^n/n!$ entering (2.62) only keep growing until $x \sim \mathcal{O}(n)$. The suppression of large-n terms implies that the dominant terms have [20]

$$n \lesssim \mathrm{e}^{-S_I/\hbar} KT. \tag{2.66}$$

In other words, this indeed confirms that the important contributions have an instanton density n/T that is exponentially small in the limit of small $\hbar$ and large T, or equivalently, a very large instanton separation.

2.6 Instantons in the periodic cosine potential

The principal reason for studying what instanton methods can teach about tunnelling phenomena is their application in gauge theories. Extending the double well to a periodic potential with an infinitely degenerate set of minima pushes the QCD analogy further, offering insights about tunnelling with less restrictions. For the difference with the double-well potential, is that the periodic cosine-well potential (Fig. 2.5a) does not require instantons and anti-instantons to alternate. Instead, a succession of multiple (anti-)instantons may occur in the sequence, enabling barrier penetration from the bottom of one well to any other well. The well-known consequence of such tunnelling is that the otherwise infinitely degenerate energy levels get smeared out into continuous bands. The energy eigenstates, called Bloch waves, are no longer labelled by a discrete

[9] Since the non-perturbative splitting is exponentially small in comparison with corrections of order $\mathcal{O}\left(\hbar^2\right)$, it should really only be kept as the leading term of the difference $E_+ - E_-$.

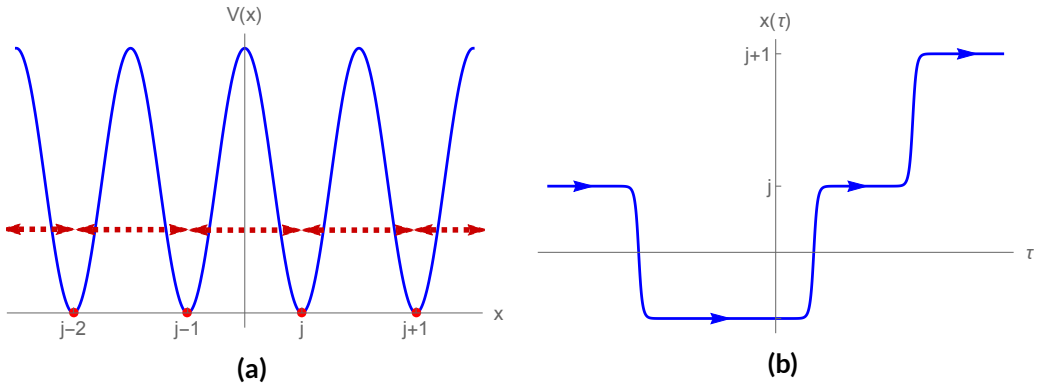

Figure 2.5: Cosine potential *(a)*, shifted to have its minimum at zero, and string of instantons and anti-instantons *(b)* representing tunnelling between vacua.

number, but by a continuous Bloch angle θ [20, 44]. This Section discusses how this picture arises when using instanton methods.

The (anti-)instantons connect adjacent wells j and $j+1$ ($j-1$), where the well indices are integers, and the next (anti-)instanton should pick up where the preceding one ended. The other constraint for tunnelling from minimum j_i to j_f is that the difference $n-\bar{n}$ between the number of instantons (n) and anti-instantons $\bar{n}$ clearly should equal the distance $\Delta j = j_f - j_i$. The summation over all allowed configurations yields the transition amplitude [20]

$$\left\langle j_f \middle| \mathrm{e}^{-HT/\hbar} \middle| j_i \right\rangle \overset{T\to\infty}{\longrightarrow} \left(\frac{\omega}{\pi\hbar}\right)^{\frac{1}{2}} \mathrm{e}^{-\frac{\omega T}{2}} \sum_{n,\bar{n}=0}^{\infty} \frac{1}{n!\,\bar{n}!} \delta_{(n-\bar{n})-\Delta j} (\mathrm{e}^{-S_I/\hbar} KT)^{n+\bar{n}} [1+\mathcal{O}(\hbar)]. \quad (2.67)$$

Combinatorics explains the origin of the factorials $n!\bar{n}!$ in the denominator, where one might expect $(n+\bar{n})!$ instead. After all, denoting the total number of instanton objects by $N = n+\bar{n}$, a factor $T^N/N!$ indeed emerges from the integration over all N zero modes. However, to account for all relevant configurations, this should still be multiplied by the number of possible reorderings of instantons and anti-instantons. Since there are $N!/n!\,\bar{n}!$ options to pick n places for the instantons among N positions, $T^N/n!\,\bar{n}!$ is the correct final factor.

Proceeding from (2.67), the Bloch angle enters when expanding into Fourier modes via

$$\delta_{ab} = \frac{1}{2\pi} \int_{-\infty}^{+\infty} \mathrm{d}\theta\, \mathrm{e}^{i\theta(a-b)}, \quad (2.68)$$

so the double sum can be rewritten as two exponentials with an emerging cosine:

$$\begin{aligned}\left\langle j_f\right|\mathrm{e}^{-HT/\hbar}\left|j_i\right\rangle &\simeq \left(\frac{\omega}{\pi\hbar}\right)^{\frac{1}{2}}\mathrm{e}^{-\frac{\omega T}{2}}\int_{-\infty}^{+\infty}\frac{\mathrm{d}\theta}{2\pi}\,\mathrm{e}^{-i\theta\Delta j}\sum_{n,\,\bar{n}=0}^{\infty}\frac{(\mathrm{e}^{i\theta-S_I/\hbar}KT)^n}{n!}\frac{(\mathrm{e}^{-i\theta-S_I/\hbar}KT)^{\bar{n}}}{\bar{n}!}\\ &= \left(\frac{\omega}{\pi\hbar}\right)^{\frac{1}{2}}\mathrm{e}^{-\frac{\omega T}{2}}\int_{-\infty}^{+\infty}\frac{\mathrm{d}\theta}{2\pi}\,\mathrm{e}^{-i\theta\Delta j}\exp\left(2\cos(\theta)\mathrm{e}^{-S_I/\hbar}KT\right). \qquad (2.69)\end{aligned}$$

This expression, valid in the limit where $T \to \infty$, allows reading off the θ-dependent ground-state energy as

$$E_0(\theta) \simeq \frac{1}{2}\hbar\omega + 2\hbar K\cos(\theta)\mathrm{e}^{-S_I/\hbar} \qquad (2.70)$$

by comparing it to (2.18). One can even immediately deduce the expression for the corresponding Bloch waves $|\theta\rangle$ in terms of position eigenstates $|j\rangle$, by fixing $j_i = j_f = j$ to determine $\langle\theta|j\rangle$:

$$|\theta\rangle = \frac{1}{\sqrt{2\pi}}\left(\frac{\omega}{\pi\hbar}\right)^{\frac{1}{4}}\sum_{j=-\infty}^{+\infty}\mathrm{e}^{ij\theta}\,|j\rangle\,. \qquad (2.71)$$

The instanton action for the cosine potential $V(x) = \cos(x)$ can be computed explicitly. Since the instanton trajectory connects minima like $x = -\pi$ and $x = +\pi$, the action is

$$S_I^{(c)} = \sqrt{2}\int_{-\pi}^{+\pi}\mathrm{d}x\,\sqrt{\cos(x)+1} = 8. \qquad (2.72)$$

The potential was shifted to $V(x) - V_{\min}$, to comply with the energy convention in this chapter: the total energy E is zero on the (classically allowed) instanton path in Euclidean space. Of course, this shift does not affect any underlying physics.

2.7 Remarks

The main purpose of this Chapter was the introduction of instantons in quantum mechanics and highlighting their use and close connection to tunnelling in two physical examples. Both the double-well and the periodic cosine potential have degenerate minima, and due to barrier penetration, non-perturbative corrections to classically expected behaviour arise. These have non-negligible, physical consequences, like the ground-state energy splitting for the double well and the energy band structure for the cosine

potential. In both cases, the leading energy correction is proportional to $e^{-S_I/\hbar}$, where S_I is the instanton action. In fact, this factor is not a surprise when thinking of the textbook formula for the WKB tunnelling amplitude between two classical turning points a and b [20]:

$$|T(E)| = \exp\left(-\frac{1}{\hbar}\int_a^b \mathrm{d}x\sqrt{2(V(x)-E)}\right)\left[1+\mathcal{O}\left(\hbar\right)\right]. \tag{2.73}$$

The integral over the barrier region gives exactly the instanton action, as in (2.52), where the potential was adjusted so $E = 0$ along the tunnelling trajectory.

This is, of course, just where the story begins. For instance, associated to instanton trajectories in the Euclidean-time framework, one can find 'bounces', trajectories starting on an inverted-potential hill and returning there after reaching a classical turning point [20, 43]. These can be used to describe tunnelling between non-degenerate vacua, enabling the calculation of the decay width for a metastable state. Furthermore, a lot is to be said about instanton methods in field theory – the principal motivation to study this framework, as explained in the Introduction. Several aspects of the discussed examples can be generalised to the context of field theory, especially when it comes to the vacuum structure. Instantons can significantly alter the naive picture of an infinitely degenerate ground state, very similar to situation of the cosine well. In Yang-Mills theories, the degenerate vacua are an infinite set of topologically inequivalent classes of gauge field configurations, and instanton field configurations interpolate between these [20, 42, 44].

Clearly, the perspective of gauge theory introduces several technicalities related to the infinite degrees of freedom of fields. Yet several insights can already be deduced from the quantum mechanical problem with infinitely degenerate vacua, and therefore another issue stands at the centre of the following chapters. As this introductory discussion has shown, perturbation theory around one of the minima has no chance to describe the relevant quantum mechanics completely on its own; it still has to be complemented by a boundary condition that will capture the non-perturbative effects. Chapters 3 and 4, then, focus on an interesting question at hand: how far can perturbative physics actually lead one? After an introduction to the mathematical point of view, the perturbative analysis of the cosine well (or rather, the equivalent sine-Gordon potential) is discussed in detail.

3

Can perturbation theory make sense?

3.1 Introduction

The problems with perturbation theory, and more generally divergent series, have plagued physicists for a long time, not too mention mathematicians. Luckily, big leaps have been made ever since Bayes, of statistics fame, branded Stirling's series for $\ln(n!)$ and the methods for its derivation completely untrustworthy due to its lack of convergence [48]. In stark contrast, any statistical mechanics student will assert Stirling's formula is quite useful. And what about perturbative expansions in QED, which Dyson revealed to be problematic, even in principle [18]? Again, their practical adequacy is beyond any doubt: the way theoretical computations of the electron's anomalous magnetic moment [6] agree with experimental results is spectacular. The pivotal point is that these examples rely on *asymptotic expansions*. Leading to accurate results in a certain limit of the involved parameters, these have become a well-appreciated tool in various branches of physics, despite their frequent divergence. Asymptotic expressions abound in quantum mechanics as well, and it is of special interest here to analyse the (divergent) perturbation series for energy eigenvalues obtained from the Schrödinger equation.

In order to make sense of perturbation theory, it pays off to review a couple of mathematical ideas, first of all making the notion of asymptotics more precise. Secondly, an attempt will be made to understand factorially divergent series through the technique of Borel resummation. However, some series are not Borel summable, and indeed, these occur in physical settings described in Chapter 2: non-perturbative effects are important for the double well and cosine well. Nevertheless, it is illuminating to see the exact point where the difficulties arise. The purpose of the next sections is to discuss the mathematical point of view; detailed results of calculations for the sine-Gordon potential follow in Chapter 4.

3.2 Asymptotic analysis

The mathematical evolutions in the field of asymptotics have not gone by without controversy and colourful opinions. Whereas Abel deemed divergent series "the invention of the devil" and refused to use them as base for anything, in Euler's point of view such series could still be meaningful when subjected to the right resummation procedure, following a careful study of the divergent behaviour [48]. This is the approach pursued until today, in order to answer the question at hand: can the exact result be reconstructed from the information encoded in a divergent perturbative expansion? On physical grounds, for instance, the energy eigenvalue E in the Schrödinger equation should be finite for a bounded potential. Yet often, its expansion in a dimensionless[1] coupling constant g,

$$\sum_{n=0}^{\infty} E_n g^n, \tag{3.1}$$

does not converge around $g = 0$. Instead, checking the large-order behaviour of the coefficients typically shows factorial divergence, $E_n \sim n!$. Clearly, the perturbation series contains some information about the exact result E, but does it contain all information?

A first important realisation is that many series like this are asymptotic expansions, valid in a certain limit of the perturbation parameter. In the considered case, that limit

[1] As is often the case, E is considered to represent a dimensionless energy. For example, starting from the Schrödinger equation $\left[-\frac{\hbar^2}{2m}\partial_x^2 + W(x)\right]\psi(x) = u\psi(x)$, one switches to a dimensionless coordinate $z = \frac{x}{\lambda_0}$ and dimensionless potential function $V(x) = \frac{W(x)}{\epsilon_0}$, and takes $g = \frac{\hbar}{\sqrt{m\epsilon_0}\lambda_0}$, $E = \frac{u}{\epsilon_0}$, where ϵ_0 and λ_0 are arbitrary energy and length scales, respectively.

is the semi-classical one, $g \to 0$, that is used to make the expansion ansatz and obtain the coefficients E_n. To clarify the notion of an asymptotic relation, Poincaré introduced the following definition, considering a sector D in the complex plane[2] restricted by $|\arg(z)| \leq \alpha$ and $|z| \leq R$. The series $\sum_n f_n z^n$ is called *asymptotic* to a function $f(z)$ on domain D if the error from truncation after any N-th term vanishes like $C_{N+1}z^{N+1}$ in the limit $z \to 0$, i. e. quicker than the last kept term [49, 50]. This means there is a neighbourhood of the origin where

$$\forall N \in \mathbb{N},\ \exists C_{N+1} \in \mathbb{R}^+ : \left| f(z) - \sum_{n=0}^{N} f_n z^n \right| \leq C_{N+1}|z|^{N+1} \quad (z \to 0). \tag{3.2}$$

The change of perspective becomes clear by comparing with the definition of a convergent series: asymptotic approximations to a function are required to become better as z tends to a specific value, for any fixed N, whereas convergence requires improvement as N tends to infinity, for a fixed z-value. Convergence is an absolute characteristic, as it can be determined from the series coefficients f_n alone, but asymptoticity is relative and depends on both the coefficients and the approximated function $f(z)$.

3.2.1 Superasymptotics

Poincaré's definition does not exclude convergent series[3]. However, it neglects typical features that are nowadays associated to asymptotic expansions and may provide a handle on the frequent divergence. First of all, an exact result represented by a divergent asymptotic series cannot be found by keeping on adding terms, it can only be estimated by partial sums and taking $|z|$ sufficiently small to obtain the desired precision. The best way to do this, as Stokes found, is not by taking a fixed number of terms N, but by truncating just before the smallest term of the series, at a z-dependent order $N(z)$. The reason is that the remainder after summing N terms is, in many cases, less than the $N+1$-th term [49]. Hence, partial sums beyond the least term will eventually

[2] The restriction to (complex paths in) a wedge-shaped region of the complex plane avoids problems in defining a complex asymptotic relation as a limit, related to the fact that a complex limit is path-independent. Paths winding around the origin as they approach it may not give unique limits for multi-valued functions with a branch point at $z = 0$ [49].

[3] However, some authors (e. g. [50]) explicitly restrict asymptotic series to divergent series complying with Poincaré's definition.

diverge anyway. To illustrate this *optimal truncation*, one can easily find the order of that least term for the example of perturbation coefficients behaving like $f_n \sim AB^{-n}n!$ for large n. To minimise the error, the series should stop where $|B^{-n}n!\,z^n|$ is at its minimum, for a fixed z-value. With Stirling's approximation ($n! \sim \sqrt{2\pi n}\mathrm{e}^{-n}n^n$), one finds

$$\frac{\mathrm{d}}{\mathrm{d}n}\ln\left|B^{-n}n!\,z^n\right| \sim \ln\left|\frac{z}{B}\right| + \ln(n) \tag{3.3}$$

at large n. Therefore, optimal truncation occurs around $N(z) \simeq |B/z|$. Beyond that, the terms start growing and lead to a divergent tail. Furthermore, the argument shows that less terms should be included for larger value of $|z|$. A quick estimate of the error due to truncation near $N(z)$ shows that it is exponentially small:

$$\epsilon_{N(z)} \approx f_{N(z)}z^{N(z)} \sim \sqrt{\frac{B}{z}}\mathrm{e}^{-|B/z|}. \tag{3.4}$$

One might even remark, in this regard, how useful asymptotic series are: in a sense, they converge excellently up to the point where they start to diverge. In physical examples like asymptotic series in QED[4], there is even no accuracy restriction in practice: $N(\alpha_e) \sim 137$, and loop calculations get very tedious much sooner.

To illustrate the optimal truncation strategy, also referred to as *superasymptotics*, one can consider the specific case of the power series with coefficients $f_n = (-1)^n n!$. It can be shown that it is the asymptotical expansion of a function involving the exponential integral $E_1(z)$, for small $z > 0$ (Sec. 3.3):

$$f(z) = \frac{1}{z}\,\mathrm{e}^{1/z}\,E_1\left(\frac{1}{z}\right) \sim \sum_{n=0}^{\infty}(-1)^n n!\,z^n \quad (z \to 0^+). \tag{3.5}$$

Hence, partial sums of the divergent asymptotic series, truncated after N terms, can be compared to the exact result. Increasing N, the remainder decreases until the optimal truncation order $N(z) \simeq 1/z$ is reached (Fig. 3.1). Beyond that point, the partial sums diverge from the correct function value.

[4]Dyson's argument is discussed in Sec. 4.4.

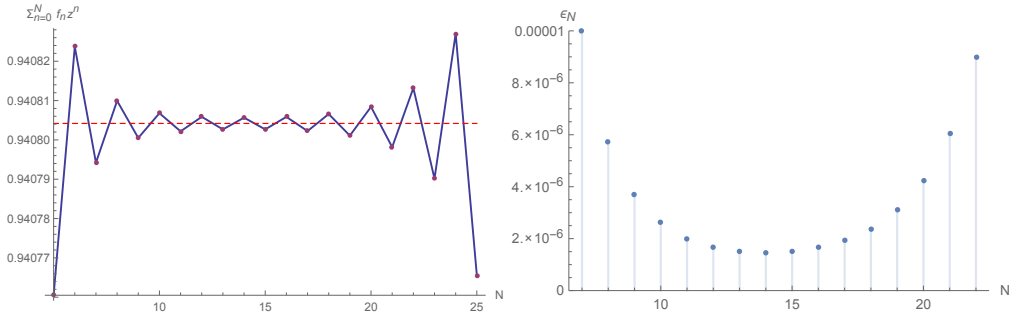

(a) Partial sum for $z = \frac{1}{15}$ as function of N. **(b)** Remainder $\epsilon_N(z = \frac{1}{15})$ for varying N.

Figure 3.1: Partial sums $\sum_{n=0}^{N} f_n z^n$ (**a**) and remainder $\epsilon_N(z) = |f(z) - \sum_{n=0}^{N} f_n z^n|$ (**b**) for a specific z-value. Optimal truncation occurs around $N = 1/z$. Beyond that point, the result starts to diverge, in stark contrast to the behaviour of convergent series.

3.2.2 Stokes phenomenon

Stokes used the superasymptotics approach to study Airy's function $\mathrm{Ai}(z)$, an oscillatory integral [48]. Unlike Poincaré's classical asymptotics, which gave polynomial accuracy, this method leads to exponential accuracy, as noted above. Stokes went even further, also resumming the divergent tails after optimal truncation (*hyperasymptotics*), and this level of numerical approximation led him to a fundamental discovery: across different sectors of the complex plane, the asymptotic behaviour of functions may vary. This *Stokes phenomenon*, the transition between different asymptotic representations of a single function, lies at the core of the modern view on divergent asymptotic expansions. For example, the dominant asymptotic behaviour of the hyperbolic sine $\sinh(z)$ jumps from one exponential ($\mathrm{e}^z/2$) to a different one ($-\mathrm{e}^{-z}/2$) when one leaves the right half-plane $\mathrm{Re}(z) > 0$ and enters the left one $\mathrm{Re}(z) < 0$. The imaginary axis acts as a boundary between these regions and is called a *Stokes line*[5]. Upon crossing this line, the dominant contribution becomes sub-dominant and vice versa, so a different leading behaviour emerges. On the line itself, both contributions are oscillatory and of equal magnitude. An *anti-Stokes line* indicates where the sub-dominant contribution is most unequal to the dominant one, in this case on the real axis, with the contrast between purely real exponentially growing and decaying contributions.

[5]Conventions about the terminology in mathematics and physics do not always agree, so the meaning of Stokes and anti-Stokes lines is often interchanged in literature.

Asymptotic expansions are practical, as they validate the use of a simpler expression in terms of elementary functions to approximate a complicated function (like the exponentials representing the transcendental $\sinh(z)$ function) in a region of the complex plane. The other side of the coin is the Stokes phenomenon. Essentially, it reflects the limited ability of a single exponential to emulate $\sinh(z)$ in this example. Rather than an intrinsic trait of the approximated function, the phenomenon exposes the limitations of the functions employed in the approximation.

3.2.3 Borel resummation

It is important to remark that distinct functions may have the same asymptotic expansion, so the information encoded in the expansion coefficients is insufficient to determine the original function uniquely. As a trivial example, the functions $f(z)$ and $f(z) + \mathrm{e}^{-1/z}$ have the same asymptotic expansion near the origin, since the Taylor series of the sub-dominant exponential addition vanishes around $z = 0$. One might think about multiplying the added exponential by a large number M, but even that will not alter the asymptotic expansion. What it will change, however, is the range where the asymptotic series approximates $f(z) + M\,\mathrm{e}^{-1/z}$ accurately. This illustrates the point that the asymptotic series on its own says nothing about its region of validity, which is instead governed by the behaviour of sub-dominant functions.

On the other hand, a given function has a unique asymptotic expansion in each complex domain. Under what conditions is it possible to reconstruct the original function $f(z)$ from its asymptotics? That is the question answered by *Watson's theorem* [50–53]. It asserts that the function[6] $f(z)$ can be uniquely determined from its asymptotic expansion $\sum_n f_n z^n$ in a complex domain, under certain conditions. Specifically, it is sufficient that

(a) f is analytic in a sector $D : |\arg(z)| < \pi/2 + \epsilon$, $|z| < R$ that exceeds the right half-plane ($\epsilon > 0$, depicted in Fig. 3.2);

(b) f has an asymptotic expansion $\sum_n f_n z^n$ in D, with a factorially bounded error[7] $|f(z) - \sum_{n=0}^{N-1} f_n z^n| \leq C\sigma^n N!\,|z|^N$ for any N and z in D (with constants C and σ).

[6] In physical examples, the studied function will be the energy $E(g)$ as a function of the coupling constant, with an asymptotic expansion $\sum_n E_n g^n$.

[7] This kind of formal power series is also called a series of Gevrey order-1.

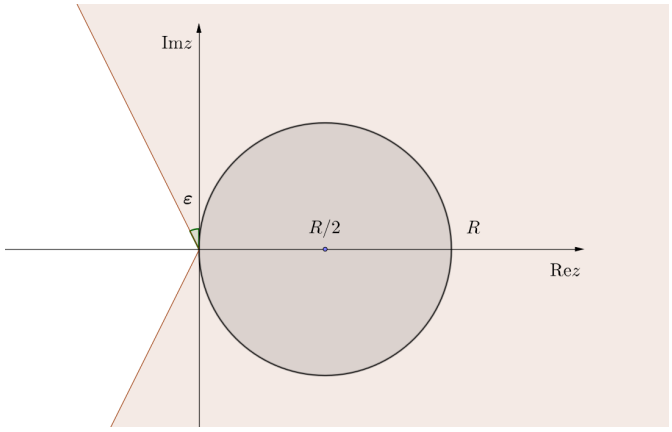

Figure 3.2: Analyticity domain D for Watson's theorem (coloured area) and convergence domain of the Borel sum $\mathcal{S}[f](z)$ (inside the circle).

In that case, the theorem[8] guarantees that the original function can be recovered as the Borel resummation of the asymptotic series, i. e. the series is *Borel summable*. In practice, the conditions ensure the convergence of the series' *Borel transform*

$$\mathcal{B}[f](t) = \sum_{n=0}^{\infty} \frac{f_n}{n!} t^n, \tag{3.6}$$

inside the circle $|t| < 1/\sigma$. This is a consequence of the bound in (b) and typically, the Borel transform encounters singularities on the circle itself [13], as in the next example in Sec. 3.3. However, Watson's theorem guarantees that $\mathcal{B}[f](t)$ has an analytic continuation in a neighbourhood $|\arg(t)| < \epsilon$ of the real axis, so that the *inverse Borel transform* $\mathcal{S}[f](z)$ converges absolutely and returns the exact function as

$$f(z) = \mathcal{S}[f](z) = \int_0^\infty \mathrm{d}t\, \mathrm{e}^{-t}\, \mathcal{B}[f](zt) = \frac{1}{z} \int_0^\infty \mathrm{d}t\, \mathrm{e}^{-t/z}\, \mathcal{B}[f](t) \tag{3.7}$$

for $\mathrm{Re}(1/z) > 1/R$, i. e. inside the circle of radius $R/2$ centred at $z = R/2$. One notices that the inverse Borel transform is essentially a Laplace transform.

[8] Actually, Watson's theorem has been superseded by the Nevanlinna-Sokal theorem [51], which is stronger due to the smaller analyticity domain it requires. It suffices that the function f is analytic inside the circle $\mathrm{Re}(1/z) > 1/R$, rather than in a sector larger than the half-plane (Fig. 3.2).

The Borel transform divides the expansion coefficients f_n by $n!$, in an attempt to tame factorial growth. For instance, for an alternating[9], divergent asymptotic series with coefficients behaving as $f_n = A(-B)^{-n}n!$ (for $B > 0$), the Borel transform becomes

$$\mathcal{B}[f](t) = A \sum_{n=0}^{\infty} \left(-\frac{t}{B}\right)^n = \frac{AB}{t+B}. \tag{3.8}$$

The last equality is not trivial: the Borel series only converges for $|t| < B$, but the rational function is meromorphic on the complex plane, with only one simple pole at $t = -B$. Indeed, the latter function is actually an analytic continuation of the Borel transform, still containing its singularity structure, but well-defined on the whole of a punctured plane. Since no singularities occur on the positive real axis, the inverse Borel transform can be performed to recover the original function $f(z)$ exactly, for a certain range of z-values, so the series is Borel summable. Explicitly, the Borel sum of the divergent series can be expressed in terms of the exponential integral $E_1(z)$, as

$$\mathcal{S}[f](z) = \int_0^{\infty} \mathrm{d}t\, \mathrm{e}^{-t}\, \frac{AB}{B+zt} = \frac{AB}{z}\, \mathrm{e}^{B/z}\, E_1\left(\frac{B}{z}\right). \tag{3.9}$$

This result converges and is hence meaningful for any $z > 0$. In particular, in the case where $A = B = z = 1$, one finds that Borel resummation even gives a precise meaning to the asymptotic series

$$\sum_{n=0}^{\infty} (-1)^n n! = \mathrm{e}\, E_1(1) \approx 0.596. \tag{3.10}$$

A physical example corresponding to this Borel summable case is the quartic anharmonic oscillator, discussed in Sec. 4.4.

How does Borel resummation repair divergent series? Firstly, one notices that by inserting a convergent Borel transform (3.6) in the inverse transformation integral, one formally retrieves the original asymptotic series, using the definition of the gamma

[9] Though often suggested, it is wrong to generalise and assume all alternating series are Borel summable. A counterexample is encountered in [3].

function,

$$n! = \Gamma(n+1) = \int_0^\infty \mathrm{d}t\, t^n\, \mathrm{e}^{-t}. \tag{3.11}$$

This illuminates why Borel resummation is effective if f_n grows factorially, in the following (formal) equality:

$$\int_0^\infty \mathrm{d}t\, \mathrm{e}^{-t} \sum_{n=0}^\infty \frac{f_n}{n!}(tz)^n = \sum_{n=0}^\infty \frac{n!\, f_n}{n!} z^n = \sum_{n=0}^\infty f_n z^n. \tag{3.12}$$

The trick is an interchange of the integral and the sum, where the sum only converges for $|tz| < 1$ for $f_n \sim n!$. Yet, the semi-infinite integral transgresses that range! This is reflected in the divergence of the series on the right-hand side. Hence, the latter should only be understood as an asymptotic expansion of the integral in the limit $z \to 0$.

3.4 Non-Borel summable series

In physics, however, not every asymptotic series should be expected to be Borel summable. A counterexample is straightforward to find: the non-alternating, divergent asymptotic series with coefficients $f_n = AB^{-n}n!$ (for $B > 0$) leads to a Borel transform

$$\mathcal{B}[f](t) = A \sum_{n=0}^\infty \left(\frac{t}{B}\right)^n = \frac{AB}{B-t} \tag{3.13}$$

with a singularity $t = B$ on the positive real axis. This obstruction on the integration path makes the Borel sum (and by extension, perturbation theory) ill-defined. To solve that, one can avoid the pole and take an integration contour tilted away from the real axis, along a ray at an angle θ. This defines the directional Borel resummation

$$\mathcal{S}_\theta[f](z) = \frac{1}{z} \int_0^{\mathrm{e}^{i\theta}\infty} \mathrm{d}t\, \mathrm{e}^{-t/z}\, \mathcal{B}[f](t). \tag{3.14}$$

Taking $\theta = \pm\epsilon$, for a small $\epsilon > 0$, dodges the pole and yields well-defined lateral resummations $\mathcal{S}_{\pm\epsilon}[f](z)$. However, due to the singularity wedged in between the corresponding rays $\mathcal{C}_\pm$ (Fig. 3.3), the result will not be the same! Instead, there will be an imaginary contribution (proportional to the residue) with an ambiguous sign, depending on whether the contour is deformed towards the region above or under the pole.

In a manifestation of the Stokes phenomenon, jumps between the integration contours cross the Stokes direction $\theta = 0$ and lead to a discontinuity.

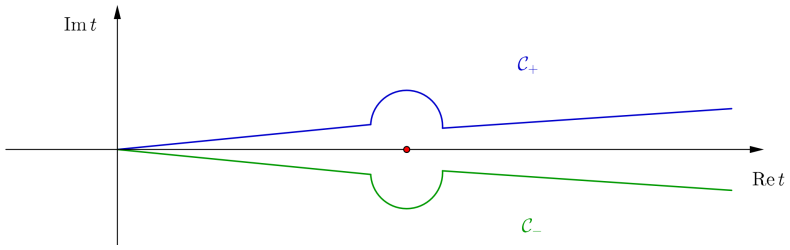

Figure 3.3: Integration contours $\mathcal{C}_+$ and $\mathcal{C}_-$, skirting the Borel transform's singularity respectively from above and under.

The double well and periodic cosine well serve as physical examples for this case, due to their structure of harmonic degenerate minima. This will be discussed in Sec. 4.3. The key point is that the Borel resummation strategy is insufficient in these cases, and one should explicitly take non-perturbative effects into account. The resummation of the ground-state energy introduces two problems: first of all the sign ambiguity and secondly the fact that there is an imaginary contribution to a bound-state energy. The resolution will only appear when considering the complete picture, which requires the resurgence framework explained in Chapter 5.

3.5 Borel-Padé approximants

In practice, one can only ever numerically compute the perturbation coefficients to a finite order, yielding a truncated Borel transform. For the physically relevant example of energy expansions, this truncated transform $\sum_{n=0}^{N_*} E_n g^n/n!$ does not give a good approximation of the analytic structure of the exact energy function $E(g)$. As the previous examples indicate, the function is expected to have a branch-cut structure along the real axis, whereas a truncated Borel transform is an entire function. Instead, *Padé approximation* can be used, employing rational functions with a pole structure that approaches the expected branch cut of the full Borel transform [13, 49, 54, 55].

More explicitly, the Padé approximant of a power series $\sum_{n=0}^{N_*} f_n z^n$ takes the form

$$\mathcal{P}_{[N/M]}[f](z) = \frac{P_N(t)}{Q_M(t)} = \frac{p_0 + p_1 z + \ldots + p_N z^N}{1 + q_1 z + \ldots + q_M z^M}, \tag{3.15}$$

the ratio of two polynomials P_N and Q_M of orders N and M, respectively. Without loss of generality, $q_0 = 1$ is fixed. The remaining $N + M + 1$ coefficients are defined by requiring that the Taylor expansion of the approximant matches the series up to order $\mathcal{O}\left(z^{N+M+1}\right)$. Alternatively, this means the coefficients can be found by solving

$$\sum_{n=0}^{N+M} f_n z^n \sum_{j=0}^{M} q_j z^j - \sum_{k=0}^{N} p_k z^k = \mathcal{O}\left(z^{N+M+1}\right) \tag{3.16}$$

order by order in z, which yields $N + M + 1$ equations for the same number of unknown coefficients p_k and q_j. The $[N/M]$ Padé approximant of a Borel transform $\mathcal{B}[f](t)$ will be called a *Borel-Padé approximant*, denoted by $\mathcal{B}_{[N/M]}[f](t)$.

Another argument in favour of Padé approximants is their rapid convergence. In practice, often diagonal approximants with $N = M$ are used, which are computed through the knowledge of $2N + 1$ coefficients $f_0, \ldots, f_{2N}$ of the asymptotic series. Hence, the next term in the Taylor series of the approximant is a prediction f_{2N+1}^{pred} of the actual coefficient f_{2N+1}. Interestingly, the estimate is often very reasonable and in several examples [3, 56], the relative error was found to vanish exponentially at large N:

$$\left| \frac{f_{2N+1}^{\text{pred}} - f_{2N+1}}{f_{2N+1}} \right| \sim C e^{-\sigma N}, \tag{3.17}$$

for constants C and $\sigma > 0$. In fact, before the analytical calculation was published, the 4-loop coefficient of the QCD β-function was predicted using this Borel-Padé method, with some sophistications to account for error estimates [56].

For completeness, it can be noted that there is a nice way to rewrite (3.16) as a matrix equation [49], which is used in numerical calculations of the Padé approximants in Chapter 4. First, one determines the q_j and subsequently the p_k coefficients, from

$$\begin{bmatrix} & & \\ & f_{N+i-j} & \\ & (1 \le i, j \le M) & \\ & & \end{bmatrix} \begin{bmatrix} q_1 \\ q_2 \\ \vdots \\ q_M \end{bmatrix} = - \begin{bmatrix} f_{N+1} \\ f_{N+2} \\ \vdots \\ f_{N+M} \end{bmatrix} \quad \text{and} \quad p_k = \sum_{j=0}^{k} f_{k-j} q_j \quad \text{for } 0 \le k \le N, \tag{3.18}$$

where $q_{j>M} = 0$ by definition.

To end this discussion about mathematical tools, it is instructive to examine the simplest non-Borel summable asymptotic series $\sum_n f_n z^n$ in some more detail. For non-alternating coefficients $f_n = n!$, the divergent series should actually be understood as the expansion of the integral

$$\mathcal{S}_{\pm\epsilon}[f](z) = \frac{1}{z}\int_0^{e^{\pm i\epsilon}\infty} \mathrm{d}t\, \mathrm{e}^{-t/z}\,\frac{1}{1-t} \sim \sum_{n=0}^{\infty} n!\, z^n \quad (z \to 0), \tag{3.19}$$

following the discussion in Sec. 3.4. The lateral Borel resummation along a ray, with $\epsilon > 0$, is necessary to avoid the singularity $t = 1$ on the positive real axis. The imaginary contribution due to passing around the (half-)pole, with a sign ambiguity depending on whether $\arg(z)$ is positive $(+)$ or negative $(-)$, is

$$\operatorname{Im} f(z) = \pm\frac{\pi}{z}\mathrm{e}^{-1/z}, \tag{3.20}$$

and it is the inevitable consequence one has to deal with to obtain a well-defined resummation. A physical interpretation will be given in Sec. 4.4.

It turns out there is a connection between the perturbation coefficients f_n and the imaginary part incurred by the Borel sum. Generally considering a function $f(z)$ with a branch-cut singularity structure along the positive part of the real axis, there is a discontinuity between $f(z \pm i\varepsilon)$ as ε tends to zero (for $z > 0$). In such cases, there is another way to express the exact function $f(z)$ at some point $z_0 \in \mathbb{C}$ not on the Stokes line. By deforming the Cauchy integration contour encircling z_0 to the one in Fig. 3.4, one has

$$f(z_0) = \frac{1}{2\pi i}\oint \mathrm{d}z \frac{f(z)}{z - z_0} = \frac{1}{2\pi i}\int_0^\infty \mathrm{d}z \frac{\operatorname{Disc}_0 f(z)}{z - z_0} = \frac{1}{\pi}\int_0^\infty \mathrm{d}z \frac{\operatorname{Im} f(z)}{z - z_0}, \tag{3.21}$$

where $\operatorname{Disc}_0 f(z) = \lim_{\varepsilon\to 0}[f(z + i\varepsilon) - f(z - i\varepsilon)]$ denotes the discontinuity along the singular direction at angle $\theta = 0$. The second equality follows assuming $f(z)$ decays fast enough, so the contributions from the circular contour vanish as its radius R tends to infinity, leaving only the integrals skirting the cut. The result (3.21) is called a *dispersion relation* and it shows how the function $f(z)$ is determined by the discontinuity[10]

[10] In the last equality, $\operatorname{Im} f(z)$ is really just shorthand for $\frac{1}{2i}\lim_{\varepsilon\to 0}[f(z + i\varepsilon) - f(z - i\varepsilon)]$.

across its cut.

Now, expanding the left-hand side $f(z_0)$ of (3.21) as an asymptotic series $\sum_n f_n z_0^n$ and recalling the geometric series

$$\frac{1}{z - z_0} = \frac{1}{z} \sum_{n=0}^{\infty} \left(\frac{z_0}{z}\right)^n, \tag{3.22}$$

one can obtain an interesting relation between the perturbation coefficients and the imaginary contribution to the function:

$$f_n = \frac{1}{\pi} \int_0^{\infty} \mathrm{d}z \frac{\operatorname{Im} f(z)}{z^{n+1}}. \tag{3.23}$$

This result holds generally for a function with a cut along the positive real axis and generalisations to multiple Stokes directions are possible [19]. Convergence issues near $z = 0$ are usually dispelled when accounting for a non-perturbative factor of the type $\mathrm{e}^{-1/z}$ frequently entering $\operatorname{Im} f(z)$.

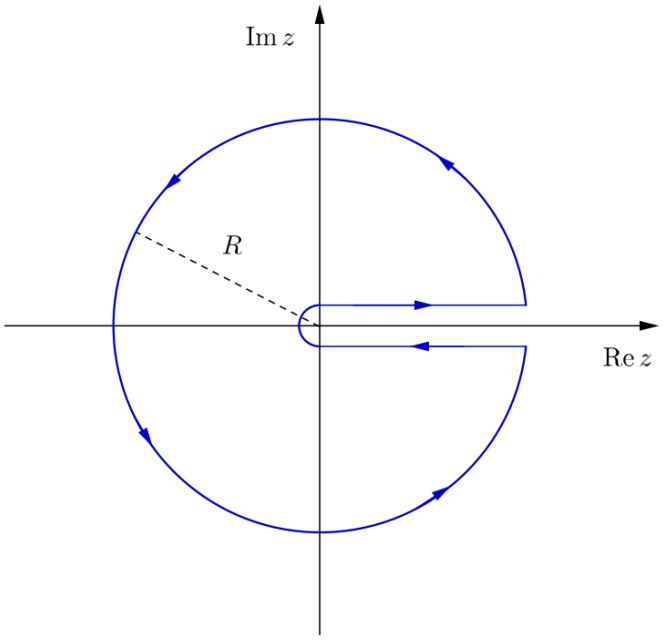

Figure 3.4: Integration contour for the dispersion relation, deformed to avoid the branch cut.

As a concrete example of the use of the dispersion relation and its corollary (3.23), the specific case where

$$\operatorname{Im} f(z) = \pm\frac{1}{z}\mathrm{e}^{-S/z}(c_0 + c_1 z + c_2 z^2 + c_3 z^3 + \ldots) \tag{3.24}$$

will be of interest in Chapters 4 and 5. The infinite power series represents fluctuations around the non-perturbative exponential factor (with $S > 0$). In physical terms, it will describe fluctuations around a non-perturbative multi-instanton sector, with S a multiple of the instanton action. It will be shown that these form an asymptotic series by themselves.

Once one has performed the integral

$$\int_0^\infty \mathrm{d}z\ \mathrm{e}^{-S/z}\frac{c_k z^k}{z^{n+2}} = c_k S^{k-n-1}(n-k)!\,, \tag{3.25}$$

the coefficients of the asymptotic series are immediately found to contain a descending factorial series:

$$f_n = \frac{1}{\pi}\left(\frac{1}{S}\right)^{n+1} n!\left[c_0 + c_1\left(\frac{S}{n}\right) + c_2\left(\frac{S^2}{n(n-1)}\right) + c_3\left(\frac{S^3}{n(n-1)(n-2)}\right) + \ldots\right]. \tag{3.26}$$

Intriguingly, this shows how the higher-order fluctuations $c_k z^k$ are directly related to a series of sub-leading corrections of order $\mathcal{O}\left(n^{-k}\right)$ to the dominating factorial growth of the perturbation coefficients f_n.

4

Asymptotics in the Mathieu problem

4.1 Introduction

Extracting the energy spectrum from the Schrödinger equation for the sine-Gordon potential is equivalent to solving an age-old mathematical problem, first described by Mathieu in his study of the vibrations of an elliptical membrane. A natural approach is perturbation theory. In general terms, one aims to approximate the solutions of a problem that can be constructed from a related, simpler one by tweaking a small parameter ε, which quantifies how the problem deviates from the unperturbed case at $\varepsilon = 0$. The solution takes the form of a power series in ε, with coefficients computed iteratively by plugging in the series ansatz and solving the problem order by order in ε.

The last step of the analysis is summing the perturbation series for the desired ε value. As indicated in Chapter 3, this is often problematic in quantum mechanics, also in the case of the sine-Gordon well. To a certain extent, the divergence issues can be interpreted as the analytic reflection of the singular character of the time-independent Schrödinger problem [57]: the energy is expanded as a series around the special value zero of the coupling constant, but the nature of that unperturbed case is very different! Indeed, the coupling multiplies the highest-order derivative ∂_x^2 in the Schrödinger equation, so setting it to zero fundamentally changes the original equation.

The aim of the following sections is to apply the mathematical machinery introduced in Chapter 3 in the study of the sine-Gordon potential. More specifically, the divergence will be shown through concrete, numerical calculations and the large-order behaviour of the perturbation coefficients will be linked to instanton effects. Afterwards, that connection will receive a more elaborate treatment in the framework of resurgent transseries (Chapter 5). Indeed, it will become apparent that only zooming out and looking at the global picture beyond perturbation theory might show how to solve the lack of Borel-summability, a resummation issue encountered here and in more general quantum problems. Mathematically, the crux of the problem is that the obtained perturbative expansions rely on local approximations. From the physical point of view, discussed at the end of this chapter, the singular nature is directly connected to global features, like instability or degenerate vacua of the potentials, beyond the grasp of a local analysis (Sec. 4.4).

4.2 Perturbative energy spectrum of the Mathieu potential

The time-independent Schrödinger equation for the sine-Gordon potential is defined as[1]

$$\left[-g^4\partial_y^2 + \sin^2(y)\right]\psi(y) = g^2 E\psi(y), \tag{4.1}$$

which can be rewritten in the form of a well-studied second-order differential equation, the *Mathieu equation*. Its textbook form[2] can be obtained by changing variables, so that

$$\left[\partial_z^2 + (a - 2q\cos(2z))\right]\psi(z) = 0, \tag{4.2}$$

where the two real parameters a (the *characteristic value*) and q are related to the energy E and coupling constant g^2 as

$$g^2 = \frac{1}{k} \quad \text{and} \quad E = \frac{1}{k}\left(a + \frac{1}{2}k^2\right), \quad \text{with } k^2 = 4q. \tag{4.3}$$

The exact solutions $\psi(z)$ of the Mathieu equation are entire functions, as the equation has no finite singularities. If the parameters are non-zero, its solutions are also tran-

[1] To avoid introducing yet another notation, the conventions in [21] will be followed: the coupling constant is g^2, which can be identified with $\hbar$ (when made dimensionless).

[2] More details on conversions between different notations can be found in App. B.

scendental, hence non-polynomial, except for the trivial solution $\psi = 0$.

In the semi-classical limit of small g^2, or equivalently $q \to \infty$, the effects of quantum tunnelling on the energy levels are minimal and one can reasonably approximate the potential by a series of independent harmonic oscillators with infinite barriers between each other [40, 58]. For a local analysis, it suffices to focus on one of the harmonic wells, for example the one located around $z = \pi/2$ or $-\pi/2$. A rewritten version of the Mathieu equation with $k^2 = 4q$,

$$\psi''(z) + \left[a + \frac{k^2}{2}\cos\left(2\left(z \pm \frac{\pi}{2}\right)\right)\right]\psi(z) = 0, \tag{4.4}$$

can then be expanded around the minimum using the first terms of the cosine's Taylor series, $\cos(z) \simeq 1 - z^2/2$. A change of variables

$$z \to \zeta = \sqrt{\frac{k}{2}}\left(z \pm \frac{\pi}{2}\right) \tag{4.5}$$

reveals that the Mathieu equation is approximately a parabolic cylinder equation in this limit:

$$\psi''(\zeta) + \left[\frac{2a + k^2}{4k} - \frac{\zeta^2}{4}\right]\psi(\zeta) \simeq 0. \tag{4.6}$$

Since this is just the Schrödinger equation for the simple harmonic oscillator, the solutions (parabolic cylinder functions) are well known to involve Hermite polynomials. Only discrete eigenvalues

$$\frac{2a + k^2}{4k} \simeq N + \frac{1}{2} = \frac{1}{2}(2N + 1), \text{ for N = 0,1,2, } \ldots \tag{4.7}$$

lead to normalisable solutions. With this information, the N-th perturbative energy level of the original Mathieu equation can be expressed as

$$a_{pt}(k, N) = -\frac{k^2}{2} + ka_0 + \Delta, \text{ with } a_0 = 2N + 1. \tag{4.8}$$

Here, Δ denotes corrections due the remainder of the cosine expansion truncated earlier and the subscript 'pt' refers to perturbation theory.

A procedure to obtain the next expansion terms for the characteristic value, due to [58], is outlined in the following. Inserting (4.8) into the complete Mathieu equation

yields

$$\psi''(z) + k\left[a_0 + \frac{\Delta}{k} - k\cos^2(z)\right]\psi(z) = 0. \tag{4.9}$$

Asymptotically for k tending to infinity, i. e. in the semi-classical approximation, one may omit the middle terms and the solution behaves as

$$\psi(z) \sim \exp\left(\pm k\int^z \cos(z')\,\mathrm{d}z'\right). \tag{4.10}$$

Then, taking $\psi(z) = v(z)\mathrm{e}^{k\sin(z)}$, the equation can be transformed into

$$D_N v(z) = \left[\cos(z)\frac{\mathrm{d}}{\mathrm{d}z} + \frac{1}{2}\left((2N+1) - \sin(z)\right)\right]v(z) = -\frac{1}{2k}\left(v''(z) + \Delta v(z)\right). \tag{4.11}$$

If one solution of the proposed form is retrieved, another linearly independent one, asymptotic to $\mathrm{e}^{-k\sin(z)}$ is obtained by the reflection $z \to -z$. In the large-k limit of (4.11), the zeroth-order solution solves the first-order differential equation $D_N v^{(0)}(z) = 0$ and one finds

$$v_{(0)}(z) = v_N(z) = \cos^N\left(\frac{1}{2}\left(z + \frac{\pi}{2}\right)\right) / \sin^{N+1}\left(\frac{1}{2}\left(z + \frac{\pi}{2}\right)\right). \tag{4.12}$$

To obtain a better approximation of the full solution, one can assess the error introduced by entering $v_{(0)}(z)$ into the right-hand side of (4.11). These uncompensated terms can be written as

$$-\frac{1}{2k}(v''_{(0)}(z) + \Delta v_{(0)}(z)) = -\frac{1}{8k}\Big[(N+1)(N+2)v_{N+2}(z) + \left(N^2 + (N+1)^2 + 4\Delta\right)v_N(z) + N(N-1)v_{N-2}(z)\Big]. \tag{4.13}$$

After calculating that

$$D_N v_{N+j}(z) = -j v_{N+j}(z) \quad \text{for } j = 0 \text{ or } \pm 2, \tag{4.14}$$

the terms in (4.13) containing $v_{N\pm j}(z)$ with $j = \pm 2$ can be cancelled by adding terms proportional to $-v_{N\pm j}/j$ to the zeroth-order solution. In this way, one finds a better

approximation $v \simeq v_{(0)} + v_{(1)}$, where

$$v_{(1)}(z) = \frac{1}{8k}\left[(N+1)(N+2)\frac{v_{N+2}(z)}{2} - N(N-1)\frac{v_{N-2}(z)}{2}\right]. \tag{4.15}$$

Now, also requiring the $v_N(z)$ term in (4.13) to vanish determines Δ to leading order:

$$\Delta \simeq -\frac{1}{4}\left(N^2 + (N+1)^2\right) = -\frac{1}{8}(a_0^2+1). \tag{4.16}$$

Of course, while adding $v_{(1)}$ cleans up the remainder terms on the right-hand side of (4.11) due to $v_{(0)}$, it introduces new unbalanced terms itself. In turn, these have to be compensated by new corrections to v and Δ, a procedure that can be repeated to yield series expansions in $1/k$:

$$v(z) = v_{(0)} + v_{(1)} + v_{(2)} + \ldots = \sum_{l=0}^{\infty} \frac{v_l(z)}{k^l} \tag{4.17}$$

$$a_{pt}(k,N) = -\frac{k^2}{2} + ka_0 + a_1 + k\sum_{l=2}^{\infty}\frac{a_l}{k^l}, \text{ with } a_1 = -\frac{1}{8}(a_0^2+1). \tag{4.18}$$

When translated to the language of energy eigenvalues, one obtains a perturbative expansion $\sum_{n=0}^{\infty} E_n(N)(g^2)^n$ around the N-th energy level of the harmonic oscillator[3] [38–40, 59, 60]:

$$\begin{aligned} E_{pt}(g^2,N) = 2&\left[N+\frac{1}{2}\right] - \frac{g^2}{2}\left[\left(N+\frac{1}{2}\right)^2 + \frac{1}{4}\right] \\ &- \frac{g^4}{8}\left[\left(N+\frac{1}{2}\right)^3 + \frac{3}{4}\left(N+\frac{1}{2}\right)\right] \\ &- \frac{g^6}{32}\left[\frac{5}{2}\left(N+\frac{1}{2}\right)^4 + \frac{17}{4}\left(N+\frac{1}{2}\right)^2 + \frac{9}{32}\right] - \ldots \end{aligned} \tag{4.19}$$

This is an asymptotic expression for the exact energy, valid in the weak-coupling limit $g^2 N \ll 1$, when $g^2 \to 0$ or the considered level number is sufficiently low. The expansion coefficients $E_n(N)$ turn out to be polynomials of n-th degree in N with alternating

[3] More details on conversions are worked out in App. B. Actually, one finds that in these conventions $E_n(N) = a_n(N)$.

parity. For reasons discussed in Chapter 5, it is instructive to view the coupling g^2 as a variable parameter of the theory, reflecting the strength of quantum effects.

4.3 Asymptotic features of the Mathieu spectrum

4.3.1 Divergence of perturbation theory

In order to expose the divergent character of the perturbative expansion $E_{pt}(g^2, N)$, it is necessary to determine the characteristic behaviour of the series coefficients $E_n(N)$ at large orders n of perturbation theory. The most straightforward way to determine their asymptotic form proceeds by writing recurrence relations for them [41, 58].

Transforming the Mathieu equation (4.2) by writing

$$\psi(z) = u(z)\mathrm{e}^{k\cos(z)} \tag{4.20}$$

and series expansions following naturally from the perturbative analysis,

$$u(z) = \sum_{l=0}^{\infty} \frac{u_l(z)}{k^l} \quad \text{and} \quad a_{pt}(N) = -\frac{k^2}{2} + k\sum_{l=0}^{\infty} \frac{a_l}{k^l}, \tag{4.21}$$

one can obtain

$$\begin{aligned} 0 = \left[-\cos(x)k + \mathcal{O}\left(k^2\right)\right] \sum_{l=0}^{\infty} \frac{u_l}{k^l} + \left[k + \mathcal{O}\left(k^2\right)\right] \sum_{l=0}^{\infty} \left(\sum_{j=0}^{l} a_j u_{l-j}\right) \frac{1}{k^l} + \\ \left[-2\sin(x)k + \mathcal{O}\left(k^2\right)\right] \sum_{l=0}^{\infty} \frac{u_l'}{k^l} + \left[k + \mathcal{O}\left(k^2\right)\right] \sum_{l=1}^{\infty} \frac{u_{l-1}''}{k^l}. \end{aligned} \tag{4.22}$$

Equating the coefficients of $1/k^l$ yields an infinite set of differential equations for the $u_l(z)$ functions:

$$2\sin(x)u_0' + (\cos(x) - a_0)u_0 = 0 \tag{4.23}$$

$$2\sin(x)u_l' + (\cos(x) - a_0)u_l = u_{l-1}'' + \sum_{j=1}^{l} a_j u_{l-j} \quad \text{for } l > 0. \tag{4.24}$$

Using the knowledge that $a_0 = 2N + 1$ is an odd integer, the zeroth-order solution

is found to be

$$u_0(z) = \sin^N\left(\frac{z}{2}\right) / \cos^{N+1}\left(\frac{z}{2}\right). \tag{4.25}$$

Inspired by this, the remaining differential equation for $l > 0$ can be rewritten by setting

$$u_l(z) = w_l(z) \sin^N\left(\frac{z}{2}\right) / \cos^{N+1}\left(\frac{z}{2}\right). \tag{4.26}$$

The problem is then reduced to determining the functions $w_l(z)$ through

$$\begin{aligned} 2\sin(x)w_l' \; &= w_{l-1}'' + \frac{a_0 - \cos(x)}{\sin(z)} w_{l-1}' + \\ &\left(\frac{\mu - a_0\cos(z)}{\sin^2(z)} - \frac{\mu}{2}\right) w_{l-1} + \sum_{j=2}^{l} a_j w_{l-j} \end{aligned} \tag{4.27}$$

where $a_1 = -(a_0^2+1)/8$ was used and $\mu = N^2 + N + 1$. The sum in the last line is only added when $l > 1$.

Now, an ansatz can be employed to expand $w_l(z)$ into a finite power series:

$$w_l(z) = \sum_{j=1}^{l} \frac{A_j^l}{\cos^{2j}(z/2)} \quad \text{for } l > 0, \tag{4.28}$$

and $w_0(z) = A_0^0 = 1$. Some algebra shows that when $\mu = a_0$ (i. e. for $N = 0$ and $N = 1$), equating the coefficients of $\cos^{-2j}(z/2)$ leads to recursive relations between the A_j^l without any z-dependence. For $1 \leq j \leq l$, one finds after index relabelling

$$4jA_j^l \; = 4(j+1)A_{j+1}^l + j\left(j + N - \frac{1}{2}\right) A_{j-1}^{l-1} - \left(j(j+1) + \frac{b_0}{2}\right) A_j^{l-1} + \sum_{n=2}^{l} a_n A_j^{l-n}. \tag{4.29}$$

The last sum only enters for $l \geq 2$, and in that case, $-4A_1^l = a_l$ holds. Implicitly, $A_0^l = \delta_{l0}$ and for $j > l$ it is fixed that $A_j^l = 0$.

All information is available at this point to calculate the A_j^l coefficients and a fortiori the a_l from the expansion of the characteristic value of the Mathieu equation. For

example, when $j = l > 0$, (4.29) simplifies to:

$$4lA_l^l = l\left(l + N - \frac{1}{2}\right) A_{l-1}^{l-1}. \tag{4.30}$$

With the initial condition $A_0^0 = 1$ one immediately finds $A_1^1 = 1/8$ for the ground state ($N = 0$), which enables calculating $a_2 = -1/16$. Subsequent coefficients easily follow, so that[4]

$$\begin{aligned} a_{pt}(k,0) = &-\frac{k^2}{2} + k - \frac{1}{4} - \frac{1}{2^4 k} - \frac{6}{2^7 k^2} - \frac{53}{2^{10} k^3} - \frac{594}{2^{13} k^4} - \frac{7922}{2^{16} k^5} - \\ &\frac{121\,452}{2^{19} k^6} - \frac{2\,095\,501}{2^{22} k^7} - \frac{40\,114\,410}{2^{25} k^8} - \frac{843\,289\,718}{2^{28} k^9} - \\ &\frac{193\,314\,816\,948}{2^{31} k^{10}} - \frac{478\,935\,069\,186}{2^{34} k^{11}} - \frac{12\,788\,293\,823\,604}{2^{37} k^{12}} - \\ &\frac{366\,006\,950\,861\,892}{2^{40} k^{13}} - \frac{11\,182\,327\,425\,508\,824}{2^{43} k^{14}} - \ldots. \end{aligned} \tag{4.31}$$

With the appropriate substitutions, the first terms of the perturbative ground state energy are thus given by

$$E_{pt}(g^2, 0) = 1 - \frac{g^2}{4} - \frac{g^4}{16} - \frac{3g^6}{64} - \frac{53g^8}{1024} - \frac{297g^{10}}{4096} - \ldots, \tag{4.32}$$

as expected from the general perturbative energy level expansion in (4.19). However, whereas extending the general formula beyond the first few orders becomes increasingly tedious, the first 600 terms in $E_{pt}(g^2, 0)$ can be calculated in just a couple of minutes of processor time using the recursion algorithm. The a_n coefficients are rational numbers and in this work, they were obtained up to $n = 1000$ in their exact rational form. Some (rescaled) numerical values[5] are shown in Table 4.1.

A plot of the expansion coefficient ratios a_{n+1}/a_n is practically a straight line (Fig. 4.1), indicating proportionality to n and hence the factorial growth of a_n. What is more, the inverse ratio is proportional to $1/n$, so as anticipated, the series has a vanishing radius of convergence:

$$R[E_{pt}(g^2, 0)] = \lim_{n\to\infty} \left| \frac{a_n}{a_{n+1}} \right| \sim \lim_{n\to\infty} \frac{1}{n} = 0. \tag{4.33}$$

[4] Terms up to k^{-11} were published previously in [41], with a few minor typographical errors.
[5] The first 100 coefficients were already found in [41], agreeing with the results in Table 4.1.

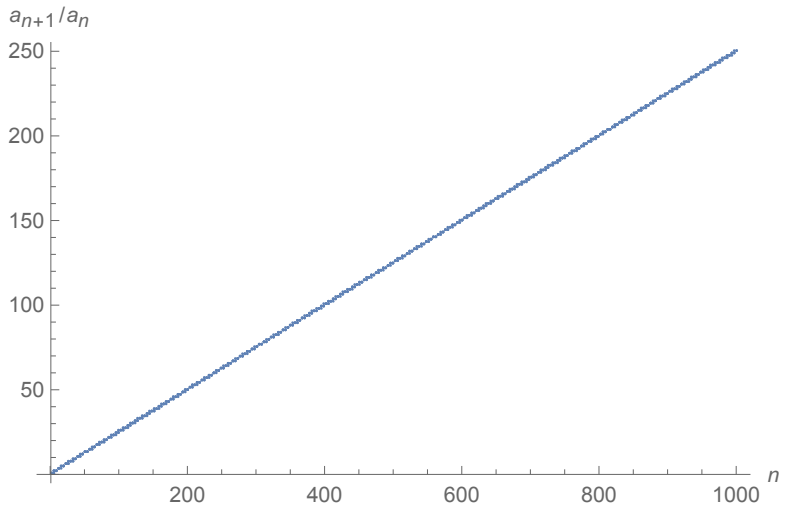

Figure 4.1: Large-order behaviour (up to $n = 1000$) of the ratio of consecutive perturbative energy expansion coefficients for the ground state.

Furthermore, it is clear that the ground-state energy perturbation series in (4.32) is non-alternating after the first two terms. As noted in Sec. 3.4, this behaviour is typical for a factorially divergent series.

4.3.2 Beyond leading-order growth

The (slow) growth of the rescaled expansion coefficients

$$b_n = -\frac{4^n}{(n+1)!}a_{n+1} \tag{4.34}$$

in Table 4.1 indicates that factorial divergence is just the leading asymptotic behaviour. There is actually more than meets the eye in Fig. 4.1, and to extract the large-order features more accurately than with a model fitting procedure, one can use *Richardson extrapolation* [49]. The idea behind this numerical method is to accelerate the convergence of a series towards its large-order form. This can be achieved by removing asymptotically negligible sub-leading terms. In practice, the goal is to find the coefficients s_m that determine the asymptotic behaviour

$$b_n \sim s_0 + \frac{s_1}{n} + \frac{s_2}{n^2} + \ldots . \tag{4.35}$$

n	$b_n = -\frac{4^n}{(n+1)!}a_{n+1}$	n	$b_n = -\frac{4^n}{(n+1)!}a_{n+1}$
1	0.125000000000000	120	0.311696174421404
2	0.125000000000000	140	0.312638991684206
3	0.138020833333333	160	0.313346507397895
4	0.154687500000000	180	0.313897045427100
5	0.171918402777778	200	0.314337636569157
6	0.188262648809524	220	0.314698228802947
7	0.203014652312748	240	0.314998798254727
8	0.215907344111690	260	0.315253180910922
9	0.226941444894834	280	0.315471263523413
10	0.236268011536261	300	0.315660298861873
11	0.244106715145603	350	0.316038455198851
12	0.250693079969985	400	0.316322148301243
13	0.256248328878023	450	0.316542843987407
14	0.260965236589615	500	0.316719429462701
15	0.265004108474712	550	0.316863927751052
20	0.278719626424706	600	0.316984356311846
30	0.291972402027155	650	0.317086266905427
40	0.298541769659101	700	0.317173625804428
50	0.302482137357013	750	0.317249342066000
60	0.305110933232159	800	0.317315597779496
70	0.306990193781085	850	0.317374061799486
80	0.308400702966648	900	0.317426032259637
90	0.309498485086778	950	0.317472534097397
100	0.310377205346367	1000	0.317514387330700

Table 4.1: Rescaled coefficients of the perturbative series for the ground-state energy.

Firstly, starting at a fixed index n and working up to order $\mathcal{O}\left(n^{-N}\right)$, one can write a system of $N+1$ equations to be solved simultaneously for the s_m:

$$b_{n+j} \simeq s_0 + \frac{s_1}{n+j} + \frac{s_2}{(n+j)^2} + \ldots + \frac{s_N}{(n+j)^N} \quad \text{for } j = 0, 1, \ldots, N. \tag{4.36}$$

As such, fitting $N+1$ known coefficients b_{n+j} to a truncated, polynomial form fixes the s_m, with an error that vanishes as n and N are increased. However, instead of risking a numerically heavy matrix inversion at large N, the leading large-order term s_0 can simply be found in closed form [49]:

$$s_0 \simeq \sum_{j=0}^{N} \frac{(-1)^{N+j}(n+j)^N b_{n+j}}{j!(N-j)!}, \tag{4.37}$$

which would be exactly $s_0 = \lim_{n\to\infty} b_n$ if the series in (4.35) were to truncate after $N+1$ terms. This method, yielding s_0, can effectively be thought of as an extrapolation to $n = \infty$. To find the next coefficient, one can create a new series where the leading behaviour is subtracted:

$$\tilde{b}_n = n(b_n - s_0) \sim s_1 + \frac{s_2}{n} + \frac{s_3}{n^2} + \ldots. \tag{4.38}$$

The Richardson transform in (4.37) for the $\tilde{b}_n$ series subsequently yields s_1. Applying this procedure iteratively, one can find the asymptotic form for the ground-state energy coefficient multiplying the $1/k^n$ term:

$$a_{n+1} \sim -\frac{1}{\pi}\left(1 - \frac{5}{2n} + \frac{7}{8n^2} - \frac{133}{16n^3} - \frac{5113}{128n^4} - \ldots\right)\frac{(n+1)!}{4^n}. \tag{4.39}$$

The first three terms were already found in [41]. By pushing the Richardson extrapolation technique towards a high number of terms and working with the exact b_n fractions, it was possible to obtain the first 32 terms s_m of the asymptotic expansion in (4.39), to a high degree of certainty, in their rational form (Table 4.2). The largest coefficient found in this form is $s_{32} \approx -1.82 \times 10^{40}$. The convergence of the first three series of b_n, $\tilde{b}_n$ and $\tilde{\tilde{b}}_n$ towards their respective asymptotic forms s_0, s_1 and s_2 as n tends to infinity is shown in Fig. 4.2. In other words, the three curves depict ratios of the perturbation coefficients to the large-order behaviour noted in (4.39), to the leading, sub-leading and sub-sub-leading levels.

m	$s_m \times \pi$	m	$s_m \times \pi$
0	1	1	$-5/2$
2	$+7/2^3$	3	$-133/2^4$
4	$-5113/2^7$	5	$-91743/2^8$
6	$-3661721/2^{10}$	7	$-84598977/2^{11}$
8	$-17590968821/2^{15}$	9	$-507207324271/2^{16}$
10	$-32088414087407/2^{18}$	11	$-1104069776270571/2^{19}$
12	$-164148193706161181/2^{22}$	13	$-6553772212163835987/2^{23}$
14	$-559481302507973028633/2^{25}$	15	$-25426483678220344595353/2^{26}$

Table 4.2: Coefficients s_m determining the large-order growth of the ground-state energy expansion coefficients a_n. The complete table is given in App. C.1.

Finding the rational representations is somewhat tricky, because the Richardson extrapolation (4.37) is an approximation; however, given the large number of a_n terms known, starting at order $n = 800$ and taking $N = 200$ terms in the summation, the conjectured fractions in Table 4.2 are correct up to at least 130 decimal places. Numerically approximate results for the sub-leading corrections s_m were obtained up to $m = 65$, with $s_{65} \approx -1.28 \times 10^{101}$. The incentive for determining as many of those correction terms as possible is that they are themselves related to specific coefficients of a divergent asymptotic series, a manifestation of resurgence which will become clear in Chapter 5.

4.3.3 Emergence of instanton effects

Anticipating connections revealed by resurgent analysis, it should already be noted that (4.39) shows the leading large-order behaviour of the energy expansion coefficients has the form

$$E_n = a_n \sim -\frac{16}{\pi}\frac{n!}{S_{I\bar{I}}^{n+1}} \tag{4.40}$$

In a suggestive way, the factor in the denominator was already identified as

$$S_{I\bar{I}} = 2S_I = 4, \tag{4.41}$$

the action of an instanton–anti-instanton ($I\bar{I}$) trajectory.

The fact that the asymptotic form contains this action is not coincidental numerology,

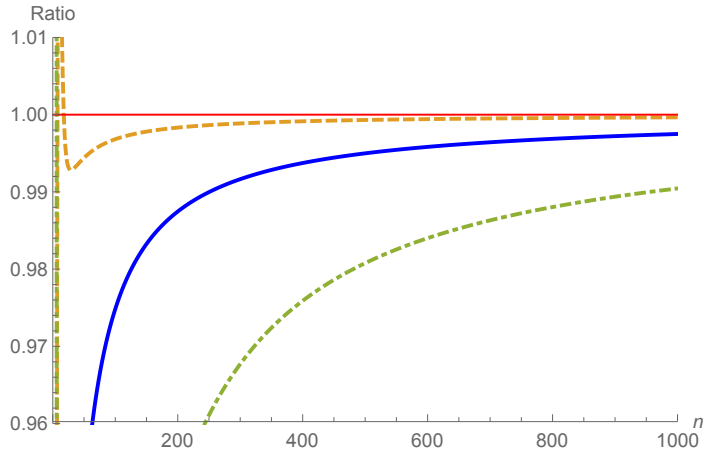

Figure 4.2: Convergence of the ratios b_n/s_0 (blue, solid line), $\tilde{b}_n/s_1$ (gold, dashed) and $\tilde{\tilde{b}}_n/s_2$ (green, dot-dashed) towards their large-order asymptotic behaviour.

but instead lifts the veil on a deeper mechanism hiding in the energy expansion. The factorial growth of the late terms in perturbation theory is connected to a two-instanton effect. A more comprehensive discussion will follow in Sec. 5.4, but at this point, one may already have noticed that (4.39) is strongly reminiscent of (3.26), the large-order features in the example of Sec. 3.6. Indeed, (4.39) can be reworked into the form of an inverse, descending factorial series:

$$a_n \sim -\frac{16}{\pi}\left(\frac{1}{S_{I\bar{I}}}\right)^{n+1} n!\left[1-\frac{5}{8}\left(\frac{S_{I\bar{I}}}{n}\right)-\frac{13}{128}\left(\frac{S_{I\bar{I}}^2}{n(n-1)}\right)-\frac{119}{1024}\left(\frac{S_{I\bar{I}}^3}{n(n-1)(n-2)}\right)+\dots\right]. \tag{4.42}$$

One can deduce that such asymptotics are the counterpart of an imaginary (sine-well perturbative ground-state) energy contribution from Borel resummation that is dominated by

$$\operatorname{Im}\mathcal{S}[E](g^2) \sim \pm\frac{\text{cst.}}{g^2}\mathrm{e}^{-S_{I\bar{I}}/g^2}\sum_{n=0}^{\infty} a_n^{I\bar{I}} g^{2n} = \mp\frac{16}{g^2}\mathrm{e}^{-S_{I\bar{I}}/g^2}\left(1-\frac{5}{8}g^2-\frac{13}{128}g^4-\frac{119}{1024}g^6+\dots\right). \tag{4.43}$$

The coefficients $a_n^{I\bar{I}}$ quantify fluctuations around the two-instanton sector. The first 65 of these were obtained numerically and the first couple of rational forms are shown in Table 4.3.

It is interesting to notice from (4.42-4.43) how the large-order perturbative-coefficient behaviour directly corresponds to a leading-order non-perturbative effect. The sign for (4.43) depends on whether $\arg(g^2)$, for the complexified coupling g^2, is positive $(-)$ or negative $(+)$. Of course, this ambiguous, purely imaginary part is highly undesirable for a bound state. The resolution is given in the framework of resurgence, which shows how an equally ambiguous term arises in the two-instanton $[\mathcal{I}\overline{\mathcal{I}}]$ sector, i. e. by explicitly accounting for non-perturbative energy contributions.

n	$a_n^{I\bar{I}}$	n	$a_n^{I\bar{I}}$
0	1	1	$-5/2^3$
2	$-13/2^7$	3	$-119/2^{10}$
4	$-5225/2^{15}$	5	$-68715/2^{18}$
6	$-2079317/2^{22}$	7	$-35323847/2^{25}$
8	$-5308543701/2^{31}$	9	$-109138963047/2^{34}$
10	$-4874789697291/2^{38}$	11	$-117581214668481/2^{41}$
12	$-12194607448373997/2^{46}$	13	$-338509879992444423/2^{49}$
14	$-20048562693726158917/2^{53}$	15	$-631295301078915611495/2^{56}$

Table 4.3: Two-instanton fluctuation coefficients $a_n^{I\bar{I}}$ corresponding to corrections to the large-order growth of the ground-state energy expansion coefficients a_n. The complete table is given in App. C.2.

4.3.4 Borel-Padé pole structure

Intuitively, the fact that the energy series coefficients are non-alternating indicates that its Borel transform has singularities on the positive real axis, as shown in Sec. 3.6. It can be shown explicitly, using the Borel-Padé approximants, that the complete Borel transform indeed has a branch cut, starting at $t = 2S_I$, along the Stokes direction $\arg(t) = 0$. By increasing the number of coefficients a_n used to obtain the rational approximation functions, as described in Sec. 3.5, one can effectively see this: extraneous poles, artefacts of the approximation, occur in the complex Borel plane yet move out towards infinite radius as the approximation is improved (Fig. 4.3). What is left is an accumulation of a growing number of poles on the real axis, precisely from $t = 2S_I$ onward. This is the rational-function approximation of a branch cut in the full Borel transform, and the location of the cut immediately suggests that integration leads to an imaginary

contribution proportional to e^{-2S_I/g^2}, confirming (4.43). In this way, the local analysis of the Borel transform near its singularities reveals non-perturbative aspects – a highly remarkable observation, since the Borel transform is constructed exclusively from perturbative information! Via the dispersion relation, one also concludes that the analytic structure of the Borel transform encodes the large-order perturbative behaviour.

The convergence of the Padé approximants has been examined in some more detail, and Fig. 4.3d illustrates the exponential decay of the relative error of the first predicted series coefficient, as the approximation is improved. A numerical fit shows the relation

$$\left| \frac{E^{(s),\,\text{pred}}_{2N+1} - E^{(s),\,\text{true}}_{2N+1}}{E^{(s),\,\text{true}}_{2N+1}} \right| \sim 1.640\, e^{-1.376\, N}. \tag{4.44}$$

As seen in the pole-structure plots, the zeros of the denominator gather on the real axis. The claim that these approach a branch cut starting at $t = 2S_I$ is supported by Fig. 4.3e: the distance from $t = 4$ to the nearest pole shrinks progressively as N is increased.

4.3.5 Asymptotics of the $[\mathcal{I}\overline{\mathcal{I}}]$ fluctuation coefficients

Thanks to the large number of sub-leading corrections found for the large-order growth of the perturbation coefficients a_n, it was possible to determine that they form a divergent asymptotic series themselves. More specifically, the series of fluctuation coefficients $a_n^{I\bar{I}}$ in (4.43), associated to the instanton–anti-instanton sector, diverges. Using the obtained numerical values for the first 65 fluctuation coefficients, a plot of the ratios of consecutive coefficients clearly shows a straight line (Fig. 4.4a), indicating factorial divergence. Considering only the last 30 points, the result of a linear fit was

$$\frac{a^{I\bar{I}}_{n+1}}{a^{I\bar{I}}_{n}} \sim 0.249n + 0.361. \tag{4.45}$$

The slope is seen to converge to $1/2S_I = 1/4$ (Fig. 4.4b), indicating a four-instanton effect since it adds a two-instanton contribution to fluctuations around the $[\mathcal{I}\overline{\mathcal{I}}]$ sector itself. Hence, the leading large-order behaviour has the form

$$a^{I\bar{I}}_{n} \sim -\frac{n!}{(2S_I)^{n+1}}. \tag{4.46}$$

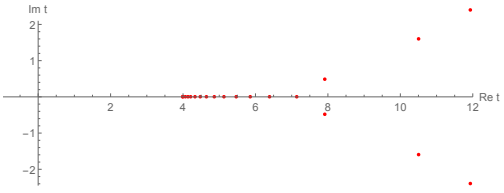

(a) Poles of $B_{[35/35]}[E_s](t)$.

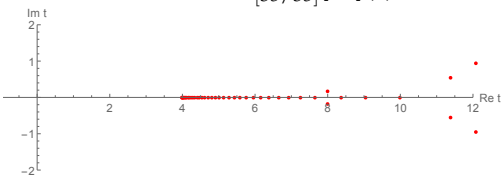

(b) Poles of $\mathcal{B}_{[75/75]}[E_s](t)$.

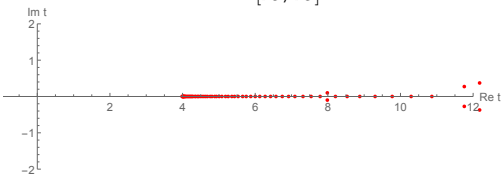

(c) Poles of $\mathcal{B}_{[115/115]}[E_s](t)$.

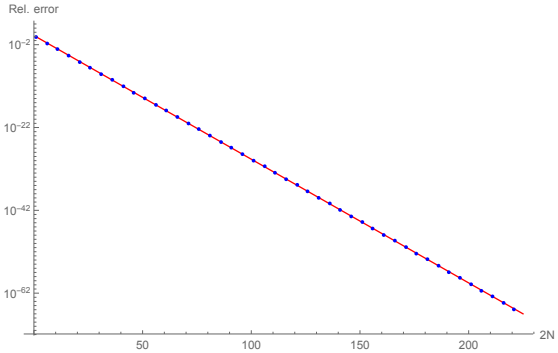

(d) Padé estimate convergence log-plot.

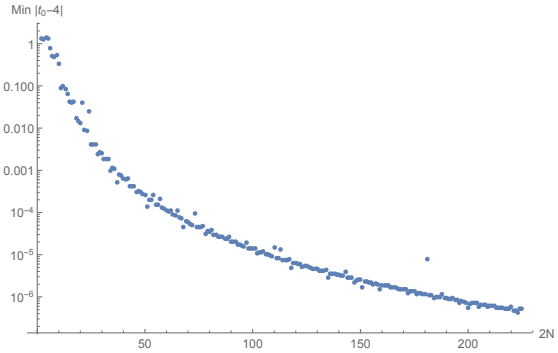

(e) Log-plot of nearest-pole distance to $t = 4$.

Figure 4.3: Gradually improved approximation (**a**-**b**-**c**) of the branch cut of the full Borel transform by diagonal Padé approximants $\mathcal{B}_{[N/N]}[E_s](t)$. Relative error of the Padé prediction (**d**) for the series coefficient $E^{(s)}_{2N+1}$, with straight-line fit (red) and only 1/5 of data points shown. Systematic convergence (**e**) towards branch-cut start at $t = 2S_I$.

This result confirms the concept of resurgence in a highly non-trivial way: the asymptotics of the asymptotics of perturbation theory is shown to bear the hallmark of a higher-order non-perturbative effect involving the four-instanton sector [1, 21]. In the next chapter, this will be made more specific

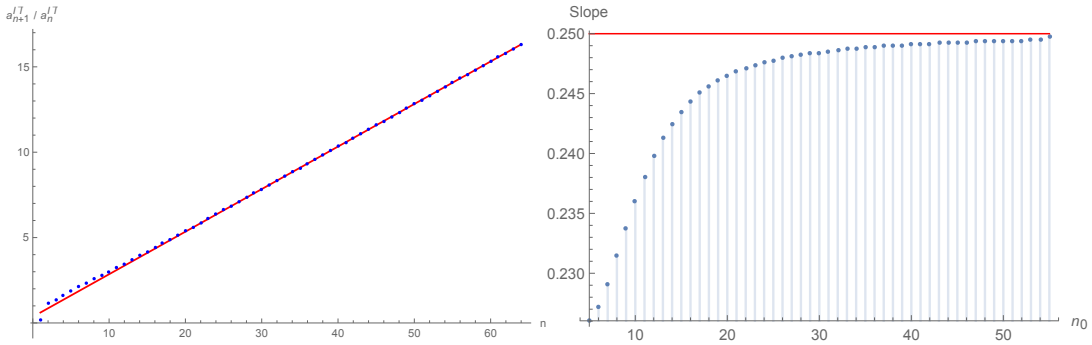

(a) $a^{I\bar{I}}_{n+1}/a^{I\bar{I}}_n$ **(b)** Slope convergence towards $1/4$.

Figure 4.4: Large-order behaviour of the ratio of consecutive two-instanton fluctuation coefficients $a^{I\bar{I}}_n$ and straight-line fit based on the last 30 points (**a**). Slope computed using 10 consecutive points, starting at varying index n_0 (**b**). The slope converges towards $1/2S_I$, as n_0 is increased.

4.4 Origins of the divergence

The factorial divergence noted for the perturbative energy series of the sine-Gordon potential is a frequent feature, also observed in other examples. Its analytic counterpart is the singularity structure of the series' Borel transform and instantons turn out to play a role here, essentially related to the energy discontinuity. Their involvement is of course due to the degeneracy of the potential, which leads to the existence of tunnelling solutions interpolating between the minima. The perturbative expansion is performed around one specific harmonic well, and instanton–anti-instanton ($I\bar{I}$) solutions represent particles jumping from one well to another and subsequently returning to the same, original well. In a sense, therefore, it is not surprising to find that the $I\bar{I}$ action affects the (asymptotics of the) perturbation series. One indeed already suspect that also the four-instanton $I\bar{I}I\bar{I}$ action is involved at some level, and by extension any configuration with a neutral *'topological charge'*, that is, with an equal number of instantons and anti-instantons [21]. This is already anticipated in Sec. 4.3.5 and will be shown ex-

plicitly using the resurgence triangle (Sec. 5.4), which illuminates the intricate relations between perturbative non-perturbative physics.

The divergence is linked to a physical instability: in the case of potentials with degenerate minima, the perturbative vacuum state is susceptible to tunnelling instabilities which effectively alter the vacuum. The connection between divergence and instability can be traced back to Dyson's argument [18] concluding the generic divergence of perturbation series in QED, on grounds of physical intuition, even after mass and charge renormalisation. The QED framework leads to formal power series expansions of physical quantities in the fine-structure constant, $\alpha_e = e^2/4\pi$, which can be represented as

$$F(e^2) = f_0 + f_1 e^2 + f_2 e^4 + \dots . \tag{4.47}$$

Then, if this expression $F(e^2)$ converges for a given value of the fundamental charge $e > 0$, $F(-e^2)$ must converge as well, because power series converge in a disk. However, the transition to a world with negative e^2 would be dramatic, Dyson argues, as the vacuum would become unstable, due to the reversal of the sign in Coulomb's law. Through like-charge attraction, unbounded e^+e^- pair production would lead to continually growing clusters of like-charge particles in a pathological state with lower energy than the conventional vacuum. In Dyson's words, *"a system once in a pathological state will not remain steady; there will be a rapid creation of more and more particles, an explosive disintegration of the vacuum by spontaneous polarization"*. It is unthinkable that such conditions could lead to the calculation of a well-defined, analytic function $F(-e^2)$. Therefore, the series for $F(e^2)$ must have zero radius of convergence and $F(e^2)$ is not analytic in $e = 0$.

The essence of Dyson's argument can immediately be seen in the simpler quantum mechanical example of the quartic anharmonic oscillator [13, 50, 61–63], with the Schrödinger equation given by

$$\left[-\frac{\hbar^2}{2m}\partial_x^2 + \frac{1}{2}m\omega^2 x^2 + \gamma x^4\right]\psi = \varepsilon\psi \quad \longrightarrow \quad \left[-\partial_z^2 + z^2 + g x^4\right]\psi = E\psi, \tag{4.48}$$

following substitutions $x \to z\sqrt{\hbar/m\omega}$, $g = 2\gamma\hbar/m^2\omega^3$ and $E = 2\varepsilon/\hbar\omega$. When the dimensionless coupling constant g is positive, Fig. 4.5a shows a stable ground state. However, for negative g the potential is not bounded from below and there is no finite-

energy ground state. The dashed states in the central, harmonic well in Fig. 4.5b are metastable, due to the possibility of tunnelling through the potential barrier. By Dyson's reasoning, one expects the energy expansion $E(g) \sim \sum_n E_n g^n$ to have zero radius of convergence. This is indeed the case, the perturbative coefficients are alternating and grow factorially [13, 50, 61].

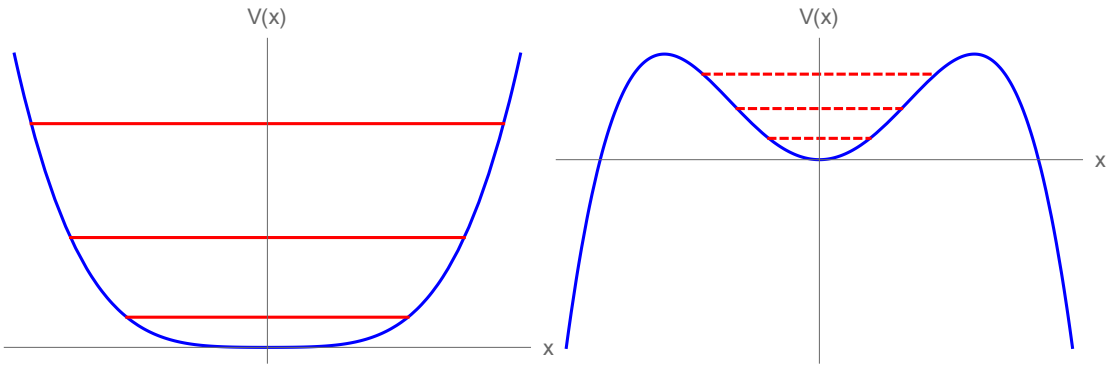

(a) $g > 0$ **(b)** $g < 0$

Figure 4.5: Anharmonic oscillator potential for positive and negative parameter g.

One concludes, for the quartic oscillator, that the non-analyticity of $E(g)$ and hence the divergence of its series expansion is the consequence of the tunnelling instability for $g < 0$. This entails that the asymptotic energy expansion diverges for $g > 0$, even though the potential cannot lead to instanton effects there. The origin of this divergence is really just the unstable situation for negative g, giving rise to instanton bounce solutions.

In the stable case ($g > 0$), the energy is Borel summable, since the singularities of the Borel transform occur on the negative real axis (as suggested[6] by the alternating perturbative coefficients) [13, 50]. However, in the unstable case ($g < 0$) the terms of the series take the form $(-1)^n E_n |g|^n$, so the Borel transform has singularities on the positive real axis and the series is not Borel summable. Lateral resummations give rise to an exponentially small imaginary contribution to the ground-state energy.

This sounds very much like the case of the sine-Gordon well, yet there is a crucial difference that should be pointed out: the quartic-oscillator ground state is fundamentally unstable due to false-vacuum decay, whereas the sine-Gordon potential has a sta-

[6] This is not a conclusive proof, though, as remarked in footnote 9.

ble ground state, albeit not a degenerate, perturbative one. Therefore, the ground-state energy should be real for this case, but is expected to be imaginary for the quartic oscillator with negative coupling! The decay width Γ of its ground state $E(g,0)$ can be found through instanton calculations or using the WKB approximation. The result can be compared to the imaginary part acquired during the resummation, and one finds [13, 50]

$$\frac{\Gamma}{2} = |\operatorname{Im} E(g,0)|, \tag{4.49}$$

as it should be if Γ is to represent the decay probability.

On the other hand, as it stands now, the imaginary part assigned to the resummed sine-Gordon energy is problematic. For the quartic oscillator, the lateral Borel resummation procedure is able to capture the non-perturbative aspect of the problem, whereas it is insufficient for the other case. To fix this, trans-series will be introduced in the next chapter. These provide a more adequate description of the non-perturbative sector and arise naturally when examining the degenerate harmonic-well problem (e. g. the double well and sine-Gordon well) from another point of view.

5

Resurgent trans-series to the rescue

5.1 Towards resurgence in the Mathieu spectrum

The framework of resurgence theory illuminates the explicit relations between perturbative and non-perturbative physics. As anticipated in the preceding chapters, a global perspective is indeed necessary to solve the problems arising in the local treatment. Perturbation theory for potentials with degenerate harmonic minima generically leads to divergent asymptotic series with non-alternating coefficients [21]. The difficulty, then, is two-fold: the series are non-Borel summable and lateral resummation results in an ambiguous, imaginary contribution to the energy eigenvalues of stable, bound states. These must be real, of course, which is the first concern, and also non-ambiguous on physical grounds, the second closely related issue.

Non-perturbative effects have to be accounted for explicitly, in order to resolve these problems, and that is the purpose of an analysis based on *resurgent trans-series*. Expressing the energy eigenvalues as a trans-series, a sum over both perturbative and non-perturbative components, enables one to capture the complete picture. Due to an elaborate set of precise relations between the perturbative series expansion and fluctuations about all of the non-perturbative sectors, the final result is real, as well as un-

ambiguous [21, 22]! The systematic cancellation of the ambiguous imaginary terms is encoded in the resurgence triangle, which also leads to a better understanding of the instanton effects mixing with perturbation theory, as encountered in the Mathieu problem in chapter 4.

This chapter reviews how trans-series and resurgent relations arise when studying the sine-Gordon potential, as described by Dunne and Ünsal in general for potentials with degenerate harmonic minima [21, 22, 59]. The key idea is the following: to obtain real, unambiguous energy eigenvalues, the local analysis from perturbation theory should be complemented with a global boundary condition containing information about the connection between the degenerate minima.

5.2 The uniform WKB strategy

As in the previous chapter, the Schrödinger equation for the sine-Gordon potential is written as

$$\left[-g^4\partial_y^2 + V(y)\right]\psi(y) = g^2 E\psi(y), \tag{5.1}$$

with $V(y) = \sin^2(y)$. The starting point of the perturbative analysis is the realisation that the sine-Gordon potential is locally harmonic, i. e. $V(y) \approx y^2$ in the limit where $g^2 \to 0$. Thus, the harmonic oscillator is a good local approximation, which motivates rewriting the wave function in terms of the parabolic cylinder functions $D_\nu(y)$ that solve the harmonic problem (previously encountered in (4.6)). Concretely, one can make the uniform WKB ansatz [21]

$$\psi(y) = \frac{D_\nu(\frac{1}{g}u(y))}{\sqrt{u'(y)}}, \tag{5.2}$$

where ν is a parameter that will be fixed by the global boundary condition. Since the problem reduces to the harmonic oscillator well when $g^2 \to 0$, it can already be seen that ν will be close to an integer N, the label of the energy level for the harmonic oscillator.

Noting that $D_\nu(y)$ is by definition the solution of the differential equation [60]

$$\partial_y^2 D_\nu(y) + \left(\nu + \frac{1}{2} - \frac{z^2}{4}\right), \tag{5.3}$$

it was verified that the Schrödinger equation (5.1) turns into a complicated nonlinear equation for $u(y)$, de facto the new wave function in the problem [21]:

$$V(y) - \frac{1}{4}(u')^2u^2 - g^2E + g^2\left(\nu + \frac{1}{2}\right)(u')^2 + \frac{1}{2}g^4\sqrt{u'}\left(\frac{u''}{(u')^{3/2}}\right)' = 0. \tag{5.4}$$

It can be noted that the ansatz parameter ν occurs in the equation, so both the energy and the wave function will depend on it. This equation can be solved perturbatively, by simultaneously expanding

$$E(\nu, g^2) = \sum_{n=0}^{\infty} g^{2n}E_n(\nu) \quad \text{and} \quad u(y, \nu, g^2) = \sum_{n=0}^{\infty} g^{2n}u_n(y, \nu). \tag{5.5}$$

To leading order in g^2, one obtains the harmonic-oscillator result $E_0 = 2\nu + 1$. An algorithm was written to obtain higher-order terms (App. D.3), leading to

$$E(B, g^2) = 2B - \frac{g^2}{2}\left[B^2 + \frac{1}{4}\right] - \frac{g^4}{8}\left[B^3 + \frac{3}{4}B\right] - \frac{g^6}{32}\left[\frac{5}{2}B^4 + \frac{17}{4}B^2 + \frac{9}{32}\right] - \dots \tag{5.6}$$

for the energy spectrum, in which $B = \nu + 1/2$. Of course, this is still merely a local analysis; if ν takes the integer value N, the standard perturbative result in (4.19) is recovered.

At this point, however, the parameter ν is not yet determined. As mentioned, it should be close to an integer N, so one may introduce a correction term $\delta\nu$, such that [**?**]

$$\nu(N, g^2) = N + \delta\nu(N, g^2). \tag{5.7}$$

Following from the global boundary condition relating the minima and properties inherent to the parabolic cylinder functions, it will be shown that $\delta\nu$ generally takes the form of a *trans-series*, incorporating summations over perturbative, exponentially small and logarithmic terms [21]:

$$\delta\nu(N, g^2) = \sum_{n=0}^{\infty}\sum_{k=1}^{\infty}\sum_{l=1}^{k-1} c_{n,k,l}\, g^{2n}\left[\frac{1}{g^{2N+1}}\mathrm{e}^{-S/g^2}\right]^k \ln\left(-\frac{1}{g^2}\right)^l, \tag{5.8}$$

where $c_{n,k,l}$ and S are constants. When $\nu(N, g^2)$ is found, it can be entered in the energy perturbation series (5.6), leading to the trans-series form of the N-th exact energy level,

obtained from an expansion around $\nu = N$:

$$E^{(N)}(g^2) = E(N, g^2) + \delta\nu \left[\frac{\partial E(\nu, g^2)}{\partial \nu}\right]_{\nu=N} + \frac{1}{2}(\delta\nu)^2 \left[\frac{\partial^2 E(\nu, g^2)}{\partial \nu^2}\right]_{\nu=N} + \dots . \tag{5.9}$$

The first term, $E(N, g^2)$, is simply the result from perturbation theory.

5.3 Global analysis: adding tunnelling to the picture

In order to get the full expression for the energy eigenvalues, beyond perturbation theory, additional information is required about the global features of the potential. After all, the perturbative result is only based on a local analysis in one specific well. As calculated in chapter 2, perturbative energy levels in the periodic sine-Gordon potential will split into a continuous energy band. It is well-known from solid-state physics that this is a consequence of Bloch's theorem. Given that the potential has period π, this theorem guarantees a basis of energy eigenstates that are Bloch waves and therefore satisfy the requirement [21]

$$\psi(y + \pi) = e^{i\theta}\psi(y), \tag{5.10}$$

for a Bloch parameter θ in $[0, \pi]$.

Luckily then, Floquet analysis ensures the existence of a non-zero solution with the required behaviour [21]. This kind of analysis of a second-order differential equation with periodic coefficients starts from the observation that two independent solutions form a complete basis of the solution space. With two different sets of initial conditions, one can define these fundamental solutions $w_1(y)$ and $w_2(y)$:

$$\begin{pmatrix} w_1(-\frac{\pi}{2}) & w_2(-\frac{\pi}{2}) \\ w_1'(-\frac{\pi}{2}) & w_2'(-\frac{\pi}{2}) \end{pmatrix} = \begin{pmatrix} 1 & 0 \\ 0 & 1 \end{pmatrix}. \tag{5.11}$$

In this way, the solutions are normalised at a point $y = -\frac{\pi}{2}$, here chosen to be the midpoint between two specific vacua of the sine-Gordon potential. It can now be shown that the desired Bloch solution $\psi(y)$ with parameter θ exists if and only if

$$\cos(\theta) = w_1\left(\frac{\pi}{2}\right). \tag{5.12}$$

The proof of such a relation was verified from [39].

In [21], explicit expressions were found for the normalised solutions $w_1(y)$ and $w_2(y)$, as combinations of the parabolic cylinder functions $D_\nu(\pm u(y)/g)$. Hence, for any angle θ in $[0,\pi]$, the Bloch condition (5.10) fixes ν as a function of g^2, at least in principle. However, the perturbative expansion of the argument function $u(y)$ diverges and is non-Borel summable on the Stokes line $g^2 > 0$ [21], which necessitates a lateral Borel resummation and leads to an ambiguous imaginary contribution to $u(y)$. Thus, the argument of the parabolic cylinder functions becomes complex, and in the limit of $|g^2| \to 0$, its asymptotic behaviour off the real axis should be used. In the end, the Bloch boundary condition can be written as [21]

$$\frac{1}{\Gamma(-\nu)}\left(\frac{2}{g^2}\right)^{-\nu} \pm i\frac{\pi}{2}\left(\frac{2\mathrm{e}^{\pm i\pi}}{g^2}\right)^{\nu}\frac{\xi^2 H_0(\nu,g^2)^2}{\Gamma(\nu+1)} = -\xi H_0(\nu,g^2)\cos(\theta). \tag{5.13}$$

In this expression, the *instanton fugacity*

$$\xi = \sqrt{\frac{2S_I}{\pi g^2}}\mathrm{e}^{-S_I/g^2} \tag{5.14}$$

is each time accompanied by a factor $H_0(\nu,g^2)$ describing a perturbative series of fluctuations around the instanton [21]. It should be stressed that the form of this equation is entirely a consequence of the Bloch condition and the analytic continuation properties of the parabolic cylinder functions in the complex plane.

Now, the boundary condition (5.13) can be expanded in $\delta\nu = \nu - N$, with $N = 0$ for the ground state. From the resulting relation, $\delta\nu$ is extracted as a trans-series, with the definitions $H_0 = H_0(0,g^2)$ and $H_0' = \partial_\nu H_0(0,g^2)$ [21]:

$$\begin{aligned}\delta\nu = &\left[-\frac{1}{2}\xi H_0\mathrm{e}^{i\theta} - \frac{1}{2}\xi H_0\mathrm{e}^{-i\theta}\right] + \\ &\left[\frac{1}{4}\xi^2(H_0H_0' + H_0^2Q_1)\mathrm{e}^{2i\theta} + \frac{1}{2}\xi^2(H_0H_0' + H_0^2Q_1^{\pm}) + \frac{1}{4}\xi^2(H_0H_0' + H_0^2Q_1)\mathrm{e}^{-2i\theta}\right] + \dots.\end{aligned} \tag{5.15}$$

Several comments are in order. Firstly, this is an expansion in powers of $\xi \sim \mathrm{e}^{-S_I/g^2}$, with ξ^n associated to a correlated n-instanton event with action nS_I, that can no longer be considered as n widely separated events as in the dilute-gas approximation. On

the first line, the term proportional to $e^{i\theta}$ is related to an instanton event $\mathcal{I}$, whereas the other one is related to an anti-instanton event $\overline{\mathcal{I}}$ [21]. In general, the power m in $e^{im\theta}$ is called a topological charge or winding number – in this context, it is simply the difference between the number of instantons and anti-instantons in the event. On the other hand, the power n in ξ^n denotes the sum of the number of instantons and anti-instantons, and necessarily $|m| \leq n$ holds.

Furthermore, the second line has contributions from the sectors $[\mathcal{I}\mathcal{I}]$, $[\mathcal{I}\overline{\mathcal{I}}]$ (and $[\overline{\mathcal{I}}\mathcal{I}]$) and $[\overline{\mathcal{I}}\overline{\mathcal{I}}]$. The Q_n and $Q_n^{\pm}$ are so-called quasi-zero mode polynomials of degree n. Physically, these arise due to instanton interaction, i. e. the fact that the action of two consecutive oscillations between vacua is slightly different from the sum of the actions of two separate, single oscillations. The $Q_n^{\pm}$ polynomials occur when instantons are combined with anti-instantons into a correlated $n+1$-instanton event, leading to an attractive interaction [32, 65]. These factors lead to an ambiguous imaginary contribution. For example, $Q_1^{\pm} = \gamma + \ln\left(2e^{\pm i\pi}/g^2\right)$, where γ is the Euler-Mascheroni constant [21]. Such ambiguities are not seen for (anti-)instanton-only events, where Q_n is a real contribution since the instanton-instanton interactions are repulsive.

Finally, it can be stressed that all building blocks of the trans-series announced in (5.8) are present: perturbative series in the H_0 fluctuations, logarithms in the quasi-zero mode polynomials and exponentially small factors in the instanton fugacity.

5.4 The resurgence triangle

The resurgence triangle (Table 5.1) provides a graphical interpretation of the structure of the contributions in a trans-series [21]. Rows in the triangle are characterised by a fixed action nS_I and columns have fixed topological charge m. A perturbative series of fluctuations around a contribution (n, m) is denoted by $f_{(n,m)}$. Standard perturbation theory corresponds to $f_{(0,0)}$, and multi-instanton events of the form $[\mathcal{I}^k\overline{\mathcal{I}}^l]$ end up classified in the cell $(k+l, k-l)$.

At this point, it can be clearly understood which sectors can interfere with perturbation theory: those with zero topological charge. This explains why the asymptotics of the perturbative ground state of the sine-Gordon potential were governed by 2- and 4-instanton effects, since an even number is necessary to ensure equal numbers of instantons and anti-instantons. Other sectors have a θ-dependence which standard pertur-

				$f_{(0,0)}$				
			$\xi e^{i\theta} f_{(1,1)}$		$\xi e^{-i\theta} f_{(1,-1)}$			
		$\xi^2 e^{2i\theta} f_{(2,2)}$		$\xi^2 f_{(2,0)}$		$\xi^2 e^{-2i\theta} f_{(2,-2)}$		
	$\xi^3 e^{3i\theta} f_{(3,3)}$		$\xi^3 e^{i\theta} f_{(3,1)}$		$\xi^3 e^{-i\theta} f_{(3,-1)}$		$\xi^3 e^{-3i\theta} f_{(3,-3)}$	
$\xi^4 e^{4i\theta} f_{(4,4)}$		$\xi^4 e^{2i\theta} f_{(4,2)}$		$\xi^4 f_{(4,0)}$		$\xi^4 e^{-2i\theta} f_{(4,-2)}$		$\xi^4 e^{-4i\theta} f_{(4,-4)}$

Table 5.1: The resurgence triangle for a periodic potential. Only the first 5 rows are shown.

bation theory does not have. Columns which have different topological charge cannot mix or cancel each other's ambiguities [21]. However, as noted above, the sectors combining instantons and anti-instantons and specifically those with zero charge like $[\mathcal{I}\overline{\mathcal{I}}]$ and $[\mathcal{I}\mathcal{I}\overline{\mathcal{I}\mathcal{I}}]$ give rise to imaginary ambiguities that open possibilities for cancelling ambiguities of the perturbative series. Indeed, it turns out that very precise cancellations do occur.

To show the cancellation mechanism explicitly for the sine-Gordon potential, one starts by writing the trans-series expansion for the ground-state energy ($N = 0$):

$$E^{(0)}(g^2) = E\left(1/2, g^2\right) + \delta\nu \left[\frac{\partial E(B, g^2)}{\partial B}\right]_{B=\frac{1}{2}} + \dots . \tag{5.16}$$

Here, the first term is the non-Borel summable series which led to an imaginary ambiguity proportional to e^{-2S_I/g^2} (4.43). Fortunately, an ambiguity occurs in $\delta\nu$ at exactly the right order ξ^2 in the two-instanton sector. Its imaginary contribution to the trans-series can be calculated and was explicitly obtained in [21]:

$$\begin{aligned} \mathrm{Im}\left[\delta\nu \frac{\partial E(B, g^2)}{\partial B}\right]_{B=\frac{1}{2}} &= \pm 2\pi\xi^2 \left(1 - \frac{3g^2}{8} - \frac{13g^4}{128} - \dots\right)\left(1 - \frac{g^2}{4} - \frac{3g^4}{32} - \dots\right) && (5.17) \\ &= \pm 2\pi\xi^2 \left(1 - \frac{5g^2}{8} - \frac{13g^4}{128} - \dots\right), && (5.18) \end{aligned}$$

which cancels the imaginary ambiguity incurred by the lateral Borel resummation (4.43) also beyond leading order, as can be seen from the agreement between the series coefficients. Such an extension of the Bogomolny–Zinn-Justin cancellation mechanism gives rise to the notion of Borel-Écalle summability, the modern understanding of resurgent asymptotics [59].

Based on multi-instanton calculus and numerical analysis, Zinn-Justin and Jentschura conjectured an exact quantisation condition to complement perturbative results for several potentials like the double well and the sine-Gordon potential [23, 24]. For the latter, the condition was given by

$$\left(\frac{2}{g^2}\right)^{-B(E,g^2)} \frac{\mathrm{e}^{A(E,g^2)/2}}{\Gamma\left(\frac{1}{2}-B(E,g^2)\right)} + \left(-\frac{2}{g^2}\right)^{B(E,g^2)} \frac{\mathrm{e}^{-A(E,g^2)/2}}{\Gamma\left(\frac{1}{2}+B(E,g^2)\right)} = \frac{2\cos(\theta)}{\sqrt{2\pi}}, \quad (5.19)$$

for which the function $B(E,g^2)$ was computed from perturbation theory and $A(E,g^2)$ was a non-perturbative function computed by a combination of numerical studies and analysis. The condition determines the energy when those two functions are known. The $B(E,g^2)$ function is in fact just the inversion of the perturbative uniform WKB result (5.6) [21, 22]. However, the uniform WKB approach is philosophically different from the Zinn-Justin–Jentschura method: the uniform WKB approach leads to a perturbative calculation of $E(B,g^2)$ and the exact quantisation condition would be considered to determine $B(g^2)$ when $A(B,g^2)$ is known, so that the exact energy eigenvalue can be obtained by plugging $B(g^2)$ into the energy series [21].

Interestingly, Dunne and Ünsal [21, 22] found an explicit relation between $E(B,g^2)$ and the non-perturbative function $A(B,g^2)$:

$$\frac{\partial E}{\partial B} = -\frac{g^2}{S}\left(2B + g^2\frac{\partial^2 A}{\partial(g^2)}\right), \quad (5.20)$$

in which S denotes the instanton action coefficient in $\xi = \mathrm{e}^{-S/g^2}/\sqrt{\pi g^2}$. Astonishingly, this result implies that all non-perturbative information of $A(B,g^2)$ is somehow encoded in perturbation theory, that is, in $E(B,g^2)$. Considering the difficult multi-instanton calculus that wasrequired to find $A(E,g^2)$, the Dunne–Ünsal relation and its simplicity are very surprising, and the sign of very tight resurgent relations between perturbative and non-perturbative sectors.

6

Conclusions and Outlook

Non-perturbative effects abound in nature, in the strongly-coupled regime of renormalisable quantum field theories like QCD, as well as in quantum mechanical systems. General arguments assert that the problems with a perturbative approach are not limited to strong-coupling phenomena, but that even expansions in quantum mechanics and QED diverge generically. The Borel resummation of factorially divergent perturbation series leads to a resolution in some cases, effectively repairing the divergence by reinterpreting the series as an asymptotic expansion of a well-defined integral.

However, non-Borel summable series arise often in quantum mechanical settings, and even generally for potentials that have degenerate, harmonic minima. For these, the resummation procedure gives rise to ambiguous imaginary contributions to observable quantities, like energies of stable states, that should be real and unambiguous on physical grounds. The conclusion is that perturbation theory, on its own, is incomplete. Nature is not bound by perturbation theory, after all, and a more comprehensive treatment is required to obtain physical results. For instance, important non-perturbative effects due to tunnelling (e. g. energy level splitting and band structures) are not accounted for in a perturbative approach. In the path integral formalism of quantum mechanics, these features arise from instantons, finite-action solutions to the classical equations of motion in Euclidean spacetime.

Motivated by its relevance in QCD toy models and as a concrete example of a quantum problem leading to a divergent expansion, the spectrum of the sine-Gordon potential was examined in more detail, starting from the perturbative treatment of the characteristic values of the Mathieu equation. For the ground-state energy, the Stone–Reeve recurrence relations were used to efficiently compute the perturbation coefficients. Using this algorithm, up to 1000 orders in perturbation theory were obtained exactly in this thesis, which enabled the assessment of the large-order behaviour to an unprecedented degree of accuracy. The determined sub-leading corrections to the asymptotics of perturbation theory correspond to fluctuations around the non-perturbative sector connected to instanton–anti-instanton $[\mathcal{I}\overline{\mathcal{I}}]$ events, as illuminated by the resurgence framework. This connection was illustrated by approximations of the singularity structure of the Borel-transformed series, converging to a branch cut at the expected location on the positive real axis of the Borel plane.

Furthermore, in this thesis it was explicitly demonstrated that the $[\mathcal{I}\overline{\mathcal{I}}]$ fluctuation coefficients form a divergent asymptotic series by themselves. Their leading asymptotics were calculated and, in a striking manifestation of the underlying resurgent structure, they were associated to a higher-order non-perturbative effect involving a part of the 4-instanton $[\mathcal{I}\mathcal{I}\overline{\mathcal{I}\mathcal{I}}]$ sector. Thus, there is much more information hidden in a divergent perturbation series than a first look would suggest.

A trans-series expansion of the energy eigenvalues shows that the subsequent divergences were in fact a blessing in disguise. Naturally arising from the uniform WKB approximation complemented with a global quantisation condition, the trans-series brings perturbative and non-perturbative multi-instanton sectors together in a unified expression, where the non-perturbative part develops imaginary ambigituities tracing back to instanton interactions. The final result is real and unambiguous, as it should be, due to intricate sequences of cancellations occurring throughout all orders in the trans-series. Moreover, for the case of potentials with degenerate harmonic minima, the non-perturbative contributions surprisingly seem to be completely encoded in the perturbation series, a sign of very tightly constrained resurgent relations between the perturbative and instanton sectors, or equivalently, between the saddle points of the path integral. Of course, this situation with degenerate harmonic minima is special, and resurgence theory does not imply that perturbation theory generally contains all information about the non-perturbative sector. Instead, the resurgence triangle regulates how sectors with the same topological charge can conspire to cancel ambiguities.

The results in this thesis provide non-trivial numerical confirmations of the resurgent structure in the quantum mechanical sine-Gordon problem. Rigorous results from path integral calculations of higher-order multi-instanton amplitudes, along the lines of [1], would provide further evidence that boundary condition used to complement the uniform WKB approach leads to the exact connection between perturbation theory and non-perturbative sectors. Furthermore, the mathematical tools described in this work were sufficient to study a special class of quantum mechanical potentials. However, more complicated situations often arise in the description of the low-energy dynamics of quantum field theories. For instance, singularies of the Borel transform are generally not restricted to the real axis, but can occur at any location in the complex Borel plane. An interesting extension of the methods used in this thesis is the study of their interpretation as complex instanton saddle points and their influence on the large-order behaviour of asymptotic series in connection to resurgence [2, 3]. In addition, transseries give potentially exact asymptotic expansions of physical observables in the calculable, semi-classical regime of field theories, but currently, it is not completely understood how to continue such a description to strongly-coupled regimes [2–5, 64]. Nevertheless, the resurgence paradigm might lead the way in connecting weak and strong coupling.

A

Schrödinger picture of quantum mechanics

In the Schrödinger picture, the time development of a quantum mechanical system is handled by letting the state kets $|\psi(t)\rangle$ carry the time-dependence and transform according to the *Schrödinger equation*:

$$i\hbar\frac{\partial}{\partial t}|\psi(t)\rangle = H|\psi(t)\rangle\,. \tag{A.1}$$

Here, H denotes the system's Hamiltonian operator in the Schrödinger picture. A formal solution for this equation in the case of a time-independent[1] Hamiltonian can be given in terms of the system state at some reference time t_0:

$$|\psi(t)\rangle = \mathrm{e}^{-iH(t-t_0)/\hbar}|\psi(t_0)\rangle\,. \tag{A.2}$$

It can be noted that $U(t,t_0) \equiv \mathrm{e}^{-iH(t-t_0)/\hbar}$ is the unitary *time evolution operator* connecting system state vectors at different times. Unitarity ensures the state stays normalised

[1] A time-dependent Hamiltonian would give a time-ordered exponential as the time evolution operator [46]: $U(t,t_0) = \mathcal{T}\left[\exp\left(-(i/\hbar)\int_{t_0}^{t}\mathrm{d}t' H(t')\right)\right]$.

at any time.

In the limit where t tends to t_0, the time evolution should logically become the identity operation:

$$\lim_{t \to t_0} U(t, t_0) = \mathbb{1}. \tag{A.3}$$

Substituting (A.2) into (A.1), one finds that $U(t, t_0)$ must also satisfy

$$i\hbar \frac{\partial U}{\partial t}(t, t_0) = HU(t, t_0) \tag{A.4}$$

Now, a non-relativistic particle with mass m can be considered, travelling in a one-dimensional space and described by the Hamiltonian

$$H = \frac{\hat{p}^2}{2m} + V(\hat{x}), \tag{A.5}$$

where $\hat{x}$ and $\hat{p}$ are the position and momentum operators, and $V(\hat{x})$ denotes the potential. The canonical commutation relations require that $[\hat{x}, \hat{p}] = \hat{x}\hat{p} - \hat{p}\hat{x} = i\hbar\mathbb{1}$.

When acting on the position eigenbasis, the operator $\hat{p}$ can be more conveniently expressed as $\hat{p} = -i\hbar(\partial/\partial x)$. Then, in terms of the matrix elements of U, (A.4) becomes

$$i\hbar \frac{\partial}{\partial t} \left\langle x_f \middle| U(t_f, t_i) \middle| x_i \right\rangle = \left[-\frac{\hbar^2}{2m} \frac{\partial^2}{\partial x^2} + V(x) \right] \left\langle x_f \middle| U(t_f, t_i) \middle| x_i \right\rangle. \tag{A.6}$$

The requirement in (A.3) translates to a boundary condition for this differential equation:

$$\left\langle x_f \middle| U(t_f, t_i) \middle| x_0 \right\rangle = \delta(x_f - x_i). \tag{A.7}$$

A formal solution of (A.6) for the matrix element can then found to be given as a path integral [46]:

$$\left\langle x_f \middle| \mathrm{e}^{-iH(t_f - t_i)/\hbar} \middle| x_i \right\rangle = N \int \mathcal{D}[x(t)] \, \mathrm{e}^{iS[x(t)]/\hbar}, \tag{A.8}$$

In this expression, N is a normalisation factor and $\int \mathcal{D}[x(t)]$ refers to integration over all trajectories satisfying the boundary conditions $x(t_i) = x_i$ and $x(t_f) = x_f$. The action $S[x(t)]$ is defined in terms of the Lagrangian by $L(x, \dot{x})$ as

$$S[x(t)] = \int_{t_i}^{t_f} \mathrm{d}t \; L(x, \dot{x}) = \int_{t_i}^{t_f} \mathrm{d}t \left[\frac{1}{2} m\dot{x}^2 - V(x) \right]. \tag{A.9}$$

B

Unifying sine-Gordon notations

The comparison between results concerning resurgence features is often complicated due to the lack of uniformity in conventions. In the relevant literature, sine-Gordon and cosine potential expressions tend to differ, for various reasons. In this section, a short dictionary is constructed to facilitate switching between notations.

B.1 Comparing energy expansions

The time-independent Schrödinger equation for the cosine potential (with $m = 1$),

$$\left[-\frac{\hbar^2}{2}\partial_x^2 + \cos(x)\right]\psi(x) = E_c\psi(x), \tag{B.1}$$

can be turned into the textbook Mathieu equation,

$$\left[\partial_z^2 + (a - 2q\cos(2z))\right]\psi(z) = 0. \tag{B.2}$$

To obtain this form, it suffices to perform a change of variables ($x \to 2z$) and relate the real parameters a (the *characteristic value*) and q of the Mathieu equation with the energy

E_c and the coupling $\hbar$:

$$a = \frac{8E_c}{\hbar^2} \quad \text{and} \quad q = \frac{4}{\hbar^2}. \tag{B.3}$$

The perturbative energy expansion coefficients a_n, as described by Stone and Reeve [41] in the notation

$$a = -\frac{k^2}{2} + k \sum_{n=0}^{\infty} \frac{a_n}{k^n} \qquad (\text{with } k^2 = 4q), \tag{B.4}$$

are also immediately related to the $E_n^{(c)}$ coefficients in

$$E_c = \sum_{n=0}^{\infty} E_n^{(c)} \hbar^n. \tag{B.5}$$

The latter form is useful to compare with results of Dunne and Ünsal [59]. Since $k = 4/\hbar$, one quickly finds

$$E_n^{(c)} = \frac{1}{2} \left(\frac{a_{n-1}}{4^{n-1}} \right). \tag{B.6}$$

To convert from the Mathieu equation (B.2) to the sine-Gordon convention used in earlier Dunne–Ünsal work [21],

$$\left[-g^4 \partial_y^2 + \sin^2(y) \right] \psi(y) = g^2 E_s \psi(y), \tag{B.7}$$

one can change variables ($x \to y + \pi/2$) to get the minus sign right and use standard trigonometry to switch to a squared sine. The correspondence is then given by

$$g^2 = \frac{1}{k} \quad \text{and} \quad E_s = \frac{1}{k} \left(a + \frac{1}{2} k^2 \right). \tag{B.8}$$

Comparing the expansions (B.4) and

$$E_s = \sum_{n=0}^{\infty} E_n^{(s)} (g^2)^n, \tag{B.9}$$

one retrieves that the expansion coefficients in both notations should be equal:

$$E_n^{(s)} = a_n. \tag{B.10}$$

Zinn-Justin and Jentschura [23, 24] use a different convention, with a somewhat pe-

culiar scaling to avoid large numerical factors in calculations:

$$\left[-\frac{g_{ZJ}}{2}\partial_y^2 + \frac{1}{16g_{ZJ}}(1-\cos(4y))\right]\psi(y) = E_{ZJ}\psi(y). \tag{B.11}$$

To make the comparison with the sine-Gordon energy in B.7, one rewrites the cosine and changes variables, yielding the conversions

$$E_s = 2E_{ZJ} \quad \text{and} \quad g^2 = 4g_{ZJ}. \tag{B.12}$$

The cosine-well energy in (B.1) can be retrieved by

$$\hbar = 16g_{ZJ} \quad \text{and} \quad E_c = -1 + \hbar E_{ZJ}. \tag{B.13}$$

B.2 Comparing instanton actions

In the discussion of the cosine potential (B.1), the energy E_c and its expansion coefficients, the relevant instanton action (connecting minima at $x = \pm\pi$) is

$$S_I^{(c)} = \sqrt{2}\int_{-\pi}^{+\pi} \mathrm{d}x\, \sqrt{\cos(x)+1} = 8. \tag{B.14}$$

To obtain this action, the potential $V(x) = \cos(x)$ was shifted by its minimum value to $V(x) - V_{\min}$, following the conventions and Chapter 2 and ensuring the integral is real. Obviously, this step does not influence the underlying physics.

To find the instanton action in the sine-Gordon case, of importance in the study of the energy expansion coefficients $E_n^{(s)} = a_n$, one should see (B.7) as the Schrödinger equation. If g^2 is identified with $\hbar$, the relevant potential is actually

$$V(y) = \frac{1}{2}\sin^2(y). \tag{B.15}$$

Hence, the instanton action becomes

$$S_I^{(s)} = \sqrt{2}\int_0^{\pi} \mathrm{d}y\, \sqrt{\frac{1}{2}\sin^2(y)} = 2. \tag{B.16}$$

With the scaling conventions (B.11) of Zinn-Justin–Jentschura, the instanton action

is given by

$$S_I^{(ZJ)} = \sqrt{2}\int_0^{\pi/2} \mathrm{d}q \sqrt{\frac{1}{8}\sin^2(2q)} = \frac{1}{2}. \tag{B.17}$$

C

Large-order behaviour of sine-well energy coefficients

C.1 Large-order growth correction terms

Table C.1 contains the continuation of Table 4.2 in Sec. 4.3.1.

C.2 Two-instanton fluctuation coefficients

Table C.2 contains the continuation of Table 4.3 in Sec. 4.3.2.

m	$s_m \times \pi$	m	$s_m \times \pi$
0	1	1	$-5/2$
2	$+7/2^3$	3	$-133/2^4$
4	$-5113/2^7$	5	$-91743/2^8$
6	$-3661721/2^{10}$	7	$-84598977/2^{11}$
8	$-17590968821/2^{15}$	9	$-507207324271/2^{16}$
10	$-32088414087407/2^{18}$	11	$-1104069776270571/2^{19}$
12	$-164148193706161181/2^{22}$	13	$-6553772212163835987/2^{23}$
14	$-559481302507973028633/2^{25}$	15	$-25426483678220344595353/2^{26}$
16	$-19615467146385102142587533/2^{31}$		
17	$-10002716443693131734120490 71/2^{32}$		
18	$-10759075809029769683253302 8915/2^{34}$		
19	$-60870974684364299185957282 26503/2^{35}$		
20	$-14458217899764880198837635 13233063/2^{38}$		
21	$-89919728321103957779354040 981269713/2^{39}$		
22	$-11691797035016873835533993 781820349263/2^{41}$		
23	$-79315602074246477236667176 2134305164727/2^{42}$		
24	$-44842435439766046011833792 1407439976223585/2^{46}$		
25	$-32962951593651299790747152 345043895174587043/2^{47}$		
26	$-50334778168105208904076527 389716032294510705 71/2^{49}$		
27	$-39863511710362479191182844 946101146415152483 8247/2^{50}$		
28	$-13082655046512316209874389 784053572604429607 2632101/2^{53}$		
29	$-11107106069040752861658113 679679183902446949 967076667/2^{54}$		
30	$-19494114468774220717418710 651937463462168610 22158561049/2^{56}$		
31	$-17664244868398197445695929 984679345192311038 7622259277001/2^{57}$		
32	$-52836391421820746493437423 877068220573611722 843961233658 1693/2^{63}$		

Table C.1: Coefficients s_m determining the large-order growth of the ground-state energy expansion coefficients a_n.

n	$a_n^{I\bar{I}}$	n	$a_n^{I\bar{I}}$
0	1	1	$-5/2^3$
2	$-13/2^7$	3	$-119/2^{10}$
4	$-5225/2^{15}$	5	$-68715/2^{18}$
6	$-2079317/2^{22}$	7	$-35323847/2^{25}$
8	$-5308543701/2^{31}$	9	$-109138963047/2^{34}$
10	$-4874789697291/2^{38}$	11	$-117581214668481/2^{41}$
12	$-12194607448373997/2^{46}$	13	$-338509879992444423/2^{49}$
14	$-20048562693726158917/2^{53}$	15	$-631295301078915611495/2^{56}$
16	$-337187598202647196312397/2^{63}$		
17	$-11900312168249161987119903/2^{66}$		
18	$-88578015288768277531556126 3/2^{70}$		
19	$-34679729040319204350926700509/2^{73}$		
20	$-57007458276977857042569339453 35/2^{78}$		
21	$-24540075526729035454187854843 1125/2^{81}$		
22	$-22088362349425969530451216139733395/2^{85}$		
23	$-10374288128319361068006319352078479 53/2^{88}$		
24	$-40612340166776845435086524411995627 8401/2^{94}$		
25	$-20673313793352749113542308294233422659819/2^{97}$		
26	$-21862884408882315706025284026065664896281 83/2^{101}$		
27	$-11992360196210668678898663683724615634438 2277/2^{104}$		
28	$-27261158628566727671572738449726810105367526325/2^{109}$		
29	$-16032225271318925803632289893986658656367638913 27/2^{112}$		
30	$-19492266772735085659523314808390115988684717681 0149/2^{116}$		
31	$-12235966038002485789598639287191177591888127470138279/2^{119}$		
32	$-25355754710505397705124008870602516379698634512652059069/2^{127}$		

Table C.2: Two-instanton fluctuation coefficients $a_n^{I\bar{I}}$ corresponding to corrections to the large-order growth of the ground-state energy expansion coefficients a_n.

D

Analysis code

```
nMax = 1002;
Module[{A, ll, sol, l, j, k},
 eq[l_, j_] := 4 j A[l, j] - 4 (j + 1) A[l, j + 1] - j (j - 1 / 2) A[l - 1, j - 1] +
   (j (j + 1) + 1 / 2) A[l - 1, j] - Sum[-4 A[n, 1] A[l - n, j], {n, 2, l}];
 A[0, 0] = 1; A[1, 1] = 1 / 8;
 For[l = 1, l < nMax, l++, For[j = 1, j < nMax, j++,
   If[l ≠ 0, A[l, 0] = 0]; If[j ≠ 0, A[0, j] = 0];
   If[l < 0, A[l, j] = 0]; If[j > l, A[l, j] = 0];
   If[j == l, A[l, j] = (l - 1 / 2) A[l - 1, l - 1] / 4;];]];
 a[0] = 1; a[1] = -1 / 4;
 For[n = 2, n < nMax, n++, For[k = 1, n - k > 0, k++,
   sol = Solve[eq[n, n - k] == 0, A[n, n - k]];
   A[n, n - k] = A[n, n - k] /. First@sol;];
  a[n] = -4 A[n, 1]; ll = n - 1;
  b[ll] = 4 A[ll + 1, 1] * 4 ^ ll / Factorial[ll + 1];
  Clear[n];]

For[l = 1, l ≤ 1000, ++l, b[l] = N[b[l], {Infinity, 10 000}]];
Block[{n = 800, NN = 200, $MaxExtraPrecision = ∞, m, l, j},
  s[0] = Sum[(b[n + j] (n + j) ^ NN (-1) ^ (NN + j)) / (Factorial[j] * Factorial[NN - j]),
    {j, 0, NN}];
  ss[0] = s[0]; s[0] = RootApproximant[N[s[0] * Pi, 25], 1] / Pi;
  b̄[m_] := b[m];
  Do[b̄[m_] = m (b̄[m] - s[l - 1]);
   s[l] = Sum[(b̄[n + j] (n + j) ^ NN (-1) ^ (NN + j)) / (Factorial[j] * Factorial[NN - j]),
     {j, 0, NN}];
   If[l < 33, s[l] = RootApproximant[N[s[l] * Pi, {∞, 130}], 1] / Pi;],
   {l, 1, 65}];];
Block[{$MaxExtraPrecision = Infinity}, growthcoeff = Table[s[l] * Pi, {l, 1, 65}];]
Print[growthcoeff[[1 ;; 10]]];

FacSeries[coeff_] :=
  Block[{$MaxExtraPrecision = Infinity, series, facseries, newfacseries,
    n, m, newcoeff, mMax, mStart},
   mMax = Length[coeff];
   mStart = 1; (*start at 1st-order term, NOT CONSTANT TERM! *)
   series = Sum[coeff[[m]] / (n - 1) ^ (m), {m, mStart, mMax}];
   facseries = Sum[newcoeff[m] Pochhammer[n, -m + 1] / n, {m, mStart, mMax}];
   newfacseries = Series[facseries, {n, Infinity, mMax}];
   Do[
    sol = Solve[SeriesCoefficient[facseries, {n, Infinity, m}] ==
       SeriesCoefficient[series, {n, Infinity, m}], newcoeff[m]];
    newcoeff[m] = newcoeff[m] /. First@sol;,
    {m, mStart, mMax}];
   Return[Table[newcoeff[m], {m, mStart, mMax}]];
  ];

facgrowthcoeff = FacSeries[growthcoeff[[1 ;; 65]]];

Block[{$MaxExtraPrecision = Infinity},
  redfacgrowthcoeff = Table[facgrowthcoeff[[n]] / (4 ^ (n)), {n, 1, 65}];];
redfacgrowthcoeff[[1 ;; 32]]

data = Table[{n, redfacgrowthcoeff[[n + 1]] / redfacgrowthcoeff[[n]]},
   {n, 1, Length[redfacgrowthcoeff] - 1}];
Block[{$MaxExtraPrecision = Infinity}, linmodel = aa + bb (n + 0);
 fitsol = FindFit[data[[35 ;; 64]], linmodel, {aa, bb}, n];
 Print[N[{aa, bb} /. fitsol]];
 fitfun = Function[{n}, Evaluate[linmodel /. fitsol]];
 plot = Plot[fitfun[n], {n, 1, Length[redfacgrowthcoeff] - 1}, PlotStyle → Red,
   Epilog → {Blue, Map[Point, data]}, AxesLabel → {"n", "a^II_{n+1} / a^II_n"}];
 Print[plot];]
```

```
PadeApprox[coeff_, g_, N_, M_] := Module[{res},
   (*coeff = list of coefficients such that Sum[c[n]g^n,{n,0,Infty}] is the power series to
     be approximated, with coeff[N+M] the last element*)
   If[Length[coeff] < N + M + 1, Print["Length[coeff]<N+M+1"],
     If[N ≥ M,
      CMatrix = Table[coeff[[N + i - j + 1]], {i, 1, M}, {j, 1, M}];,
      CMatrix = PadRight[Table[coeff[[N + i - j + 1]], {i, 1, M}, {j, 1, Min[M, N + i]}]]];
     (*i list outermost in nested structure,
     pad with zeros for square matrix: to implement coeff[l≤0]=0*)
     CMatrixInv = Inverse[CMatrix];
     (*DenomCoeff[[0+1]]=1;*)
     DenomCoeff = -CMatrixInv.Table[coeff[[N + i + 1]], {i, 1, M}];
     DenomCoeff = Prepend[DenomCoeff, 1];

     NumCoeff = Table[Sum[coeff[[n - j + 1]] DenomCoeff[[j + 1]], {j, 0, n}], {n, 0, N}];
     res = Sum[NumCoeff[[n + 1]] g^n, {n, 0, N}] / Sum[DenomCoeff[[m + 1]] g^m, {m, 0, M}];
     Return[res];
    ];
  ];

PadeRatio[lMax_] := Block[{$MaxExtraPrecision = Infinity, TrueCoeff, s, p, cEst, cTrue, cRatio},
  TrueCoeff = Table[c[l], {l, 0, lMax}];
  s = SeriesData[g, 0, TrueCoeff, 0, lMax + 1, 1]; (*TrueCoeff[[1;;lMax+1]]*)
  pa = PadeApproximant[Normal[s], {g, 0, {Floor[lMax / 2], Floor[lMax / 2] + Mod[lMax, 2]}}];
  cEst = SeriesCoefficient[pa, {g, 0, lMax + 1}];
  cTrue = c[lMax + 1];
  cRatio = Abs[(cEst - cTrue) / cTrue];
  Return[cRatio];
 ]


PadeRatioDetails[lMax_] := Module[{TrueCoeff, s, p, cEst, cTrue, cRatio},
  TrueCoeff = Table[c[l], {l, 0, lMax}];
  s = SeriesData[g, 0, TrueCoeff[[1 ;; lMax + 1]], 0, lMax + 1, 1];
  p = PadeApproximant[Normal[s], {g, 0, {Floor[lMax / 2], Floor[lMax / 2] + Mod[lMax, 2]}}];
  cEst = SeriesCoefficient[p, {g, 0, lMax + 1}];
  cTrue = c[lMax + 1];
  cRatio = Abs[(cEst - cTrue) / cTrue];
  Print["s = ", s];
  Print["p = ", Series[p, {g, 0, lMax + 1}]];
  Print["cEst = ", cEst];
  Print["cTrue = ", cTrue];
  Print["cRatio = ", cRatio];
  Return[cRatio];
 ]

PadeZeros[lMax_] := Block[{$MaxExtraPrecision = Infinity, TrueCoeff, s, p, DenomZeros},
  TrueCoeff = Table[c[l] / Factorial[l], {l, 0, lMax}];
  s = SeriesData[g, 0, TrueCoeff, 0, lMax + 1, 1];
  p = PadeApproximant[Normal[s], {g, 0, {Floor[lMax / 2], Floor[lMax / 2] + Mod[lMax, 2]}}];
  DenomZeros = NSolve[Denominator[p] == 0, g];
  Return[DenomZeros];
 ]

Manipulate[DenomZeros = PadeZeros[lMax];
 Show[
  Graphics[{Red, PointSize[Medium], Point[{Re[g], Im[g]} /. DenomZeros]}, Axes → True,
   PlotRange → {{-50, 50}, {-50, 50}}]],
 {lMax, 1, 190, 25}]
```

In[108]:=
```
ClearAll["Global`*"];
SetAttributes[CalcEnergy, HoldAll];
CalcEnergy[V_[y], y_, NmaxMax_] :=
 Module[{u, ud, udd, uddd, U, Ud, Udd, Uddd, H, f, h, SeriesF, CoeffG,
   SeriesY, CoeffY, EqY},
  Do[(
    (*B=1/2;*)
    u[n_][y] := Sum[u[n, k] y^k, {k, 0, Nmax - n}]; (*+O[y]^(Nmax-n+1)*)
    ud[n_][y] := Sum[k*u[n, k] y^(k - 1), {k, 1, Nmax - n}];
    udd[n_][y] := Sum[k*(k - 1)*u[n, k] y^(k - 2), {k, 2, Nmax - n}];
    uddd[n_][y] := Sum[k*(k - 1)*(k - 2)*u[n, k] y^(k - 3), {k, 3, Nmax - n}];
    u[0, 0] = 0; (* harmonic potential *)
    U[y] := Sum[u[n][y] g^n, {n, 0, Nmax}] + O[g]^(Nmax + 1);
    Ud[y] := Sum[ud[n][y] g^n, {n, 0, Nmax}] + O[g]^(Nmax + 1);
    Udd[y] := Sum[udd[n][y] g^n, {n, 0, Nmax}] + O[g]^(Nmax + 1);
    Uddd[y] := Sum[uddd[n][y] g^n, {n, 0, Nmax}] + O[g]^(Nmax + 1);
    H = Sum[h[n] g^n, {n, 0, Nmax}] + O[g]^(Nmax + 1);

    f[y] := V[y] + (g B - (1/4) U[y]^2) Ud[y]^2 - g H +
      (g^2/2) (-3 Udd[y]^2 + 2 Uddd[y] Ud[y])/(2 Ud[y]^2) + O[g]^(Nmax + 1) + O[y]^(Nmax + 2);
    (* immediately discard higher orders *)
    SeriesF = Normal[Series[f[y], {g, 0, Nmax}]]; (* slow step *)
    CoeffG = CoefficientList[SeriesF, g];
    SeriesY[n_] := Normal[Series[Part[CoeffG, n + 1], {y, 0, Nmax + 1}]];
    (* only need up to (g^0, y^Nmax+1) eq *)
    CoeffY[n_] := CoefficientList[SeriesY[n], y];
    EqY[n_, k_] := (Part[CoeffY[n], k + 1] == 0);
    (*EqY[n_,k_]:=(SeriesCoefficient[SeriesF,{g,0,n},{y,0,k}]==0)*);

    (* Compute terms if not yet defined, but limit to correct range *)
    Do[If[! With[{k = k}, ValueQ[u[0, k]]],
      u[0, k] = Last @@ Last@Solve[EqY[0, k + 1], u[0, k]]], {k, 1, Nmax}];
    Do[Do[If[! With[{n = n, k = k}, ValueQ[u[n, k]]],
       u[n, k] = Last @@ Last@Solve[EqY[n, k + 1], u[n, k]]], {k, 0, Nmax - 2 n}],
     {n, 1, Ceiling[Nmax/2]}]; (* only correct up to k=Nmax-2n *)
    Do[If[! With[{n = n}, ValueQ[h[n]]],
      h[n] = Last @@ Last@Solve[EqY[n + 1, 0], h[n]] // Simplify;
      Print["h[", n, "] = ", h[n]]],
     {n, 0, Ceiling[Nmax/2] - 1}];
   ), {Nmax, 2, NmaxMax}]]

(* example use: V[y_]:=y^2(1+y)^2; CalcEnergy[V[y],y,7]

Vdw[y_] := y^2 (1 + y)^2; CalcEnergy[Vdw[y], y, 12] // Timing
```

In[114]:=
```
Vsg[y_] := Sin[y]^2; CalcEnergy[Vsg[y], y, 6] // Timing
```

$$h[0] = 2B$$

$$h[1] = \frac{1}{8}\left(-1 - 4B^2\right)$$

$$h[2] = -\frac{1}{32}B\left(3 + 4B^2\right)$$

References

[1] T. Misumi, M. Nitta, and N. Sakai, "Resurgence in sine-Gordon quantum mechanics: exact agreement between multi-instantons and uniform WKB," *Journal of High Energy Physics* **9** (Sept., 2015) , arXiv:1507.00408 [hep-th].

[2] G. Basar, G. V. Dunne, and M. Ünsal, "Resurgence theory, ghost-instantons, and analytic continuation of path integrals," *Journal of High Energy Physics* **10** (Oct., 2013) , arXiv:1308.1108 [hep-th].

[3] S. Demulder, D. Dorigoni, and D. C. Thompson, "Resurgence in η-deformed Principal Chiral Models," (Apr., 2016) , arXiv:1604.07851 [hep-th].

[4] G. V. Dunne and M. Ünsal, "Resurgence and trans-series in Quantum Field Theory: the $\mathbb{CP}^{N-1}$ model," *Journal of High Energy Physics* **11** (Nov., 2012) , arXiv:1210.2423 [hep-th].

[5] A. Cherman, D. Dorigoni, G. V. Dunne, and M. Ünsal, "Resurgence in quantum field theory: Nonperturbative effects in the principal chiral model," *Phys. Rev. Lett.* **112** (Jan, 2014) .

[6] T. Aoyama, M. Hayakawa, T. Kinoshita, and M. Nio, "Tenth-Order QED Contribution to the Electron $g-2$ and an Improved Value of the Fine Structure Constant," *Phys. Rev. Lett.* **109** no. 11, (Sept., 2012) 111807, arXiv:1205.5368 [hep-ph].

[7] B. Delamotte, "A hint of renormalization," *American Journal of Physics* **72** (Feb., 2004) 170–184, hep-th/0212049.

[8] L. Alvarez-Gaume and M. A. Vazquez-Mozo, "Introductory Lectures on Quantum Field Theory," (Oct., 2005) , arXiv:hep-th/0510040.

[9] D. J. Gross and F. Wilczek, "Ultraviolet behavior of non-abelian gauge theories," *Phys. Rev. Lett.* **30** (Jun, 1973) 1343–1346.

[10] H. D. Politzer, "Reliable perturbative results for strong interactions?," *Phys. Rev. Lett.* **30** (Jun, 1973) 1346–1349.

[11] **Particle Data Group** Collaboration, K. A. Olive *et al.*, "Review of Particle Physics," *Chin. Phys.* **C38** (2014) 090001.

[12] A. Pich, "Effective Field Theory," (June, 1998) , hep-ph/9806303.

[13] M. Marino, "Lectures on non-perturbative effects in large-N gauge theories, matrix models and strings," (June, 2012) , arXiv:1206.6272 [hep-th].

[14] A. Jaffe and E. Witten, "Quantum Yang-Mills Theory,". http://www.claymath.org/sites/default/files/yangmills.pdf.

[15] C. J. Morningstar and M. Peardon, "Glueball spectrum from an anisotropic lattice study," *Phys. Rev. D* **60** (Jul, 1999) 034509. http://link.aps.org/doi/10.1103/PhysRevD.60.034509.

[16] V. Crede and C. A. Meyer, "The experimental status of glueballs," *Progress in Particle and Nuclear Physics* **63** (July, 2009) 74–116, arXiv:0812.0600 [hep-ex].

[17] W. Ochs, "The status of glueballs," *Journal of Physics G Nuclear Physics* **40** no. 4, (Apr., 2013) , arXiv:1301.5183 [hep-ph].

[18] F. J. Dyson, "Divergence of perturbation theory in quantum electrodynamics," *Phys. Rev.* **85** (Feb, 1952) 631–632.

[19] D. Dorigoni, "An Introduction to Resurgence, Trans-Series and Alien Calculus," (Nov., 2014) , arXiv:1411.3585 [hep-th].

[20] S. Coleman, "The uses of instantons," in *Aspects of Symmetry: Selected Erice Lectures*, pp. 265–350. Cambridge University Press, 1985. Cambridge Books Online.

[21] G. V. Dunne and M. Ünsal, "Uniform WKB, multi-instantons, and resurgent trans-series," *Phys. Rev. D* **89** no. 10, (May, 2014) , arXiv:1401.5202 [hep-th].

[22] G. V. Dunne and M. Ünsal, "Generating nonperturbative physics from perturbation theory," *Phys. Rev. D* **89** no. 4, (Feb., 2014) , arXiv:1306.4405 [hep-th].

[23] J. Zinn-Justin and U. D. Jentschura, "Multi-instantons and exact results I: conjectures, WKB expansions, and instanton interactions," *Annals of Physics* **313** (Sept., 2004) 197–267, arXiv:quant-ph/0501136.

[24] J. Zinn-Justin and U. D. Jentschura, "Multi-instantons and exact results II: specific cases, higher-order effects, and numerical calculations," *Annals of Physics* **313** (Oct., 2004) 269–325, arXiv:quant-ph/0501137.

[25] P. C. Argyres and M. Ünsal, "The semi-classical expansion and resurgence in gauge theories: new perturbative, instanton, bion, and renormalon effects," *Journal of High Energy Physics* **8** (Aug., 2012) , arXiv:1206.1890 [hep-th].

[26] I. Aniceto, R. Schiappa, and M. Vonk, "The Resurgence of Instantons in String Theory," (June, 2011) , arXiv:1106.5922 [hep-th].

[27] A. Cherman, D. Dorigoni, and M. Ünsal, "Decoding perturbation theory using resurgence: Stokes phenomena, new saddle points and Lefschetz thimbles," *Journal of High Energy Physics* **2015** no. 10, (2015) .

[28] G. Basar and G. V. Dunne, "Resurgence and the Nekrasov-Shatashvili limit: connecting weak and strong coupling in the Mathieu and Lamé systems," *Journal of High Energy Physics* **2** (Feb., 2015) , arXiv:1501.05671 [hep-th].

[29] G. Başar and G. V. Dunne, "Hydrodynamics, resurgence, and transasymptotics," *Phys. Rev. D* **92** no. 12, (Dec., 2015) , arXiv:1509.05046 [hep-th].

[30] A. Grassi, M. Mariño, and S. Zakany, "Resumming the string perturbation series," *Journal of High Energy Physics* **5** (May, 2015) , arXiv:1405.4214 [hep-th].

[31] J. Écalle, *Les Fonctions Resurgentes*, vol. I - III. Publications Mathématiques d'Orsay, 1981. http://sites.mathdoc.fr/PMO/PDF/E_ECALLE_81_05.pdf.

[32] E. Bogomolny, "Calculation of instanton-anti-instanton contributions in quantum mechanics," *Phys. Lett. B* **91** no. 3, (1980) 431 – 435. http://www.sciencedirect.com/science/article/pii/037026938091014X.

[33] J. Zinn-Justin, "Multi - Instanton Contributions in Quantum Mechanics," *Nucl. Phys.* **B192** (1981) 125–140.

[34] J. Zinn-Justin, "Multi - Instanton Contributions in Quantum Mechanics. 2.," *Nucl. Phys.* **B218** (1983) 333–348.

[35] G. 't Hooft, "The whys of subnuclear physics," ch. Can We Make Sense Out of "Quantum Chromodynamics"?, pp. 943–982. Springer US, 1979.

[36] M. Beneke, "Renormalons," *Phys. Rep.* **317** (Aug., 1999) , arXiv:hep-ph/9807443.

[37] M. Beneke and V. M. Braun, "Renormalons and Power Corrections," *ArXiv High Energy Physics - Phenomenology e-prints* (Oct., 2000) , hep-ph/0010208.

[38] N. W. McLachlan, *Theory and Application of Mathieu Functions*. Oxford University Press, 1947.

[39] J. Meixner and F. W. Schäfke, *Mathieusche Funktionen und Sphäroidfunktionen*. Springer-Verlag, 1954.

[40] H. Müller-Kirsten, *Introduction to Quantum Mechanics: Schrödinger Equation and Path Integral*. World Scientific, 2006.

[41] M. Stone and J. Reeve, "Late terms in the asymptotic expansion for the energy levels of a periodic potential," *Phys. Rev. D* **18** (1978) 4746–4751.

[42] V. Novikov, M. Shifman, V. Zakharov, and A. Vainshtein, "ABC of Instantons," in *ITEP Lectures on Particle Physics and Field Theory*, vol. 1, ch. III, pp. 201–299. World Scientific, 1999. http://www.tpi.umn.edu/shifman/lectures4students/ABC_of_Instantons.pdf.

[43] E. J. Weinberg, *Classical solutions in quantum field theory: solitons and instantons in high energy physics*. Cambridge Monographs on Mathematical Physics. Cambridge University Press, 2012.

[44] H. Forkel, "A Primer on Instantons in QCD," (Sept., 2000) , arXiv:hep-ph/0009136.

[45] M. Peskin and D. Schroeder, *An Introduction to Quantum Field Theory*. Advanced book classics. Addison-Wesley Publishing Company, 1995.

[46] M. Blau, "Notes on (semi-)advanced quantum mechanics: The path integral approach to quantum mechanics," lecture notes, Universität Bern, 2014. http://www.blau.itp.unibe.ch/Lecturenotes.html.

[47] S. A. Albeverio, R. J. Høegh-Krohn, and S. Mazzucchi, *Mathematical Theory of Feynman Path Integrals: An Introduction*, vol. 523 of *Lecture Notes in Mathematics*. Springer-Verlag, 2nd ed., 2008.

[48] M. Berry and C. Howls, *Divergent series: taming the tails*. Princeton University Press, January, 2014. http://eprints.soton.ac.uk/360980/.

[49] C. M. Bender and S. A. Orszag, *Advanced Mathematical Methods for Scientists and Engineers I: Asymptotic Methods and Perturbation Theory*. Springer-Verlag, 1999.

[50] K. Konishi and G. Paffuti, *Quantum mechanics: a new introduction*. Oxford University Press, 2009.

[51] A. D. Sokal, "An improvement of Watson's theorem on Borel summability," *Journal of Mathematical Physics* **21** (Feb., 1980) 261–263.

[52] M. Flory, R. C. Helling, and C. Sluka, "How I Learned to Stop Worrying and Love QFT," arXiv:1201.2714 [math-ph].

[53] B. Simon, "The anharmonic oscillator: A singular perturbation theory," in *Cargese Lectures in Theoretical Physics*, no. 5. Gordon and Breach, 1972. http://math.caltech.edu/SimonPapers/R2.pdf.

[54] K. Hagen and V. Schulte-Frohlinde, *Critical Properties of φ^4 Theories*. World Scientific Publishing Company, 1st ed., 2001. http://users.physik.fu-berlin.de/~kleinert/kleiner_reb8/psfiles/phi4.pdf.

[55] G. A. Baker, *Essentials of Padé approximants*. Academic Press, 1975.

[56] M. Karliner, "Precise Estimates of High Orders in QCD," *Acta Physica Polonica B* **29** (May, 1998) , hep-ph/9804381.

[57] T. Kawai and Y. Takei, *Algebraic analysis of singular perturbation theory*. No. 227 in Translations of mathematical monographs. American Mathematical Society, 2005.

[58] R. Dingle and H. Müller, "Asymptotic expansions of mathieu functions and their characteristic numbers," *Journal für die reine und angewandte Mathematik* **211** (1962) 11–32. http://eudml.org/doc/150544.

[59] G. V. Dunne and M. Ünsal, "WKB and Resurgence in the Mathieu Equation," (Mar., 2016) , arXiv:1603.04924 [math-ph].

[60] "NIST Digital Library of Mathematical Functions." Release 1.0.10 of 2015-08-07. http://dlmf.nist.gov/.

[61] C. M. Bender and T. T. Wu, "Anharmonic oscillator," *Phys. Rev.* **184** (Aug, 1969) 1231–1260. http://link.aps.org/doi/10.1103/PhysRev.184.1231.

[62] C. M. Bender and T. T. Wu, "Anharmonic Oscillator. II. A Study of Perturbation Theory in Large Order," *Phys. Rev. D* **7** (Mar, 1973) 1620–1636.

[63] I. M. Suslov, "Divergent perturbation series," *Soviet Journal of Experimental and Theoretical Physics* **100** (June, 2005) 1188–1233, hep-ph/0510142.

[64] A. Cherman, P. Koroteev, and M. Ünsal, "Resurgence and holomorphy: From weak to strong coupling," *Journal of Mathematical Physics* **56** no. 5, (May, 2015) 053505, arXiv:1410.0388 [hep-th].

[65] M. Ünsal, "Theta dependence, sign problems, and topological interference," *Phys. Rev. D* **86** no. 10, (Nov., 2012) 105012, arXiv:1201.6426 [hep-th].

[66] J. Le Guillou and J. Zinn-Justin, eds., *Large-Order Behaviour of Perturbation Theory*, vol. 7 of *Current Physics--Sources and Comments*. North Holland, 1990.

[67] A. Mironov and A. Morozov, "Nekrasov functions and exact Bohr-Sommerfeld integrals," *Journal of High Energy Physics* **4** (Apr., 2010) , arXiv:0910.5670 [hep-th].

[68] W. He and Y.-G. Miao, "Magnetic expansion of Nekrasov theory: The SU(2) pure gauge theory," *Phys. Rev. D* **82** no. 2, (July, 2010) , arXiv:1006.1214 [hep-th].

[69] W. He and Y.-G. Miao, "Mathieu Equation and Elliptic Curve," *Communications in Theoretical Physics* **58** (Dec., 2012) 827–834, arXiv:1006.5185 [math-ph].

[70] A.-K. Kashani-Poor and J. Troost, "Pure N=2 Super Yang-Mills and Exact WKB," arXiv:1504.08324 [hep-th].

[71] J. L. Dunham, "The Wentzel-Brillouin-Kramers method of solving the wave equation," *Phys. Rev.* **41** (Sep, 1932) 713–720.

[72] A. Galindo and P. Pascual, *Quantum Mechanics II*. Texts and Monographs in Physics. Springer, 1991.